

Biophysical principles underlying electrical activity in nervous networks

Marco Arieli Herrera Valdez

Associate Professor, Department of Mathematics

Laboratory of Systems Physiology
Universidad Nacional Autónoma de México

*Life Sciences Seminar,
Biozentrum, University of Würzburg
October 22, 2018*

Acknowledgments

Martin Strube-Bloss and Wolfgang Rössler, Life Sciences Graduate Program, Department of Behavioral Physiology & Sociobiology, Theodor-Boveri-Institute of Bioscience, Biocenter, University of Würzburg

Thank you for the invitation

SCAB232:

Carlos Monsalvo (MSc Geometrical analysis behind neuronal excitability),
Roberto García-Medina (PhD Mappings between graphs defined by synaptic connections and based on functional connectivity),
Alfredo Antonio López-Castillo (Biol, transcription regulation in *B subtilis*, biophysics and metabolism in pancreas),
Laurent Parmentier (Math, bifurcation structures in hierarchical families of biophysical models),
César Flores-López (Biol, nearly coincident spiking in neurons with common synaptic innervation),
Carlos Andrés Gil-Gómez (Biol, biophysics and metabolic traits underlying energy consumption and storage in stratal muscles),
Olyn Castañeda Ramírez (Math, randomness in spike trains from biophysical neuronal models),
Noe Plascencia-Díaz (Phys, topological classification of dynamic motifs from EEG recordings in epileptic patients),
Guillermo Olicón (MSc Simple model of short term synaptic plasticity),
Augusto Cabrera (MSc Non-independent ion-channel gating).

Galarraga & Bargas labs:

Janet Barroso-Flores, Alejandra Cáceres-Chávez, Esther Martínez, Mariana Duhne, Mario Arias, Jesús Pérez-Ortega

Colaborators and some sources of funding

Elvira Galarraga y José Bargas. Biophysics and microcircuits in the basal ganglia (CONACyT-Frontera 57).

Tatiana Fiordelisio y Erin McKiernan (ECM). Co-directors of the Laboratory of Physiology and Quantitative Imaging.

Alessio Franci (AF). Mathematics underlying circadian rhythms and excitability in regulation of transcription.

Ayari Fuentes-Hernández (AFH) y Rafael Peña-Miller (RPM) (Phenotypical diversity, antibiotic resistance, and transcription regulation.)

Krasimira Atzaneva, Eder Zavala, Kyle Wedgwood (Exeter University, UK, Biomedical modelling of hormone dynamics at the interface of stress and metabolism, Royal Society, NI170267)

DGAPA-UNAM PAPIIT IA208618

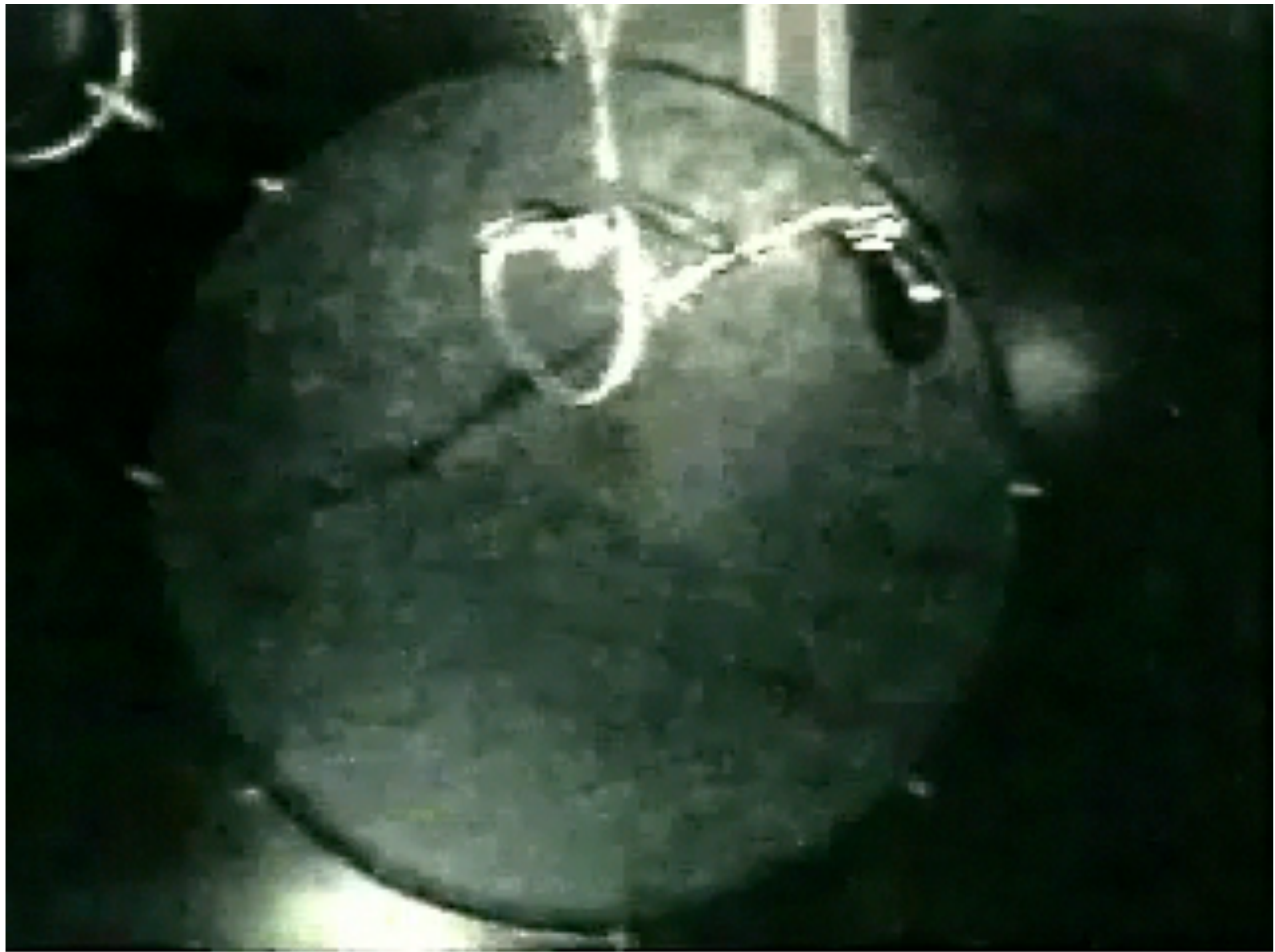
Outline:

The nervous system is a complex adaptive system. Biophysical properties of cells affect activity at different levels, including networks.

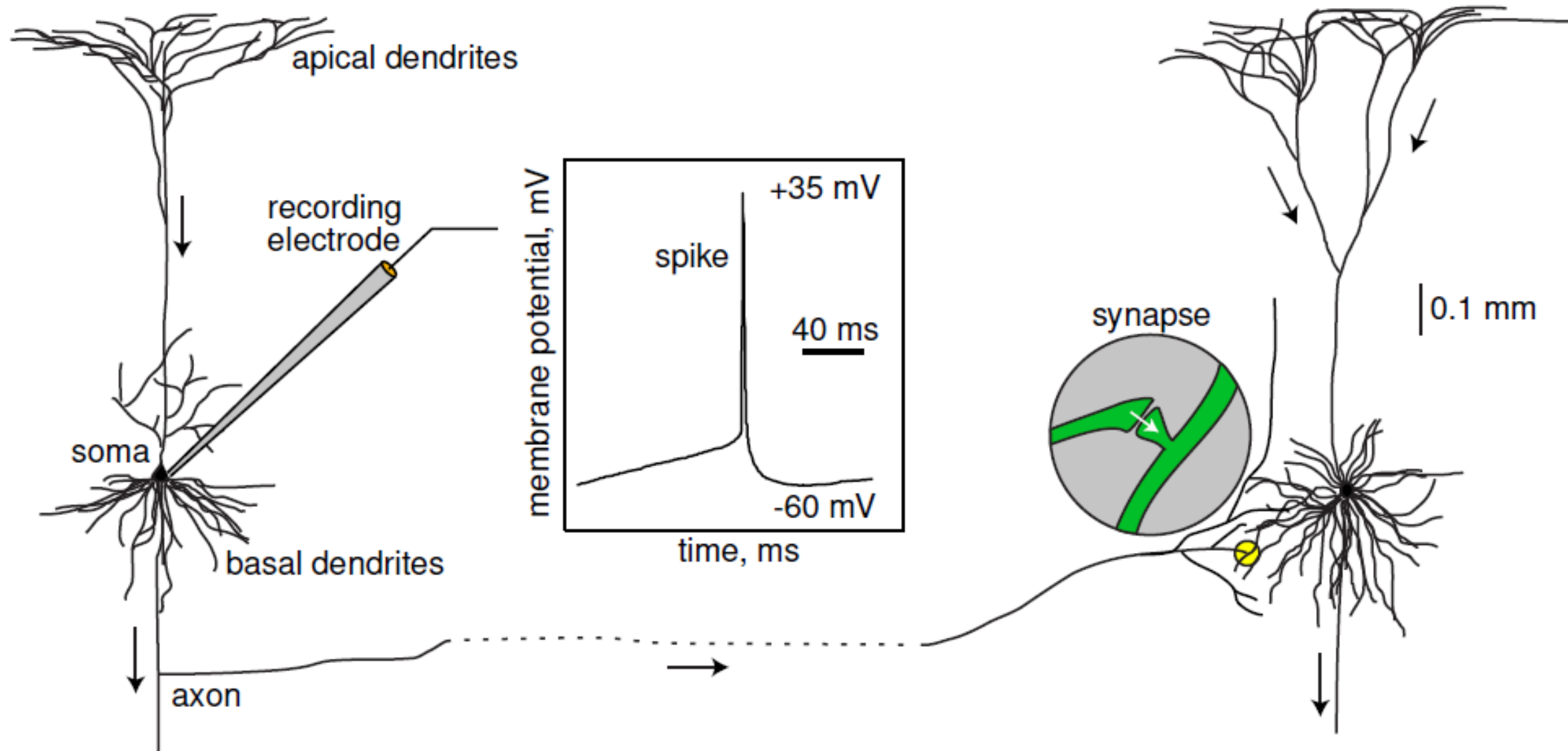
Biophysics of transmembrane transport biophysics and cellular excitability:
A thermodynamic transport model beyond the conductance-based model
Logistic model of gating dynamics

Dynamical Systems: Bifurcation structures accurately describe the relationship between the electrophysiological phenotype and the patterns of expression of transmembrane proteins mediating transport

Cellular excitability in networks: Nearly coincident spiking as a function of common synaptic input



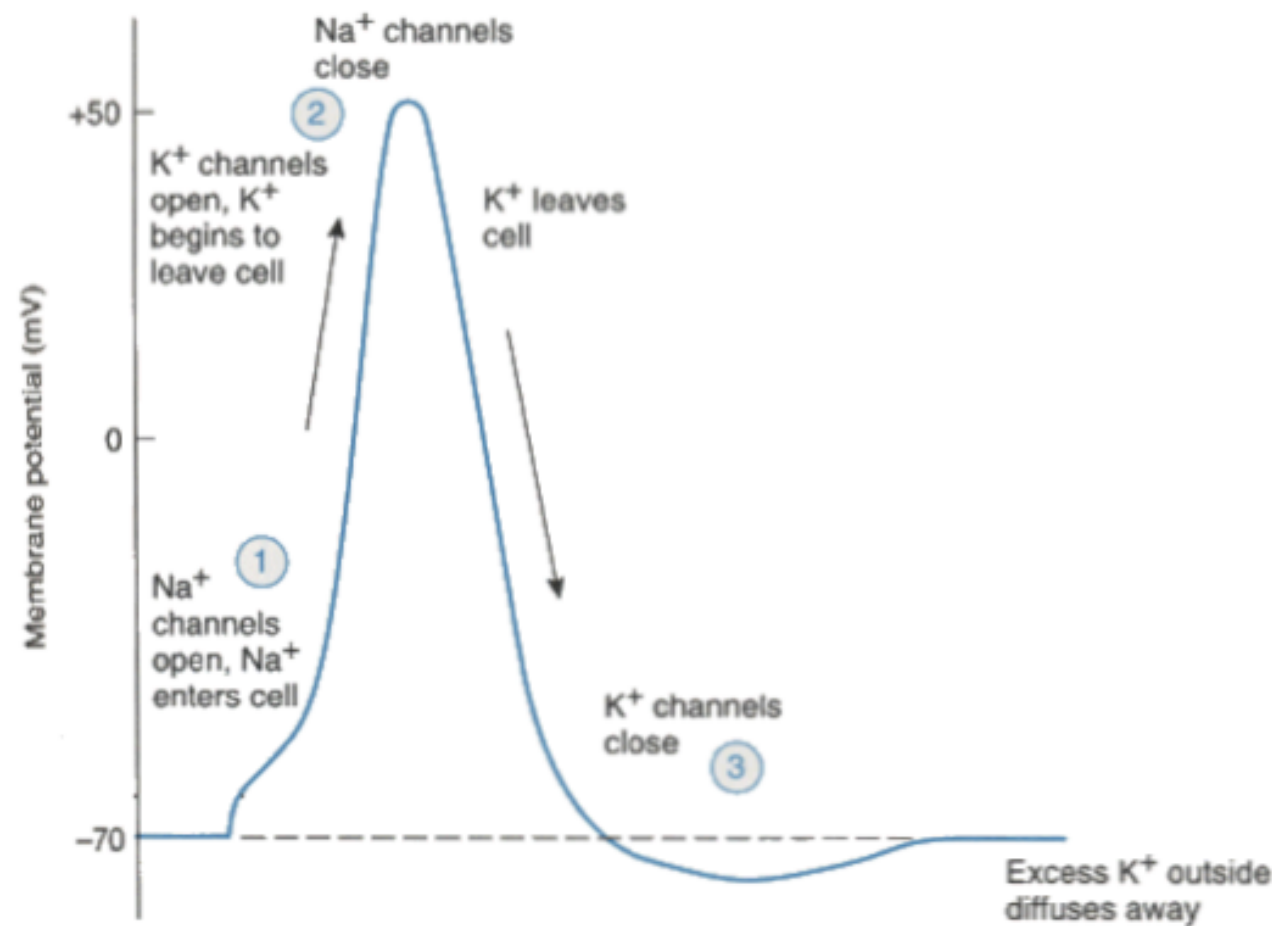
The biophysical properties of cells influence network activity and viceversa



The input from many synapses is integrated to produce more electrical activity

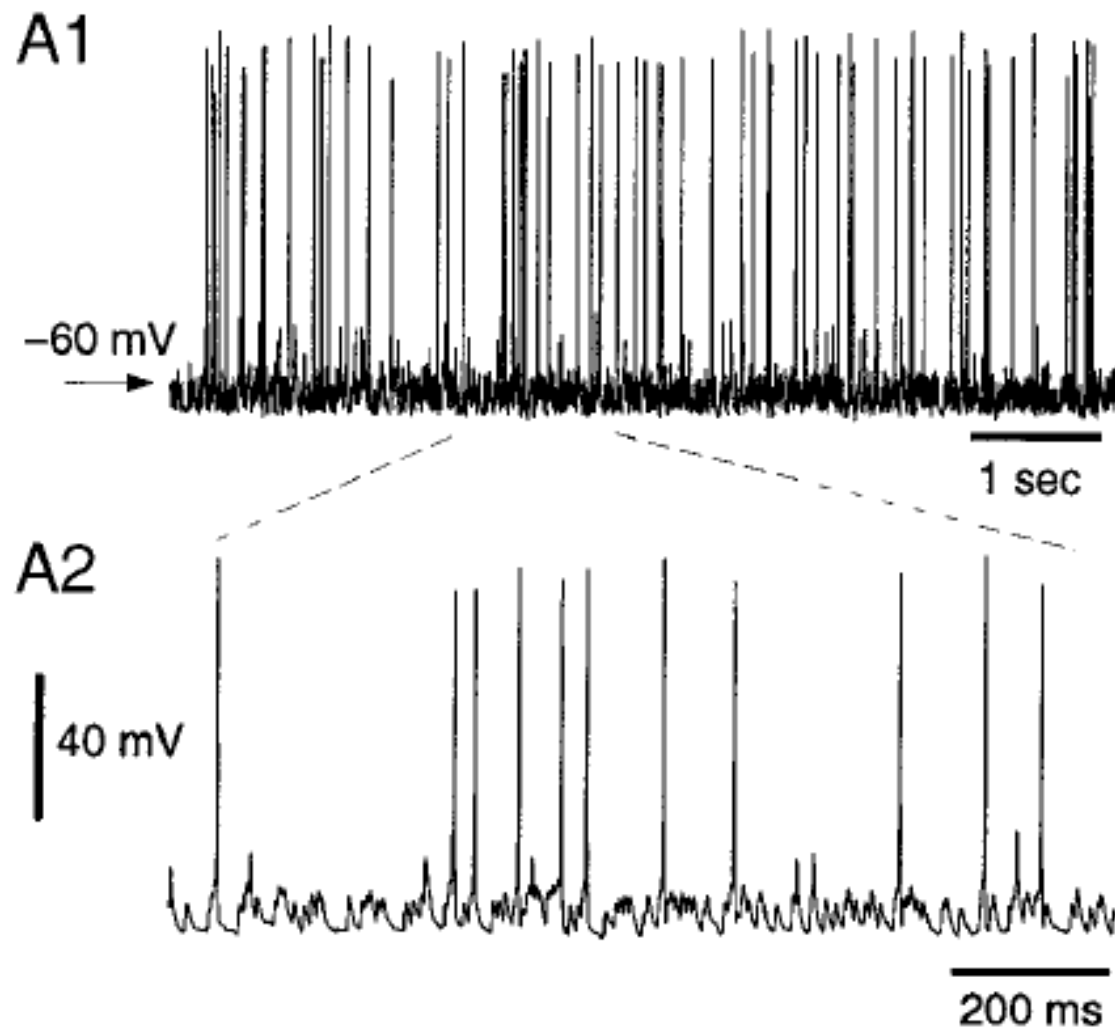
Mechanism of generation of action potentials: Hodgkin & Huxley, 1952

Cations in (Na, Ca push v up), cations out (K outflow pushes v down)
... in plants this may be a bit different, but the idea is the same



Transmembrane motion (transport) generates currents

At a single cell level, the dynamics seem to be autonomous (within short time scales)



Reliability of Spike Timing in Neocortical Neurons, Zachary F. Mainen* and Terrence J. Sejnowski (1995)

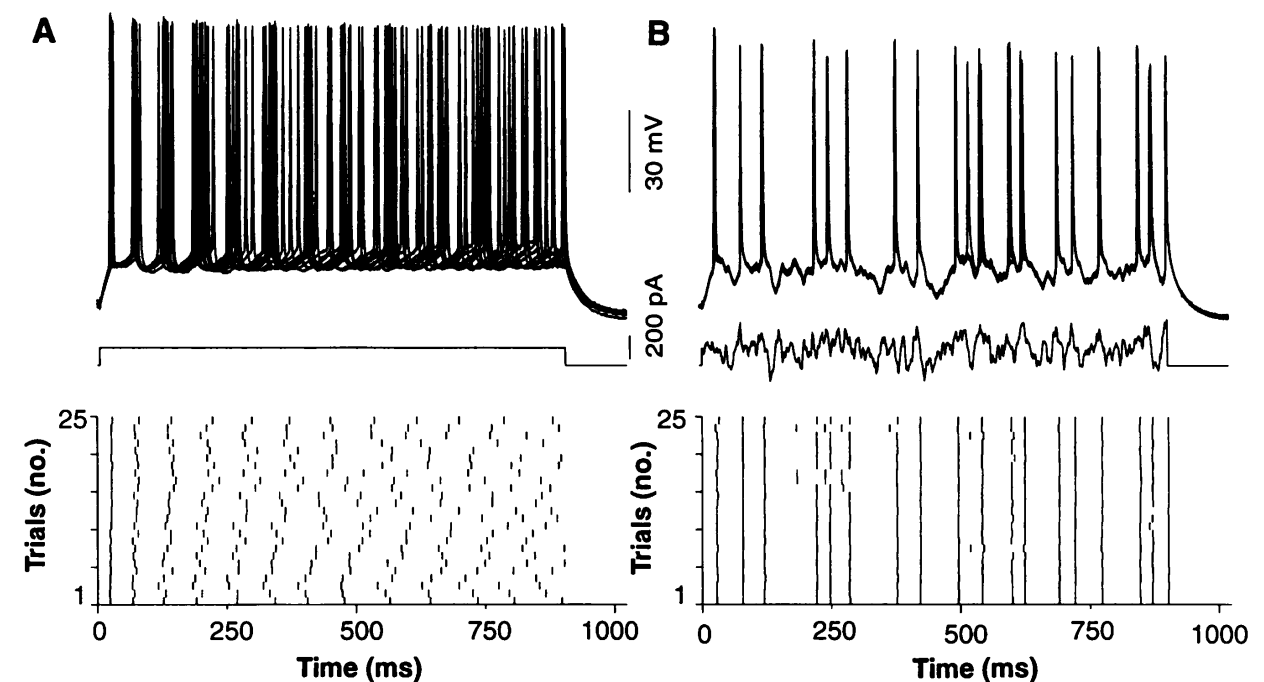


Fig. 1. Reliability of firing patterns of cortical neurons evoked by constant and fluctuating current. **(A)** In this example, a superthreshold dc current pulse (150 pA, 900 ms; middle) evoked trains of action potentials (approximately 14 Hz) in a regular-firing layer-5 neuron. Responses are shown superimposed (first 10 trials, top) and as a raster plot of spike times over spike times (25 consecutive trials, bottom). **(B)** The same cell as in (A) was again stimulated repeatedly, but this time with a fluctuating stimulus [Gaussian white noise, $\mu_s = 150$ pA, $\sigma_s = 100$ pA, $\tau_s = 3$ ms; see (14)].

The system behaves reliably in response to repeated presentations of the same noisy stimulus

Change in membrane potential:

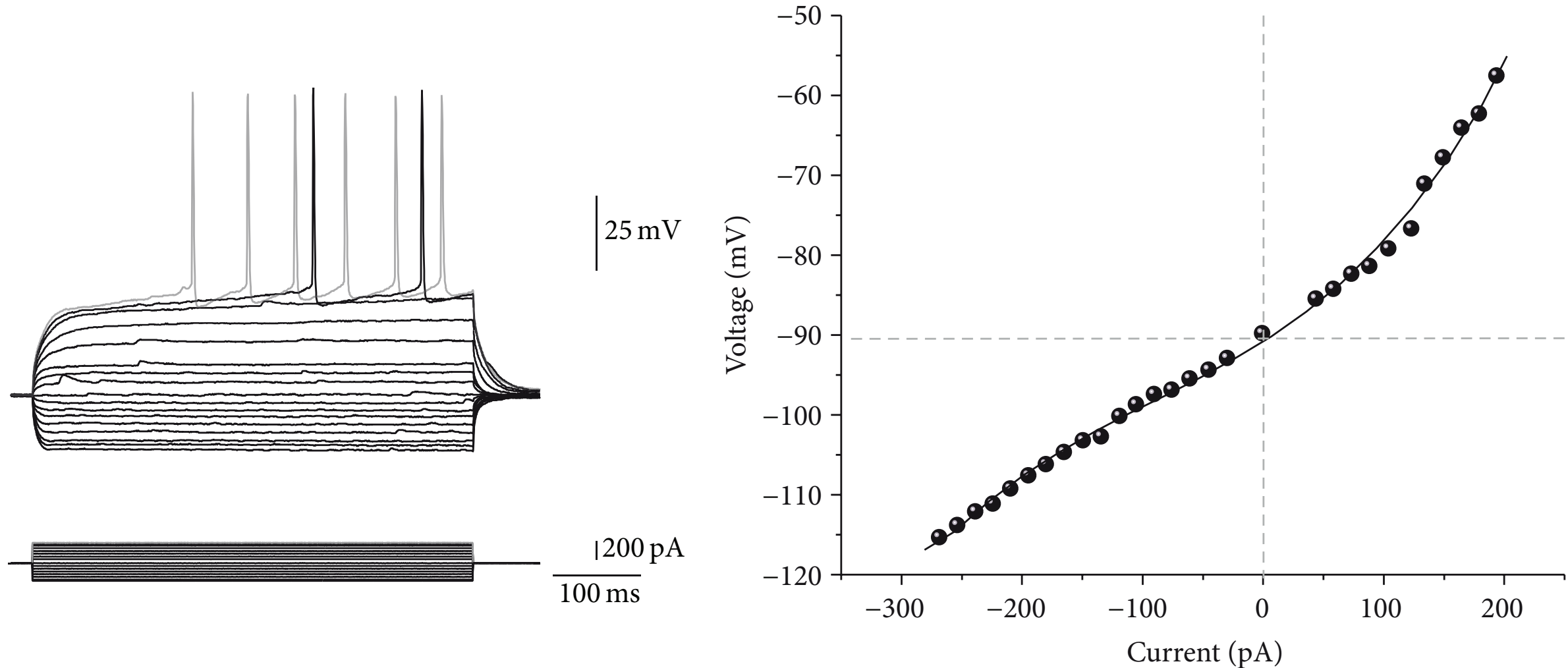
$$\partial_t v = f_i(v, w; p) + f_s(v; p) + I_F$$

Proportion of open K channels:

$$\partial_t w = g(v, w; p)$$

Synaptic plasticity

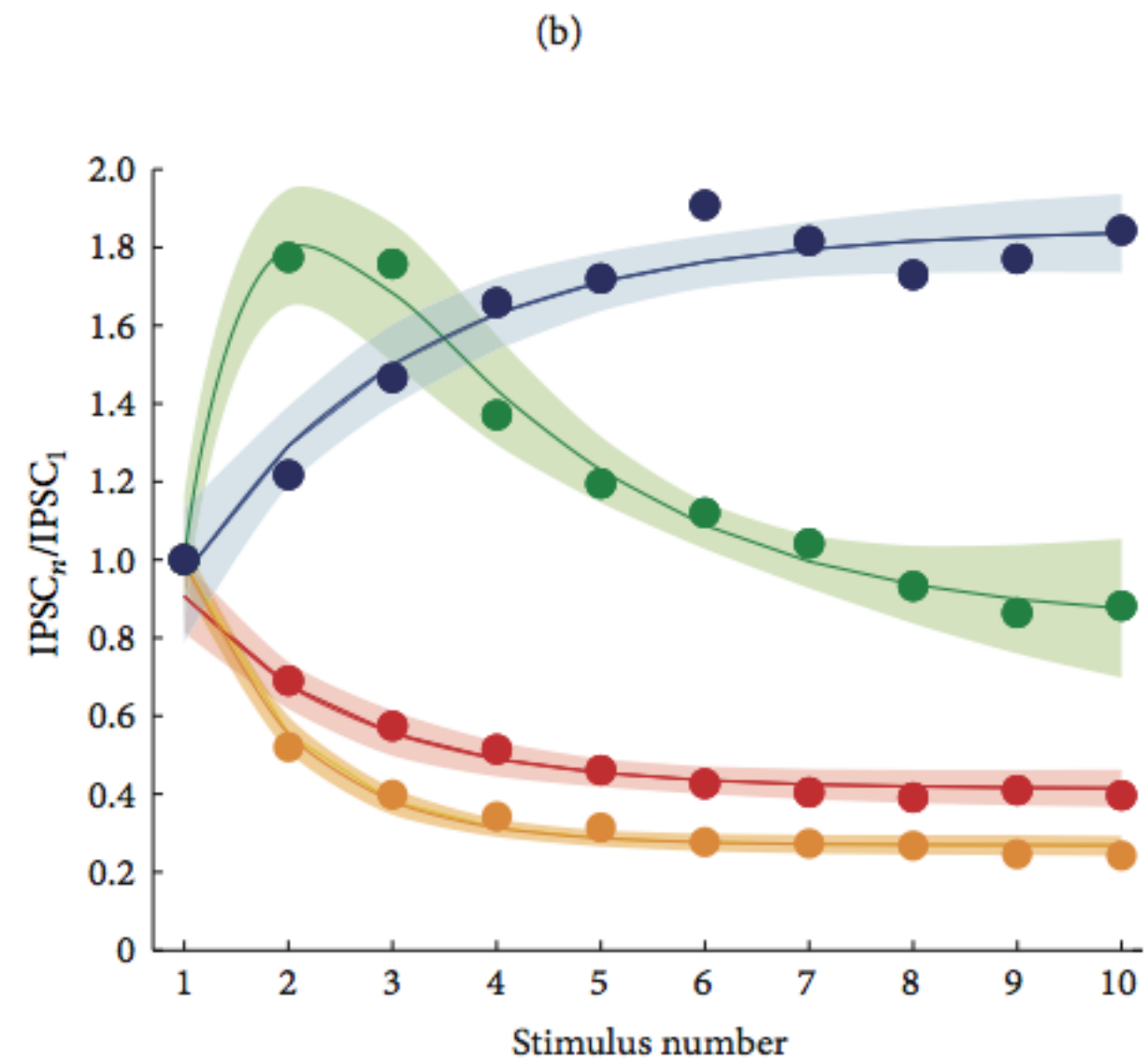
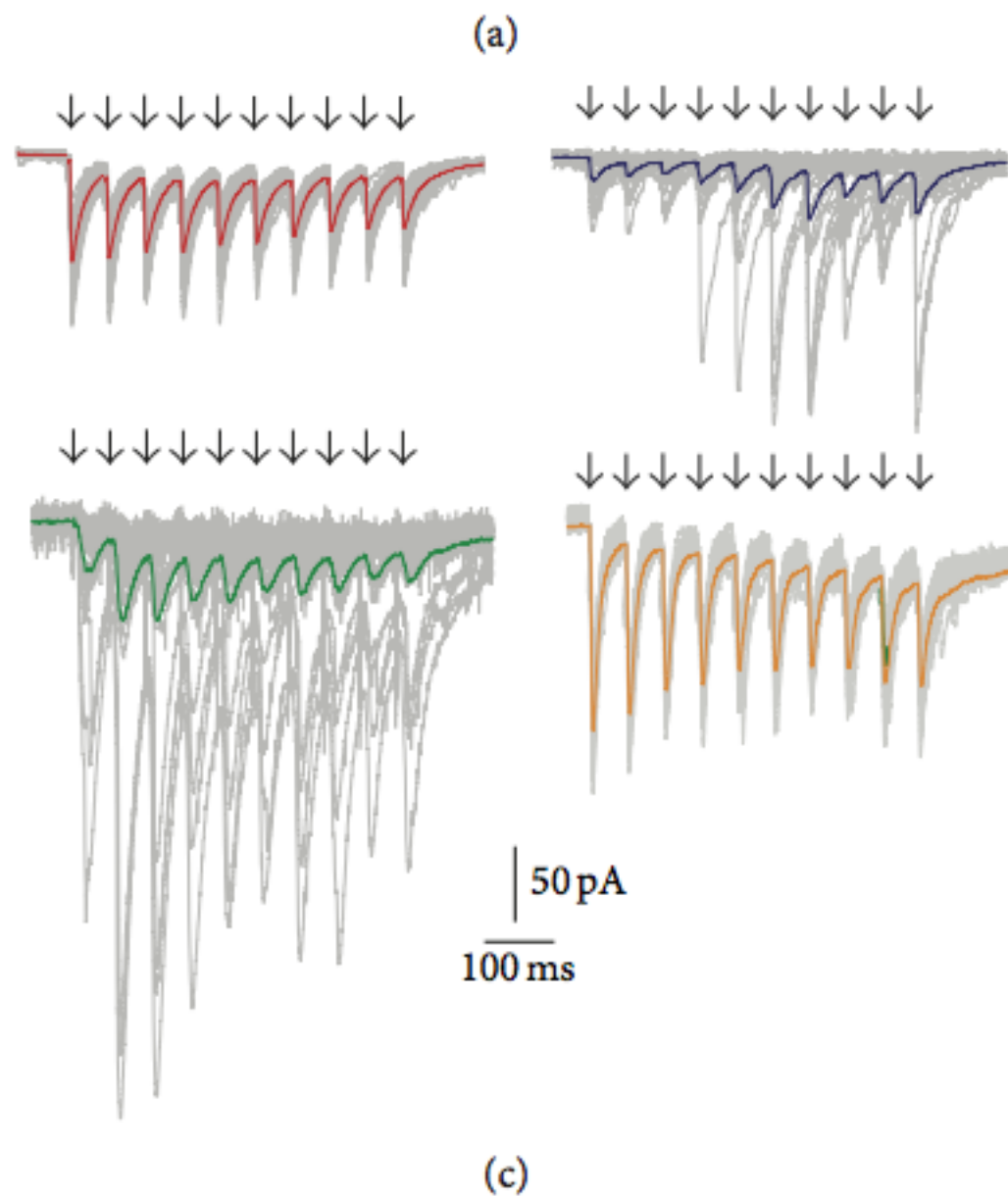
Responses to current injection in striatal spiny projection



Barroso-Flores, Herrera-Valdez, et al. 2015

Striatal spiny projection neuron plasticity

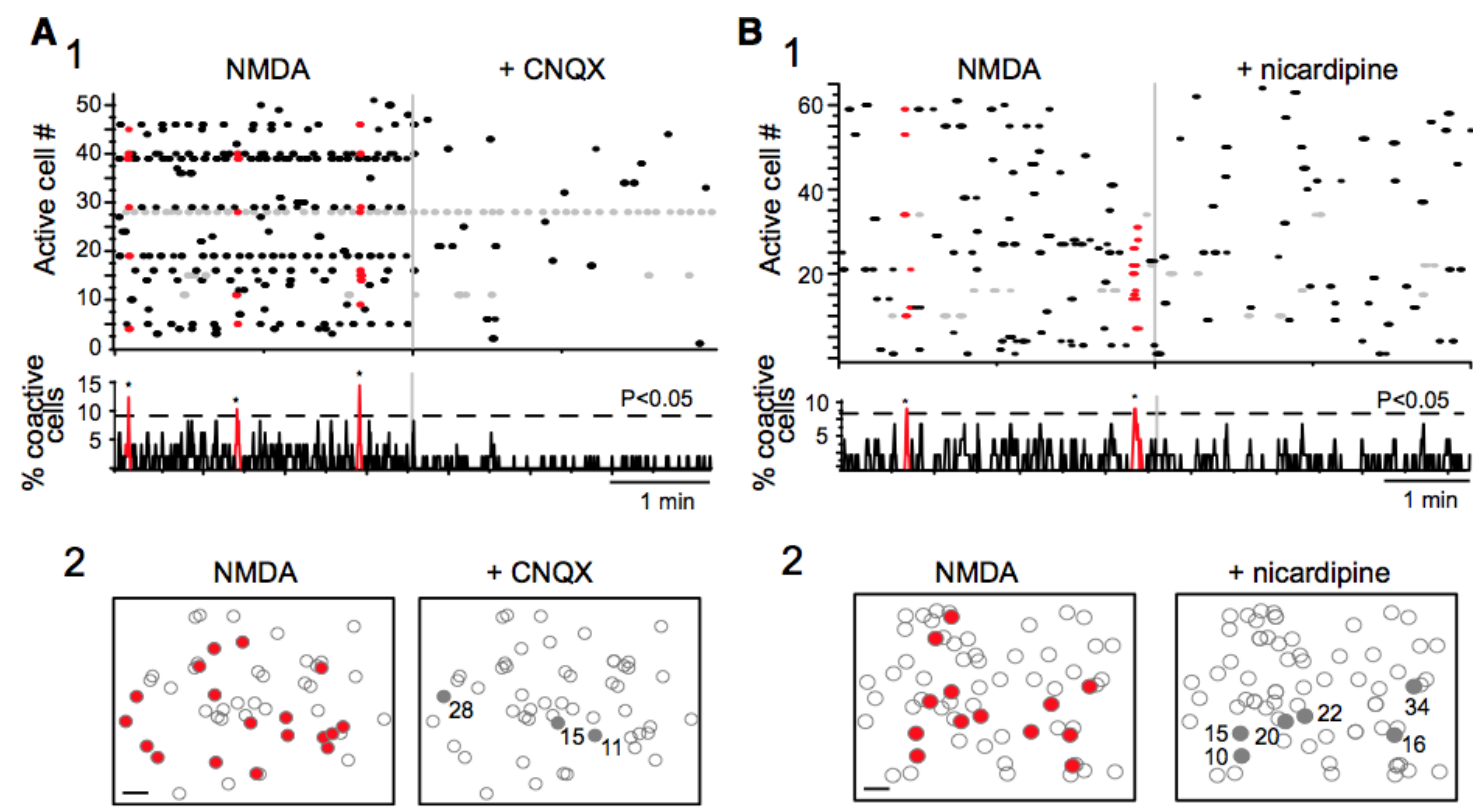
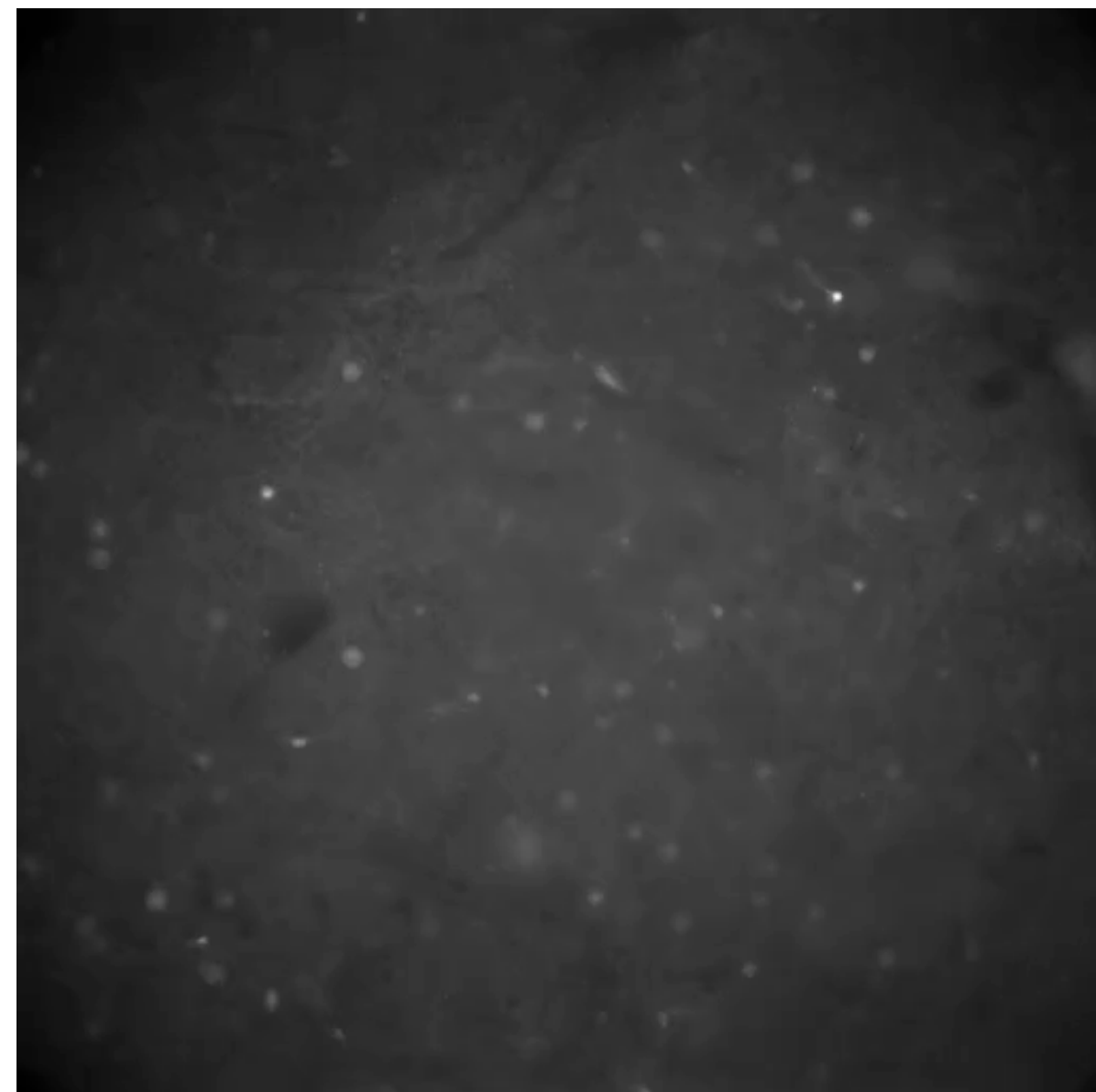
Responses in SPNs to synaptic stimulation from long range interneurons



(c)

(d)

Disruption of stratal network activity *in vitro*



CNQX~ AMPA receptor antagonist,
nicardipine~L-type Ca channel blocker.

Carrillo-Reid et al. 2008

How can we systematically study these changes at the level of the microcircuit to better understand the network as a function of the intrinsic properties of the cells?

Outline:

The nervous system is a complex adaptive system. Biophysical properties of cells affect activity at different levels, including networks.

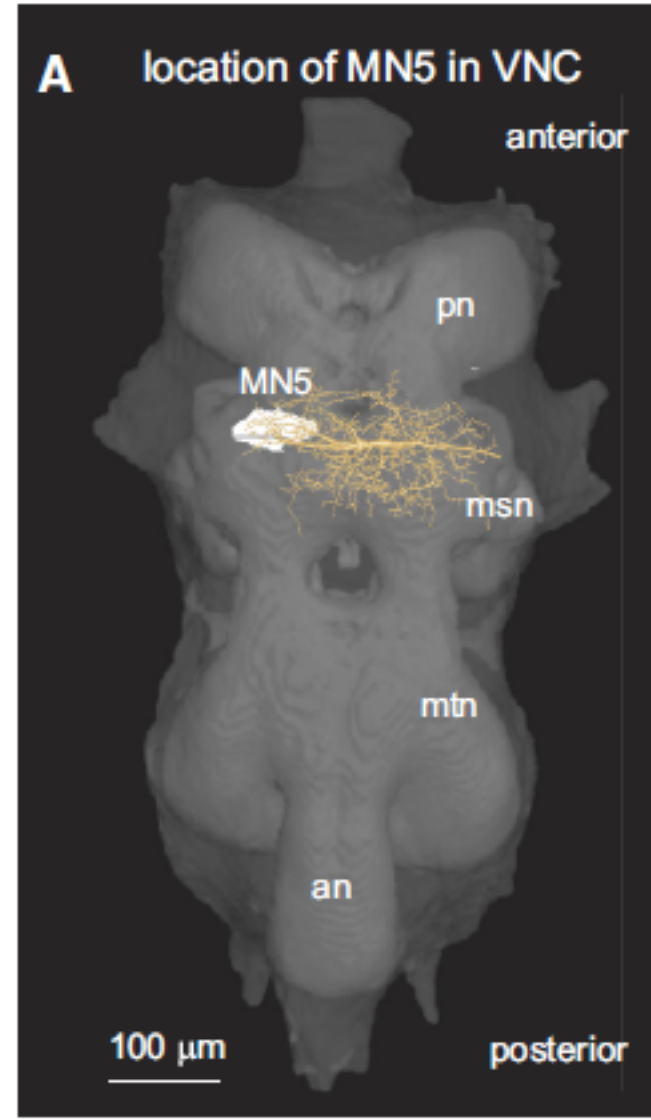
Current projects: Short term synaptic plasticity, network dynamics in the mushroom bodies

Biophysics of transmembrane transport biophysics and cellular excitability:
A thermodynamic transport model beyond the conductance-based model
Logistic model of gating dynamics

Past modeling and ongoing projects

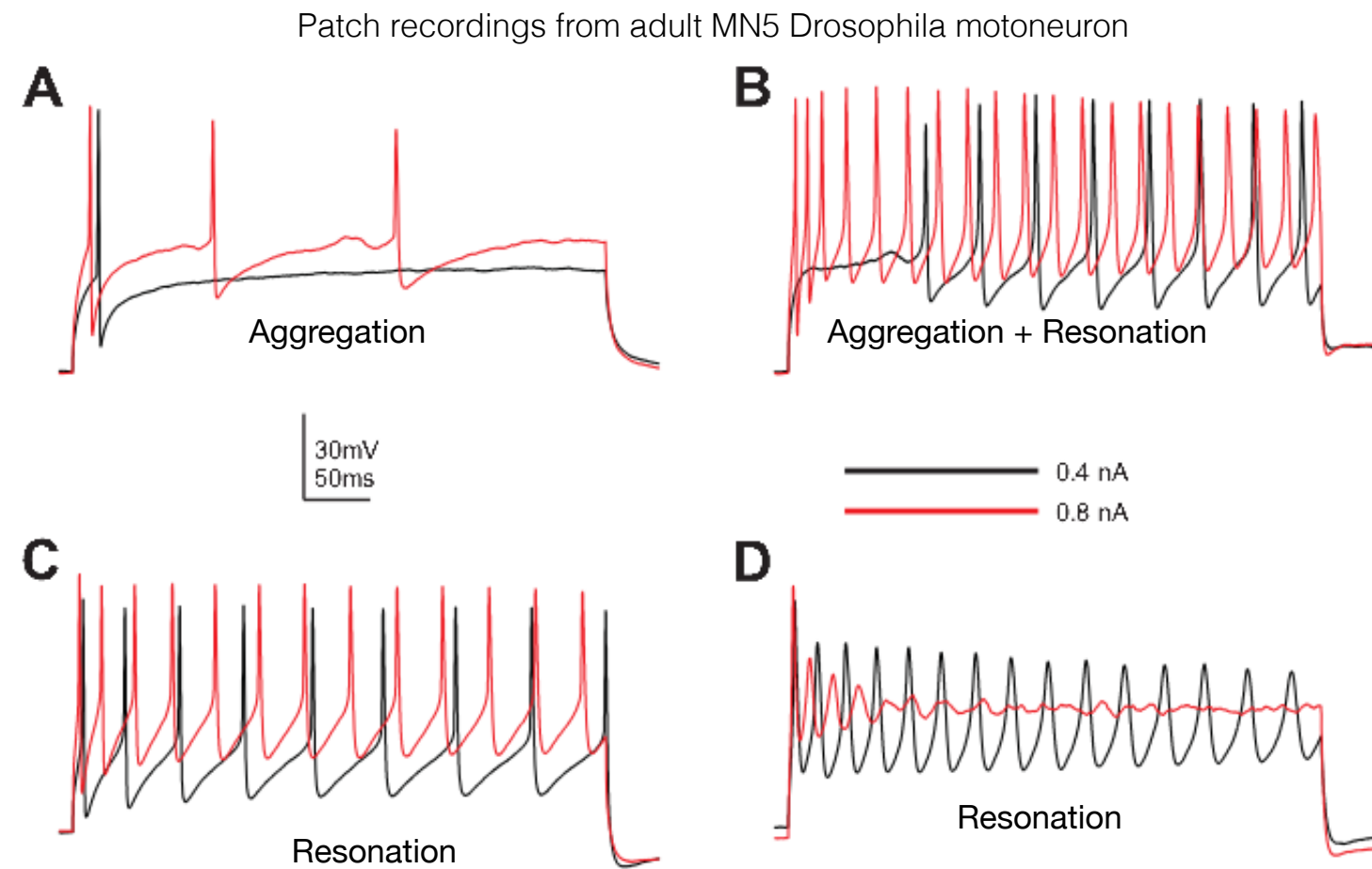
Why are the patterns from the same identified neuron so different?

MN5 controls the dorsolateral wing muscle in adult Drosophila.

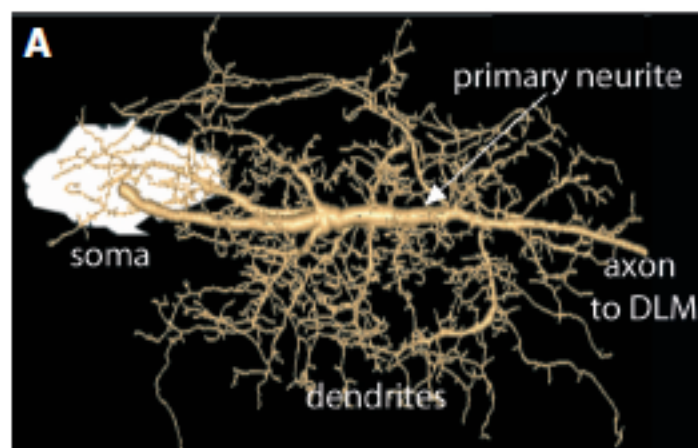


While freely behaving, wing beat can be over 200 Hz

Motoneurones MN1-5 fire at a maximum of 30 Hz



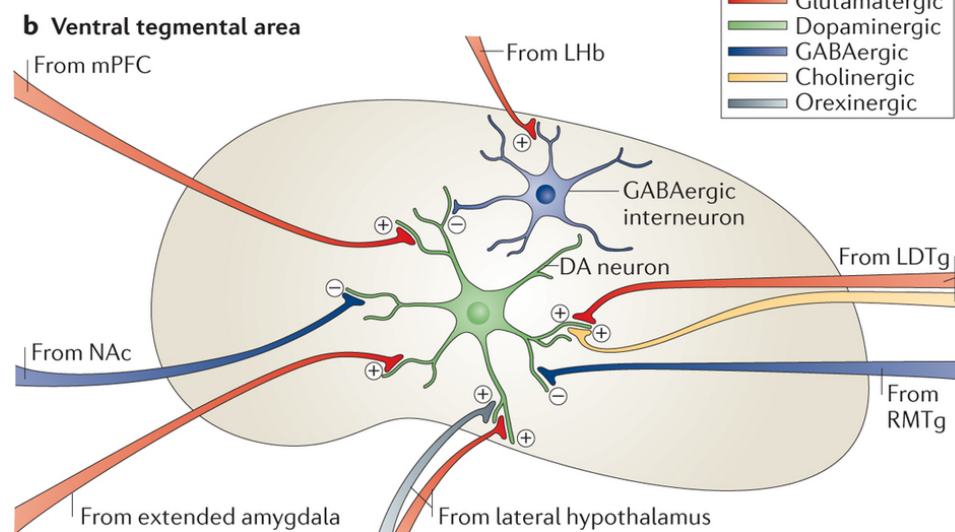
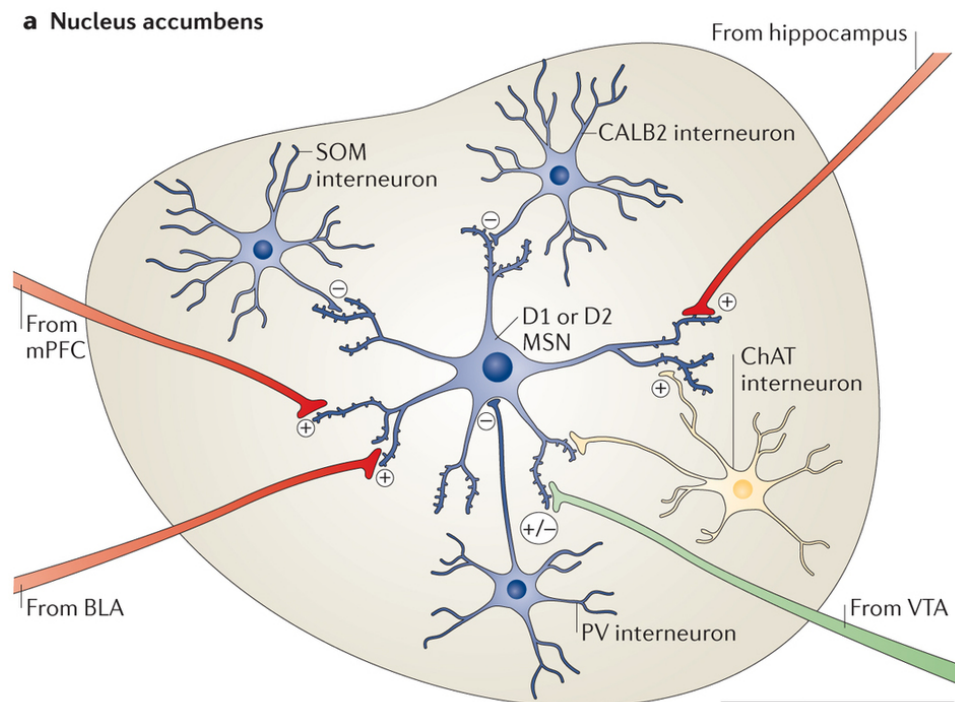
Herrera-Valdez & McKiernan, et al. 2013



The dynamics suggest resonation as a mechanism for excitability.

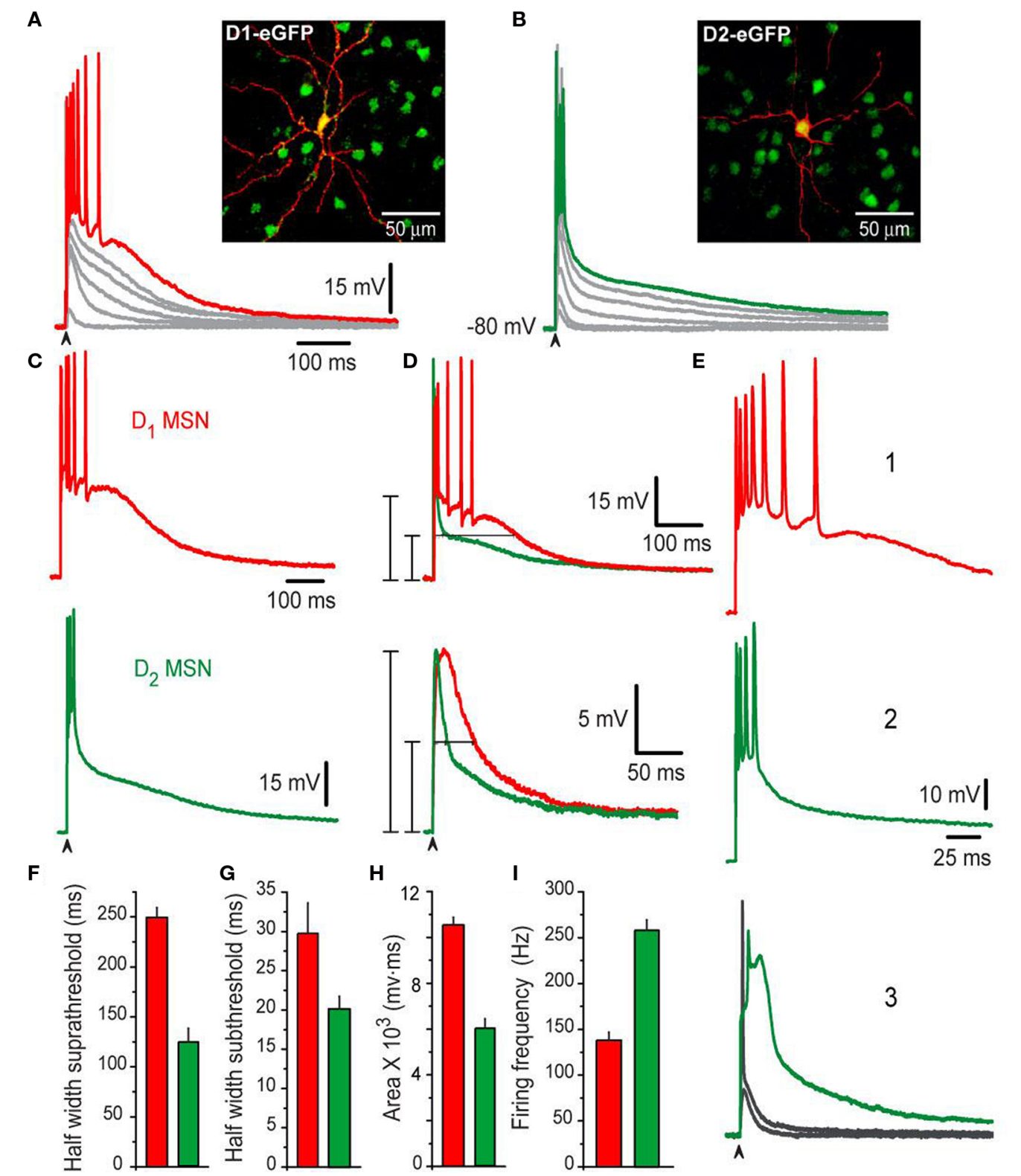
H: Differences in the patterns of ion channel expression. There is no systematic way of testing ...

Medium spiny projection neurons from the striatum display different excitabilities, but not necessarily differences in morphology, connectivity, number of spines, etc



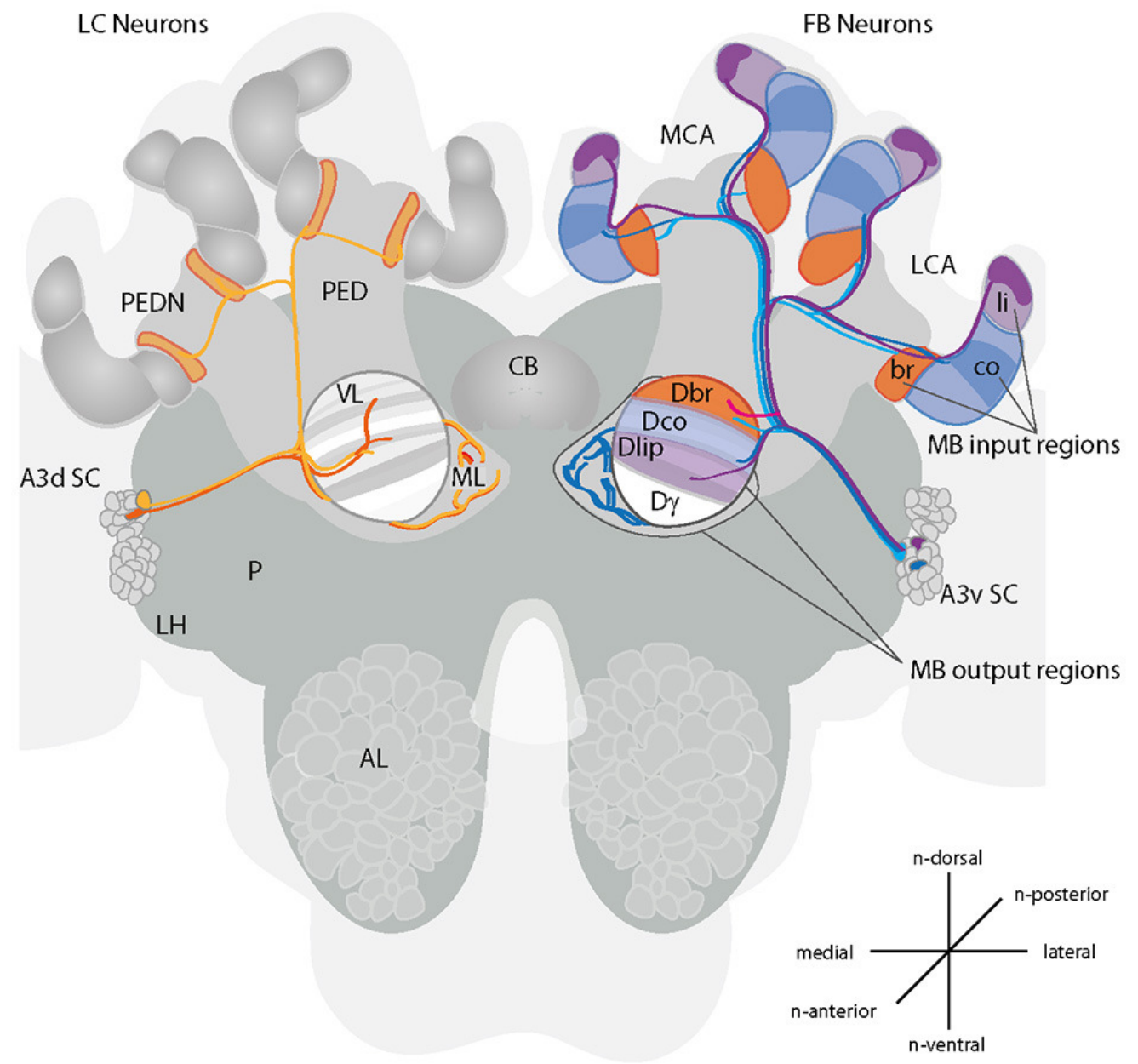
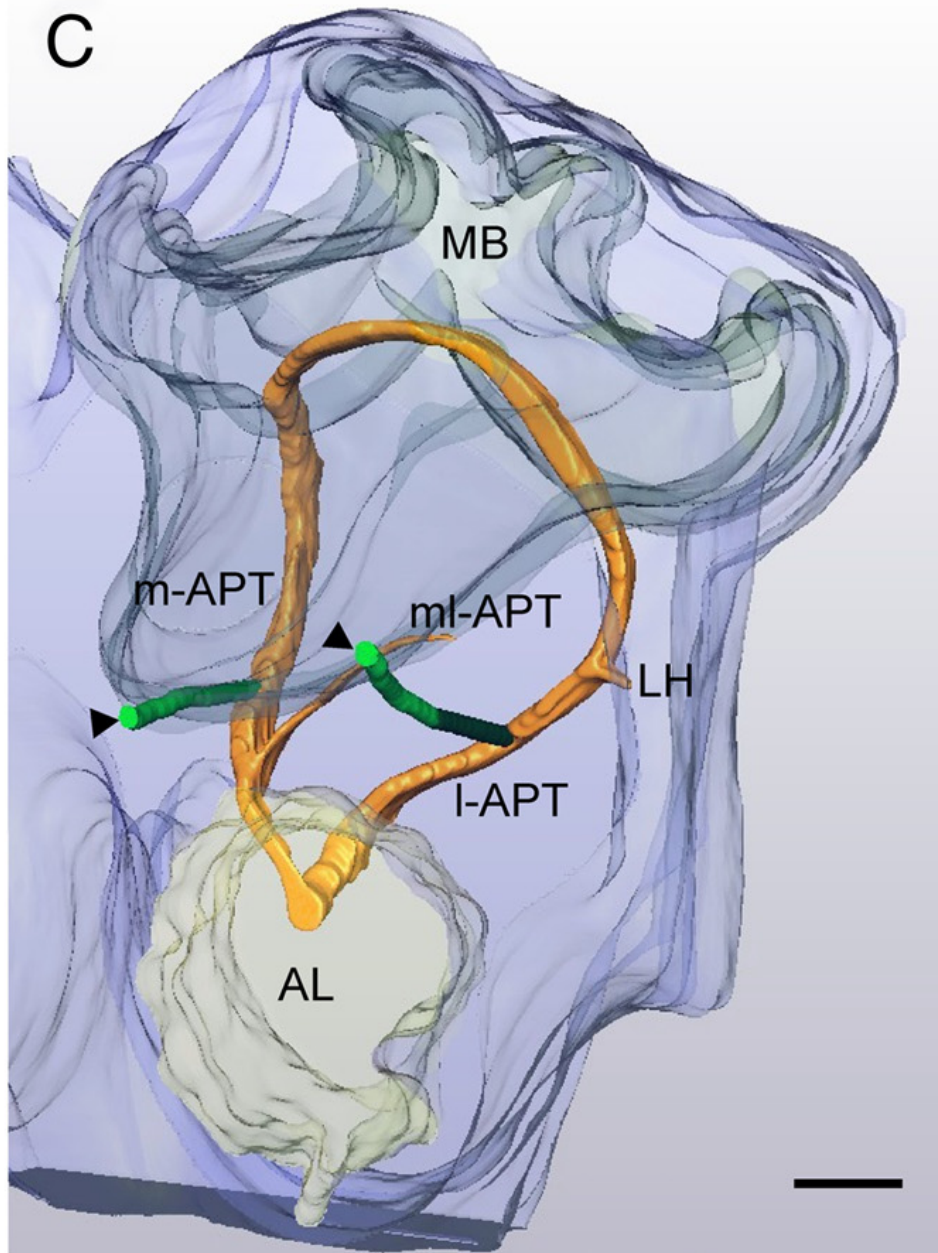
Nature Reviews | Neuroscience

Damodaran, et al. 2014



Flores-Barrera, et al 2015

Olfactory processing in the honey bee



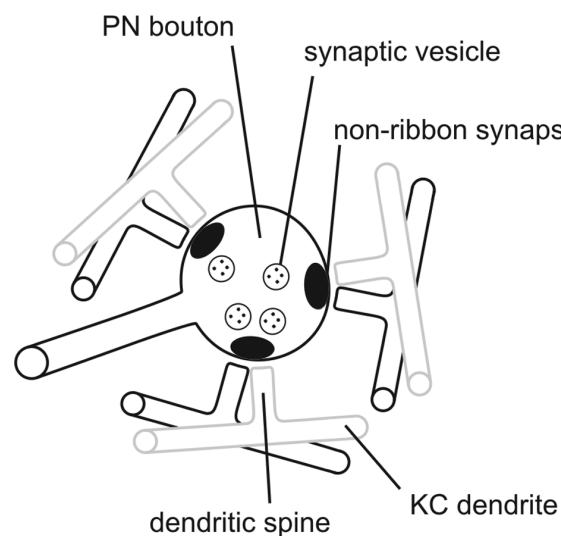
Olfactory processing in the honey bee

**AL layer (PNs from AL):
(many KC spines synaptically
connected with one PN bouton)**



**KC layer (PNs from AL):
(many KC terminals making
synapses with MBONs)**

A



B

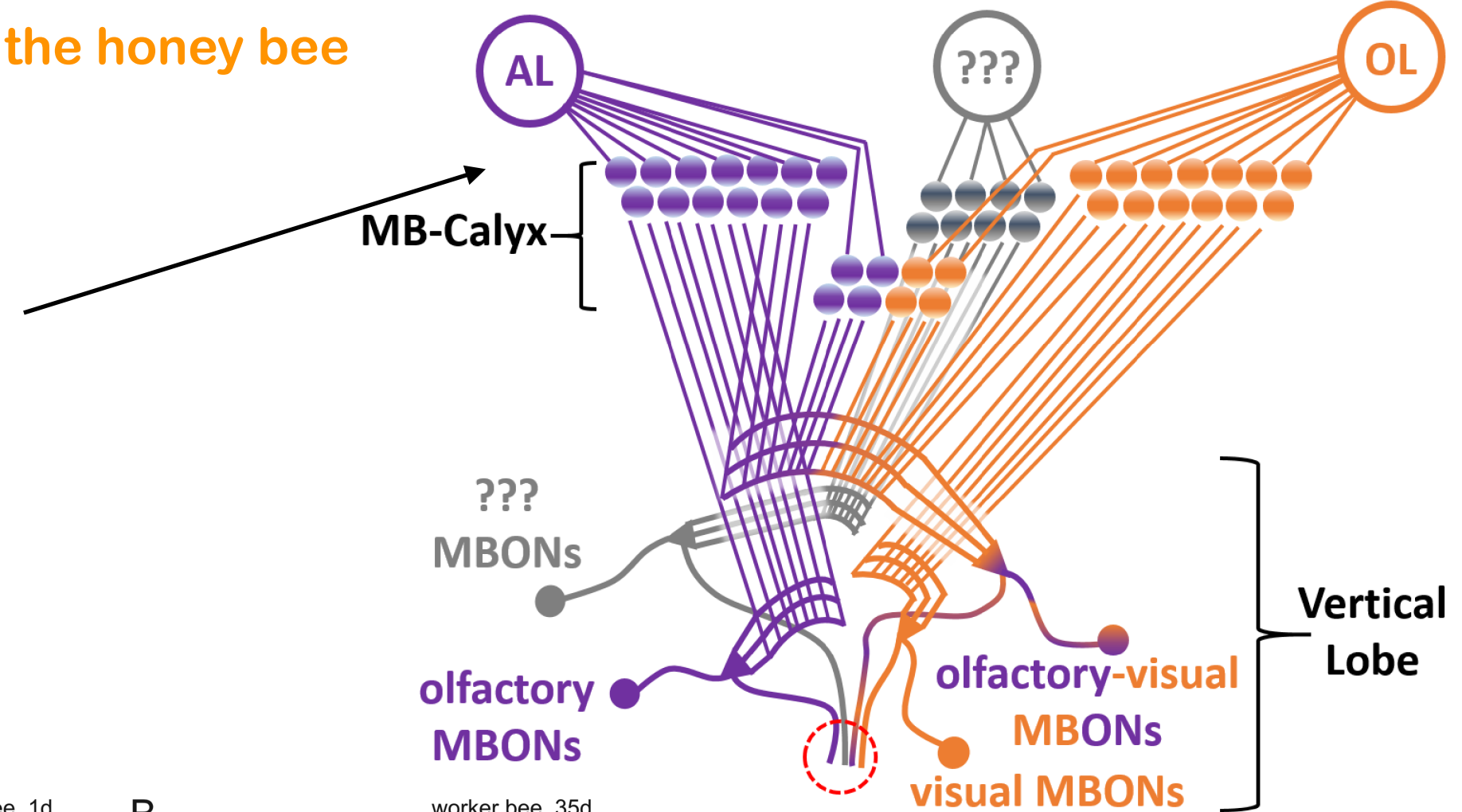
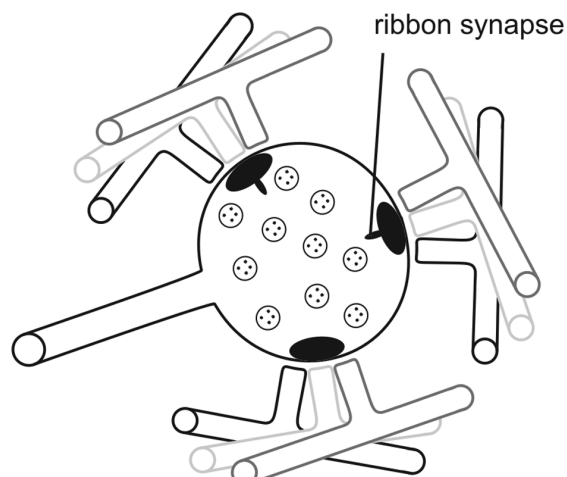


Figure 8. Diagram illustrating age-related synaptic rearrangement of projection neuron (PN) synapses in the calyx. A: In freshly emerged 1-day-old bees, mostly two postsynaptic elements, primarily tiny Kenyon cell dendritic spines, abut a single bouton release site. B: A month later, 35-day-old forager projection neuron boutons are larger and have more synaptic vesicles, more ribbon synapses, and a larger average number of postsynaptic partners. To effect these changes, the Kenyon cell (KC) dendrites undergo increased branching to form a dense network surrounding the bouton, thereby increasing the distance between individual boutons and the total volume of the calyx.

Outline:

Intro. The nervous system is a complex adaptive system.

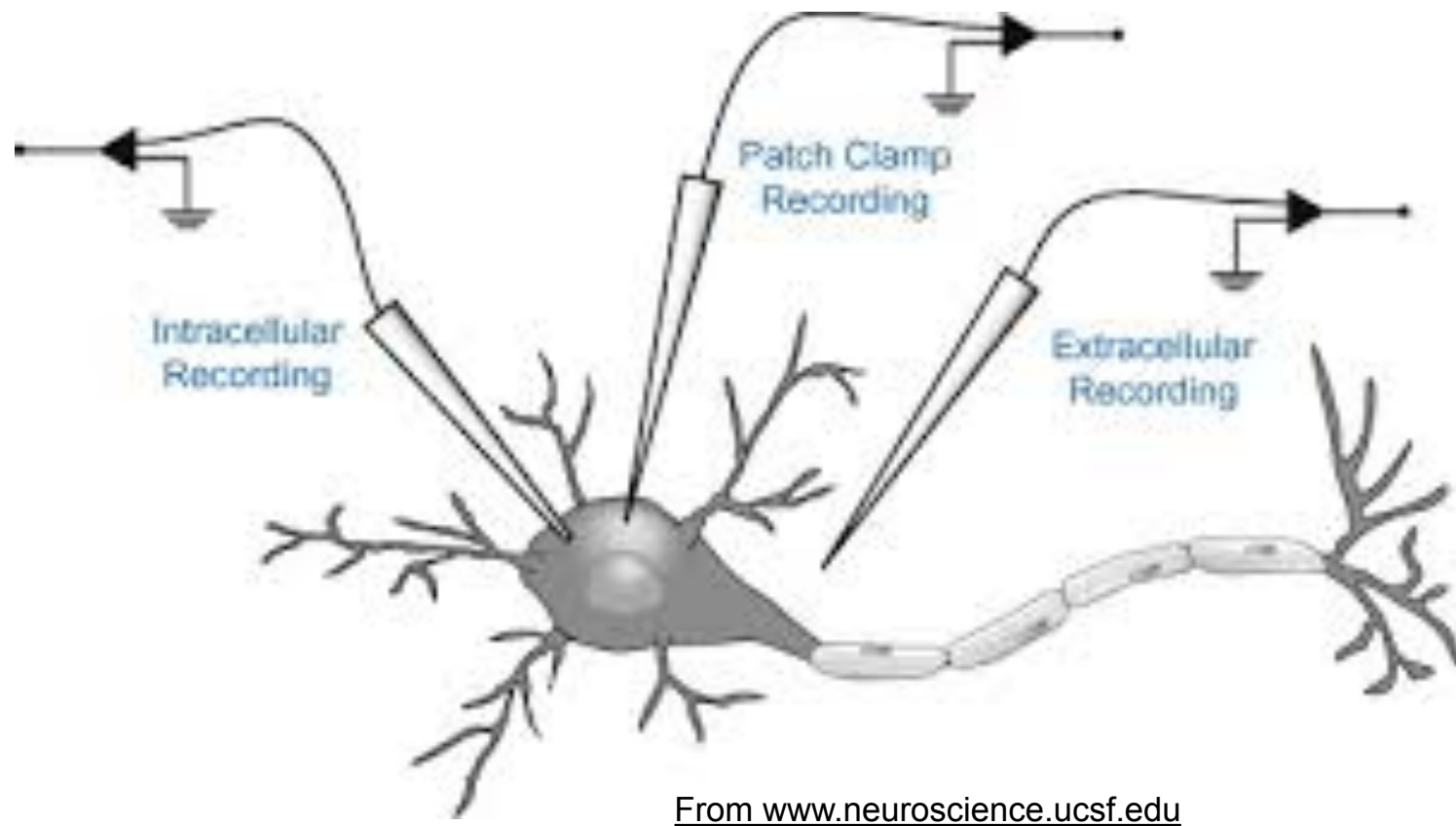
Biophysics of transmembrane transport biophysics and cellular excitability.

A thermodynamic transport model beyond the conductance-based model

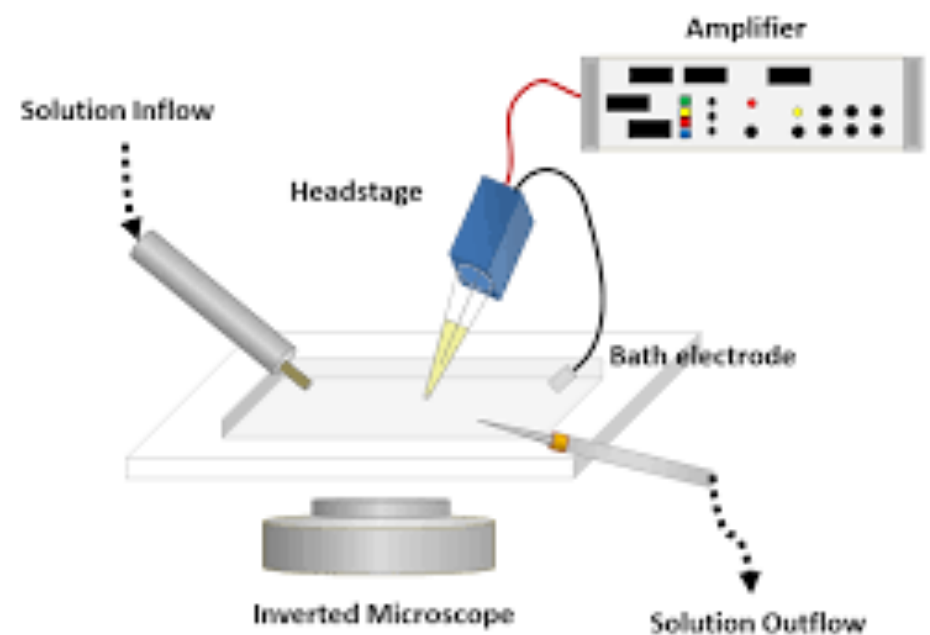
Logistic model of gating dynamics

Cellular excitability in networks: Nearly coincident spiking as a function of common synaptic input

Electrophysiology

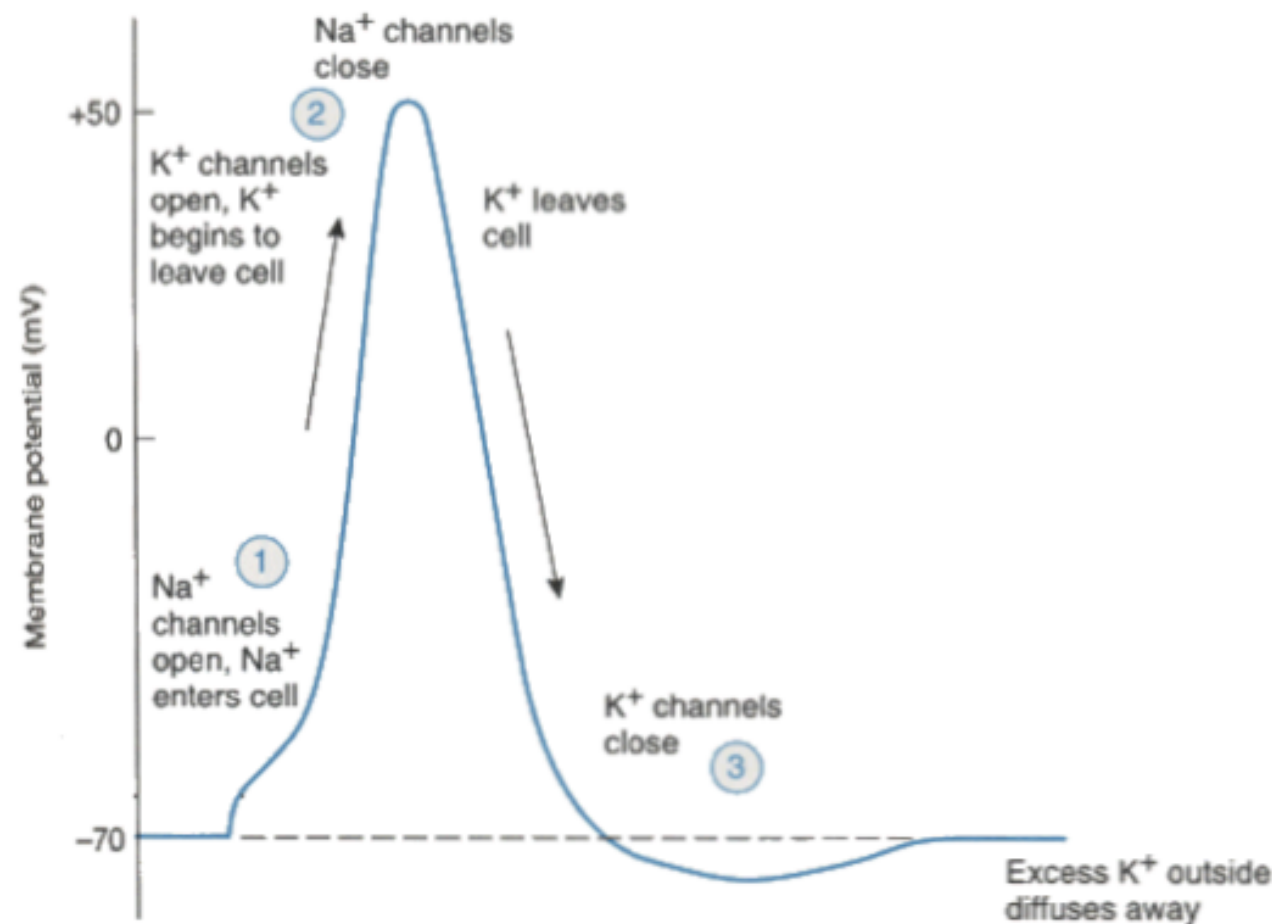


Voltage clamp = injection of current to fix voltage



Mechanism of generation of action potentials: Hodgkin & Huxley, 1952

Cations in (Na, Ca push v up), cations out (K outflow pushes v down)
... in plants this may be a bit different, but the idea is the same



Transmembrane motion (transport) generates currents

Hodgkin & Huxley (1952)
Nobel prize in Physiology and Medicine, 1963

Equivalent circuit formed by a capacitor in parallel with resistors

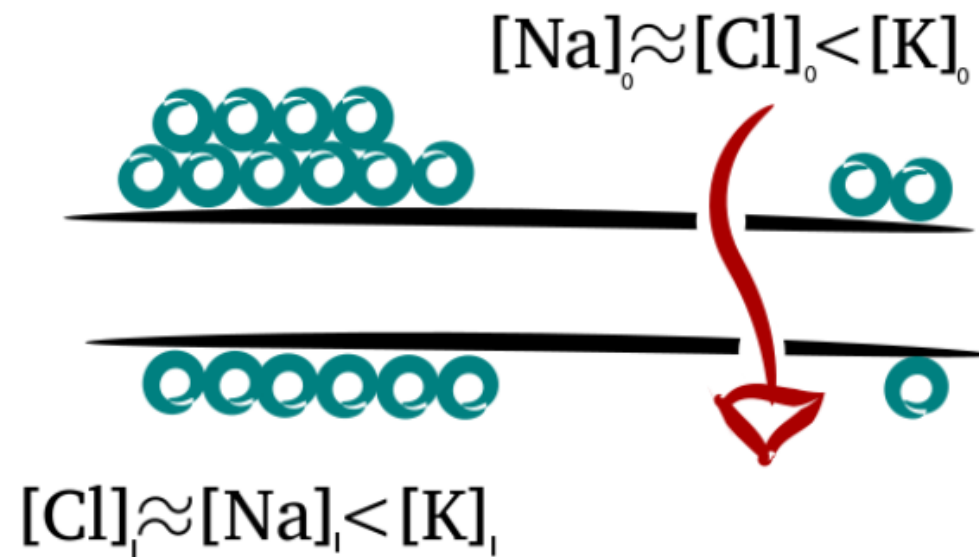


Figure 2: Flujo de iones a través de la membrana

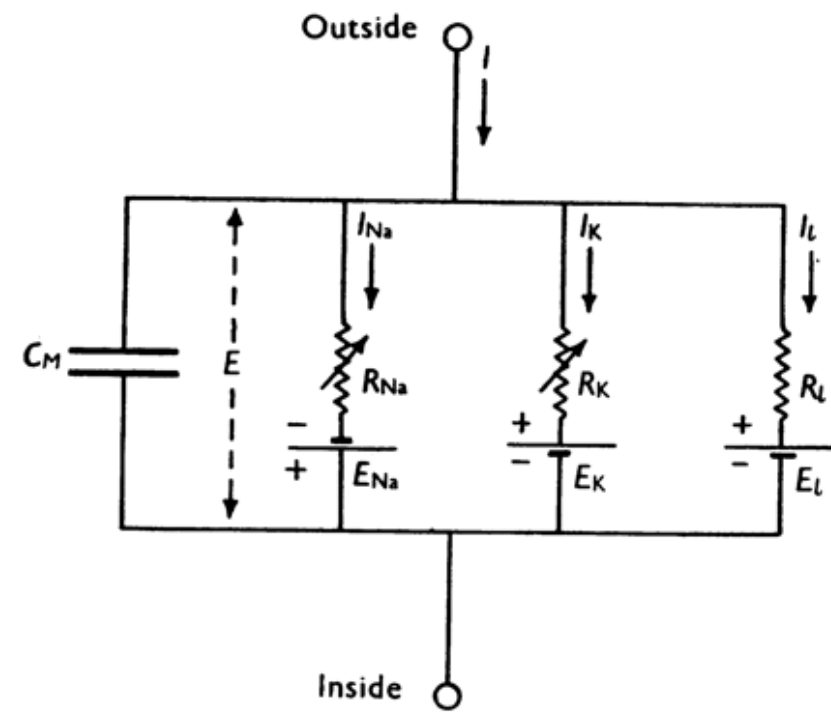


Fig. 1. Electrical circuit representing membrane. $R_{Na} = 1/g_{Na}$; $R_K = 1/g_K$; $R_L = 1/\bar{g}_L$. R_{Na} and R_K vary with time and membrane potential; the other components are constant.

$$0 = C_m \partial_t v + I_T$$

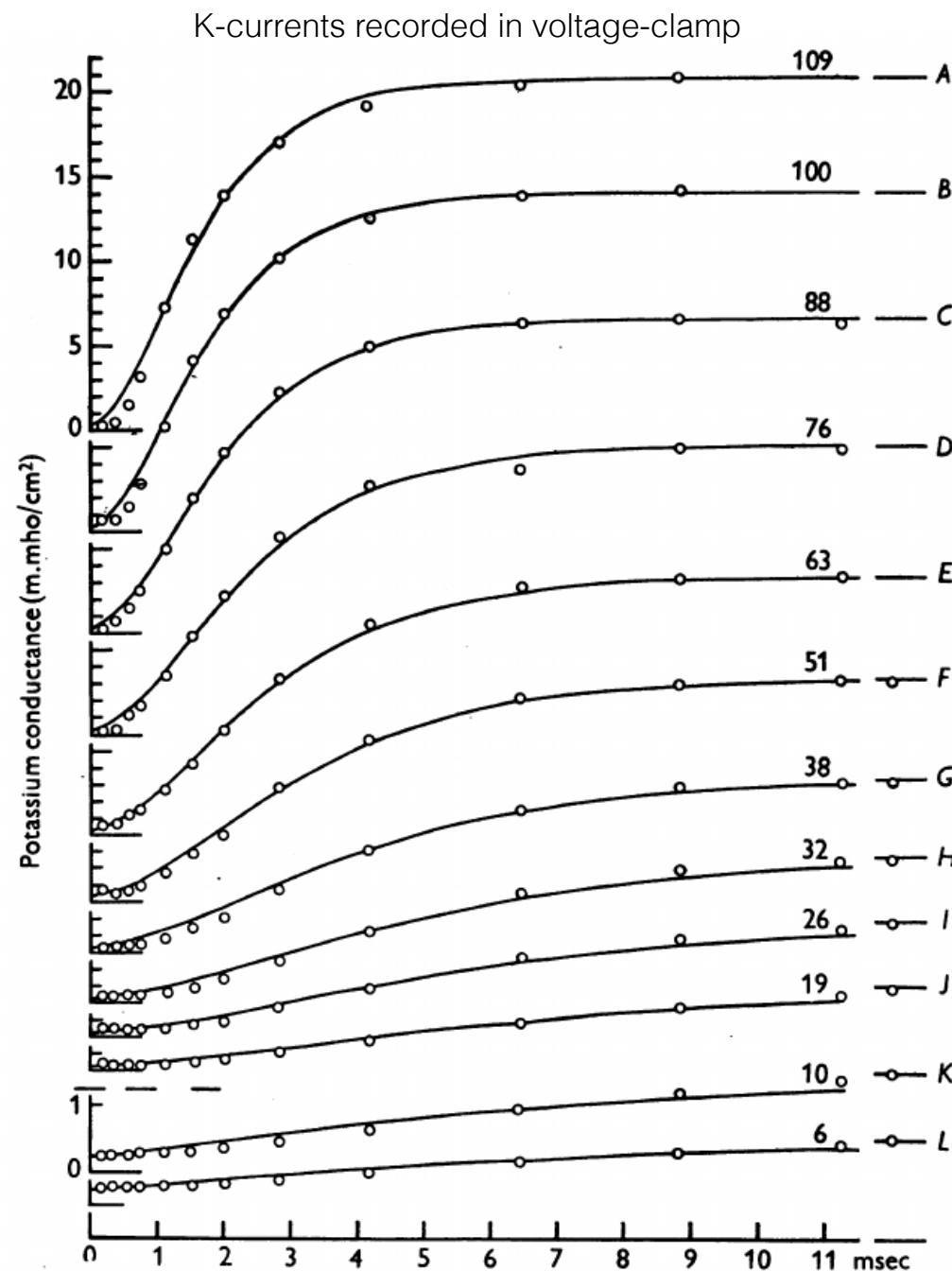
$$I_T = I_{Na} + I_K + I_L$$

$$I_i = g_i(v)(v - v_i), \quad i \in \{Na, K, L\}$$

However, when ions flow across the membrane, they carry their charge along generating a flow of charge electrodiffusively or via pumping mechanisms.

The current carried by ions across the membrane is NOT resistive.

The dynamics of voltage-dependent gating in ion channels are NOT linear



$$\begin{aligned}\partial_t x &= \frac{x_\infty(v) - x}{\tau_x(v)}, \quad x \in \{h, m, n\} \\ &= \alpha(v)(1 - x) - \beta(v)x\end{aligned}$$

$$x(t) = x_\infty(v) - (x_\infty(v) - x_0) \exp(-t/\tau_x(v))$$

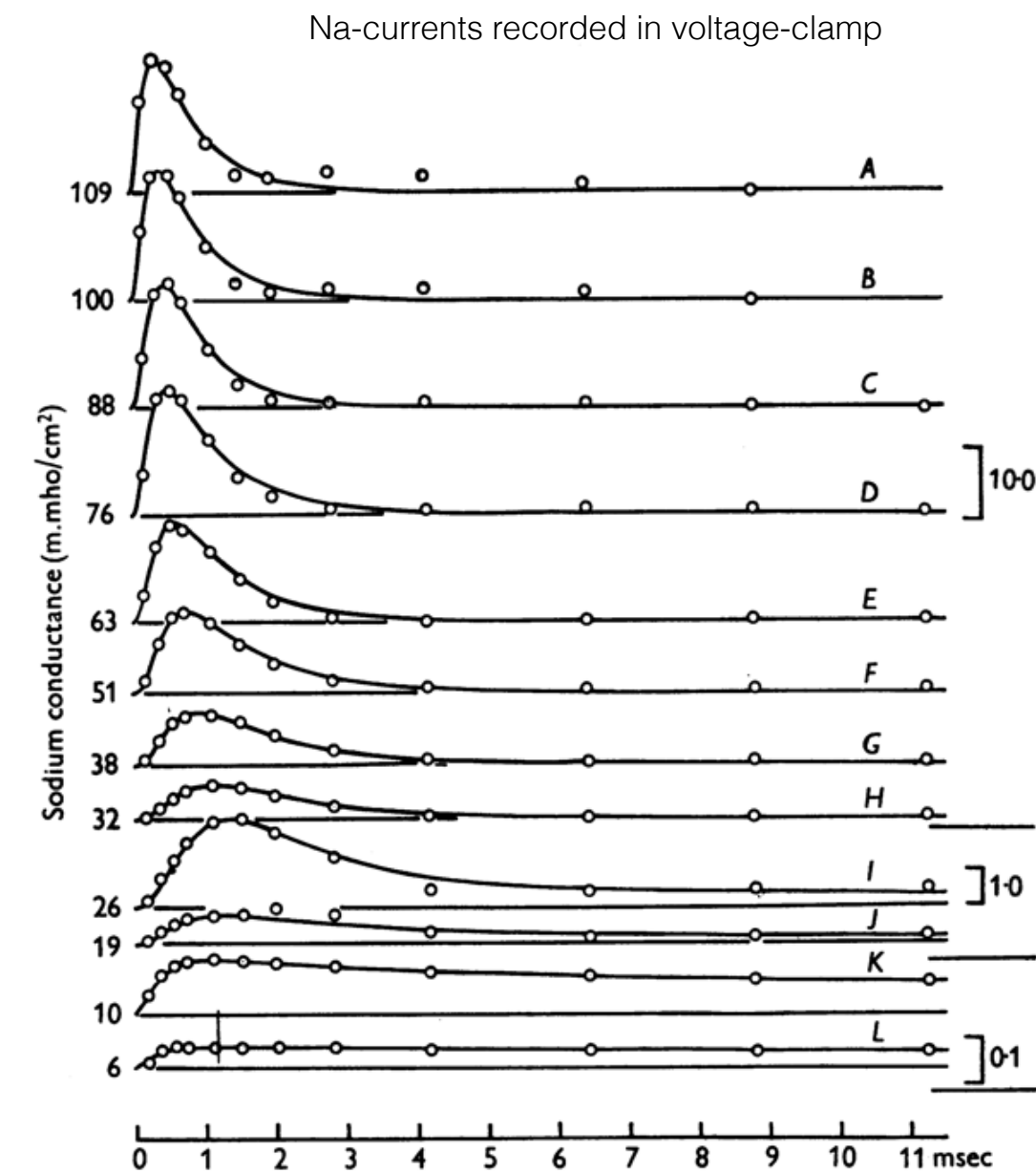


Fig. 6. Changes of sodium conductance associated with different depolarizations. The circles are experimental estimates of sodium conductance obtained on axon 17, temperature 6–7°C (cf. Fig. 3). The smooth curves are theoretical curves with parameters shown in Table 2; A to H drawn from eqn. 19, I to L from 14, 17, 18 with $\bar{g}_{Na} = 70.7 \text{ m.mho/cm}^2$. The ordinate scales on the right are given in m.mho/cm^2 . The numbers on the left show the depolarization in mV. The time scale applies to all curves.

Fits:

$$\begin{aligned}I_{Na} &= \bar{g}_{Na} m h^3 (v - v_{Na}) \\ I_K &= \bar{g}_K n^4 (v - v_K) \\ I_L &= \bar{g}_L (v - v_L)\end{aligned}$$

This model predicts there are about 3x as many sodium channels in comparison to potassium channels

Seminal work: Hodgkin & Huxley, 1952 (Nobel, 1963)

Transmembrane potential: $v = U_{out} - U_{in}$, U electrochemical potential.

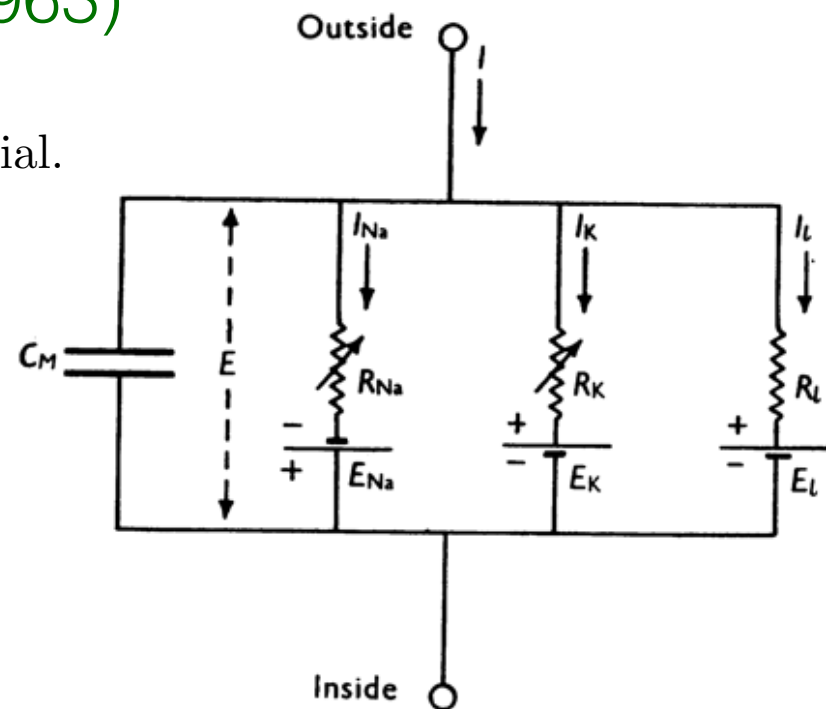
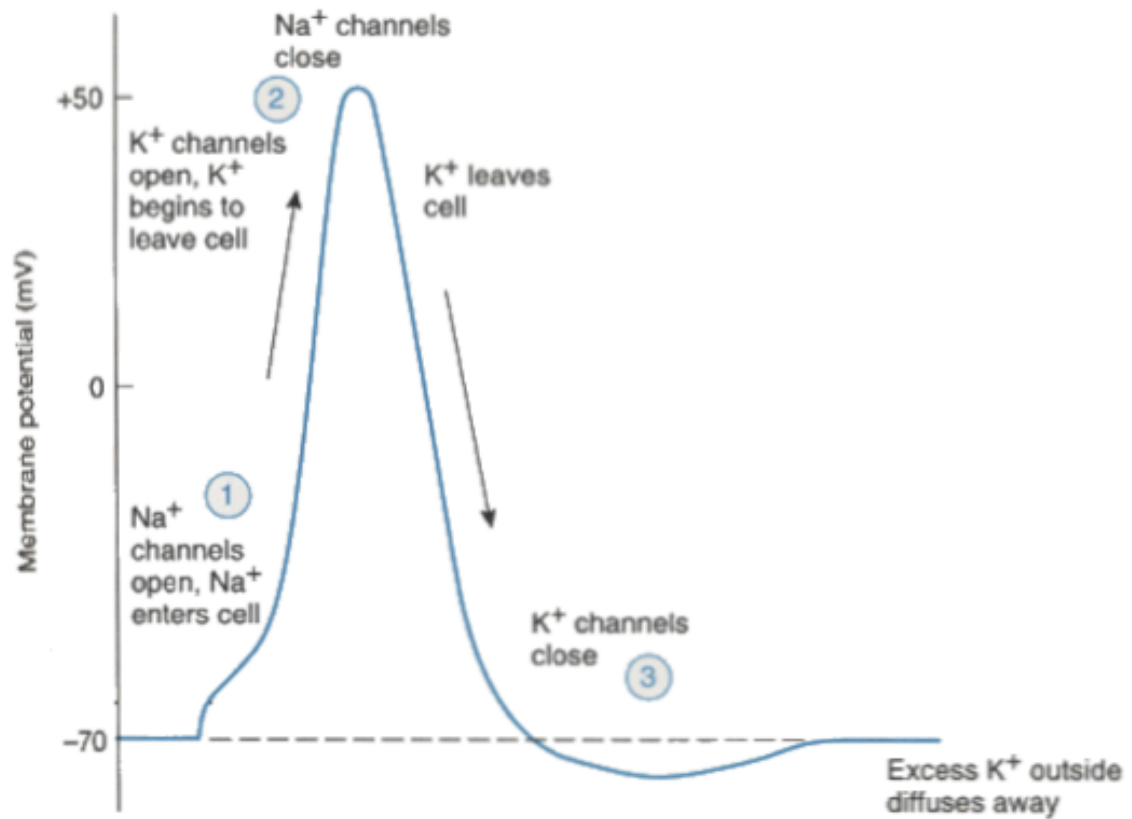
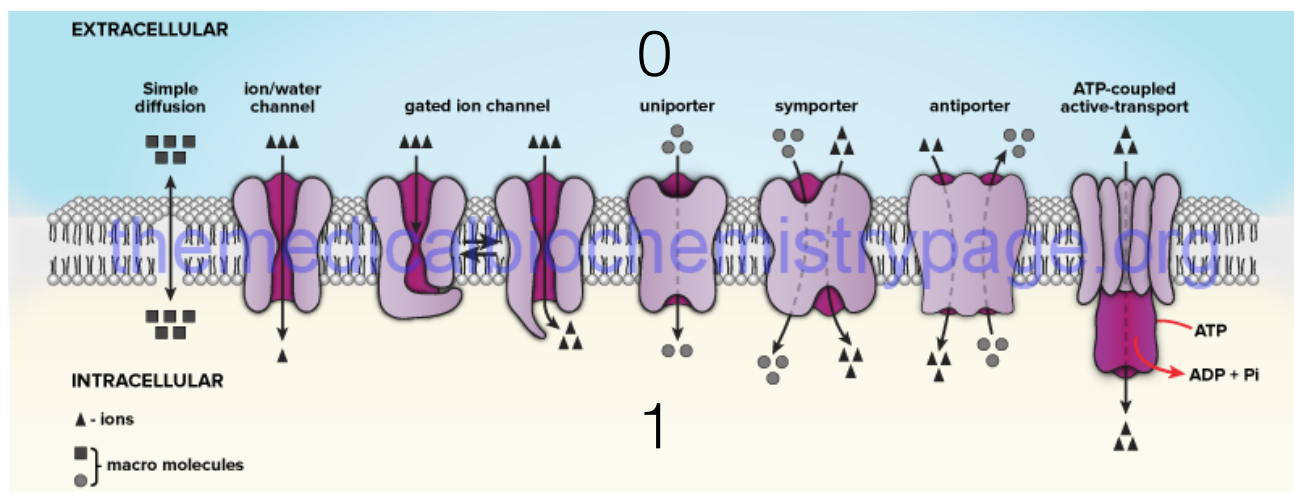


Fig. 1. Electrical circuit representing membrane. $R_{Na} = 1/g_{Na}$; $R_K = 1/g_K$; $R_L = 1/\bar{g}_L$. R_{Na} and R_K vary with time and membrane potential; the other components are constant.

$$0 = C_m \partial_t v + I_T$$

$$I_T = I_{Na} + I_K + I_L$$

$$I_i = g_i(v)(v - v_i), \quad i \in \{Na, K, L\}$$



However, when ions flow across the membrane, they carry their charge along generating a flow of charge electrodifusively or via pumping mechanisms.

The current carried by ions across the membrane is NOT resistive.

Biophysical models of transmembrane currents: cardiophysiology

The work of Rasmusson et al. (1990b) for the bullfrog *sinus venosus* provides a state-of-the-art example of how to obtain a reasonably faithful description of relevant channel dynamics and cellular processes by fitting parameters to experimental data. The resulting model consists of the following 14 ordinary differential equations¹:

$$C_m \frac{dv}{dt} = -I_{Kd} - I_{CaL} - I_{NaK} - I_{NaCa} - I_{NaB} - I_{CaP} - I_{CaB}, \quad (6)$$

$$\frac{da}{dt} = \frac{a_\infty - a}{\tau_a}, \quad a \in \{n, f, d\}, \quad (7)$$

$$\frac{d[x]_c}{dt} = \frac{[x]_b - [x]_c}{\tau_x} + \frac{I_x}{z_x F V_c}, \quad x \in \{\text{Na, K, Ca}\}, \quad (8)$$

$$\frac{d[x]_i}{dt} = -\frac{I_x}{z_x F V_i}, \quad x \in \{\text{Na, K}\}, \quad (9)$$

$$\frac{d[\text{Ca}^{2+}]_i}{dt} = \frac{2I_{NaCa} - I_{CaL} - I_{CaP} - I_{CaB}}{2FV_i} - \frac{1}{Vi} \frac{dO_B}{dt}, \quad (10)$$

$$\frac{dO_C}{dt} = 100[\text{Ca}^{2+}]_i(1 - O_C) - 0.238O_C, \quad (11)$$

¹ Some of the signs were off in Rasmusson et al. (1990b) but have been corrected, in agreement with Rasmusson et al. (1990a).

This model has 15 equations...
Are all the variables needed to model the cardiac dynamics?

$$\frac{dO_{TC}}{dt} = 39[\text{Ca}^{2+}]_i(1 - O_{TC}) - 0.196O_{TC}, \quad (12)$$

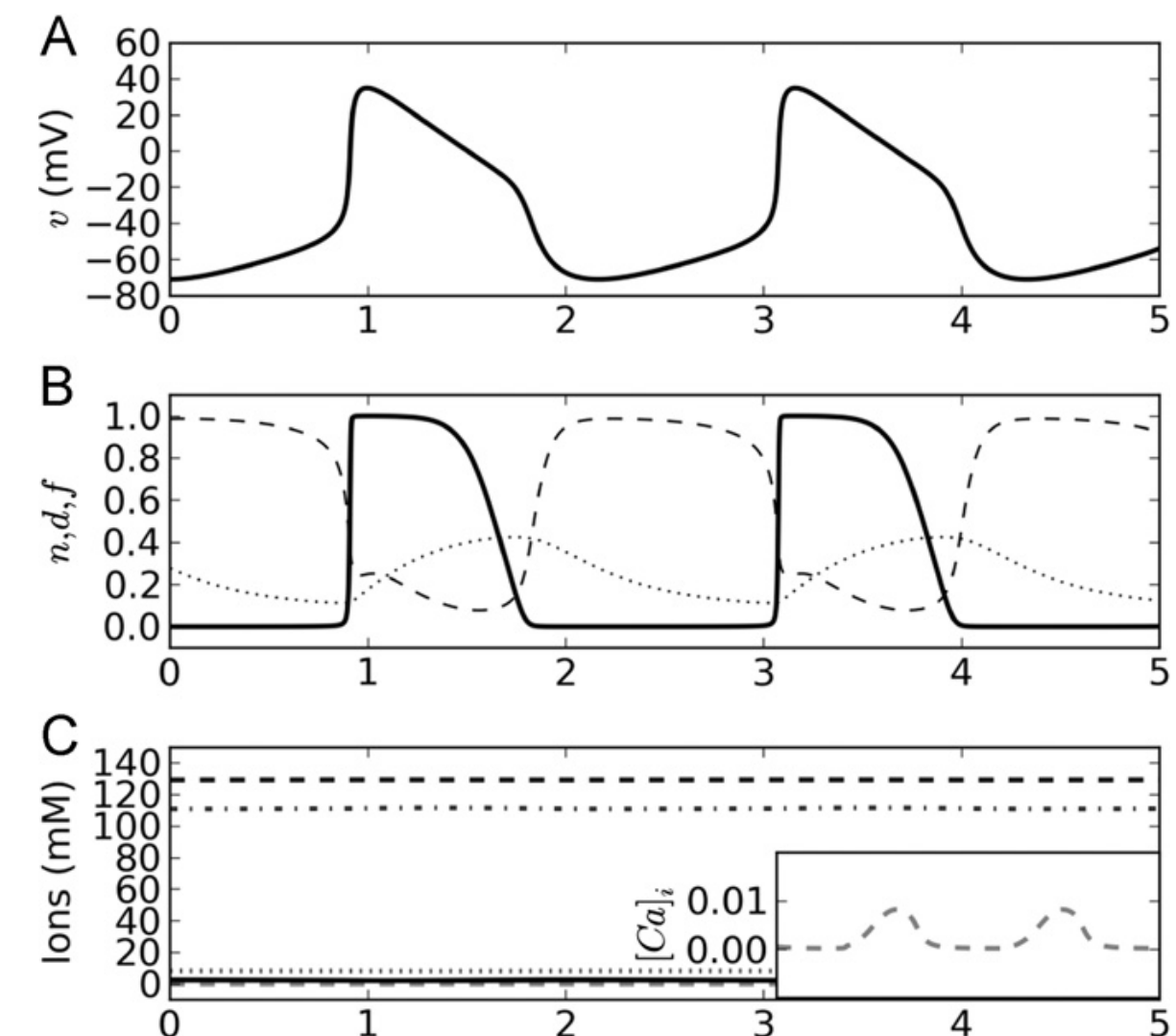
$$\frac{dO_{TMgC}}{dt} = 100[\text{Ca}^{2+}]_i(1 - O_{TMgC} - O_{TMgM}) - 0.0033O_{TMgC}, \quad (13)$$

$$\frac{dO_{TMgM}}{dt} = 0.1[\text{Mg}^{2+}]_i(1 - O_{TMgC} - O_{TMgM}) - 0.333O_{TMgM}, \quad (14)$$

with dO_B/dt in Eq. (10) given by

$$\frac{dO_B}{dt} = 0.000045 \frac{dO_C}{dt} + 0.0000842 \frac{dO_{TC}}{dt} + 0.0001684 \frac{dO_{TMgC}}{dt}. \quad (15)$$

From Rasmusson et al. 1991, Reviewed in Herrera-Valdez & Lega, 2011



The *whole-membrane delayed-rectifier K⁺ current* (I_{Kd}) is written by Rasmusson et al. as

$$I_{Kd} = n^2 \mathfrak{J}_K = n^2 \cdot 0.0115[v - (v_K + v_R)], \quad (16)$$

where v_K is the Nernst potential for K⁺ ions and

$$v_R = 95[1 + \exp(-(v - v_K - 78)/25)]^{-1} \quad (17)$$

is a rectifying term which, as reported by Giles and Shibata (1985), becomes noticeable for v -values larger than or equal to -30 mV. The gating functions, α_n and β_n used by Rasmusson et al. are given by

$$\alpha_n = \frac{0.0000144(v + 26.5)}{1 - \exp(-0.128(v + 26.5))}, \quad (18)$$

$$\beta_n = 0.000286 \exp(-0.0381(v + 26.5)). \quad (19)$$

The *whole-membrane Ca²⁺ current* in Rasmusson et al. (1990b) is written as

$$I_{CaL} = df \mathfrak{J}_{Ca}, \quad (20)$$

where d and f satisfy a differential equation like Eq. (7). The corresponding functions d_∞ , τ_d , f_∞ , and τ_f are given by

$$d_\infty = [1 + \exp(-(v + 10)/6.24)]^{-1}, \quad (21)$$

$$\tau_d = \frac{d_\infty[1 - \exp(-(v + 10)/6.24)]}{0.035(v + 10)}, \quad (22)$$

$$f_\infty = \frac{1}{1 + \exp((v + 35.06)/8.6)} + \frac{0.8}{1 + \exp((50 - v)/20)}, \quad (23)$$

$$\tau_f = [0.0197 \exp(-[0.0337(v + 10)]^2) + 0.02]^{-1}. \quad (24)$$

The expression for \mathfrak{J}_{Ca} given in Rasmusson et al. (1990b) corresponds to the Goldman constant field approximation. It reads

$$\mathfrak{J}_{Ca} = 0.0274v \frac{[\text{Ca}^{2+}]_i \exp(0.078v) - [\text{Ca}^{2+}]_c}{\exp(0.078v) - 1}.$$

Indeed, at 24 °C

$$\frac{z_{Ca}q}{kT} \simeq \frac{2 \times 1.602174 \times 10^{-19} \times 10^{-3}}{1.38065 \times 10^{-23}(273.15 + 24)} \simeq 0.0781,$$

and the expression for \mathfrak{J}_{Ca} can thus be re-written as

$$\mathfrak{J}_{Ca} = g_{Ca} \frac{v \sqrt{[\text{Ca}^{2+}]_i [\text{Ca}^{2+}]_c}}{\sinh(\frac{qz_{Ca}}{2kT} v)} \sinh\left(\frac{qz_{Ca}}{2kT} (v - v_{Ca})\right), \quad (25)$$

The rest of the currents are listed below:

1. Sodium-potassium pump current:

$$I_{NaK} = 0.145 \left(\frac{[\text{K}^+]_c}{[\text{K}^+]_c + 0.621} \right)^2 \left(\frac{[\text{Na}^+]_i}{[\text{Na}^+]_i + 5.46} \right)^3 \frac{v + 150}{v + 200}. \quad (27)$$

2. Sodium background current:

$$I_{NaB} = 0.00015(v - v_{Na}). \quad (28)$$

3. Sodium-calcium exchanger current:

$$I_{NaCa} = 0.000004 \frac{[\text{Na}^+]_i^3 [\text{Ca}^{2+}]_c \exp(0.0195v) - [\text{Na}^+]_c^3 [\text{Ca}^{2+}]_i \exp(-0.0195v)}{1 + 0.0001([\text{Na}^+]_i^3 [\text{Ca}^{2+}]_c + [\text{Na}^+]_c^3 [\text{Ca}^{2+}]_i)}. \quad (29)$$

4. Calcium pump current:

$$I_{CaP} = 0.00675 \frac{[\text{Ca}^{2+}]_i}{[\text{Ca}^{2+}]_i + 0.001}. \quad (30)$$

5. Calcium background current:

$$I_{CaB} = 0.0000003(v - v_{Ca}). \quad (31)$$

Why are all these functional forms for the currents so different?

Logistic activation and gating

Alternative approach: The dynamics of the family

$$\left\{ \partial_t u = u^k (F_u - u) C_u, \quad k = 0, 1, \dots \right\}, \quad (1)$$

include sigmoidal behaviours when $k > 0$ (Herrera-Valdez, 2014). Voltage-dependent gating with steady state F and rate C can be written explicitly as

$$F_u(v) = \frac{\exp\left(g_u \frac{v-v_u}{v_T}\right)}{1 + \exp\left(g_u \frac{v-v_u}{v_T}\right)}, \quad C_u(v) = r_u \left[\exp\left(s_u g_u \frac{v-v_u}{v_T}\right) + \exp\left(g_u(s_u - 1) \frac{v-v_u}{v_T}\right) \right]$$

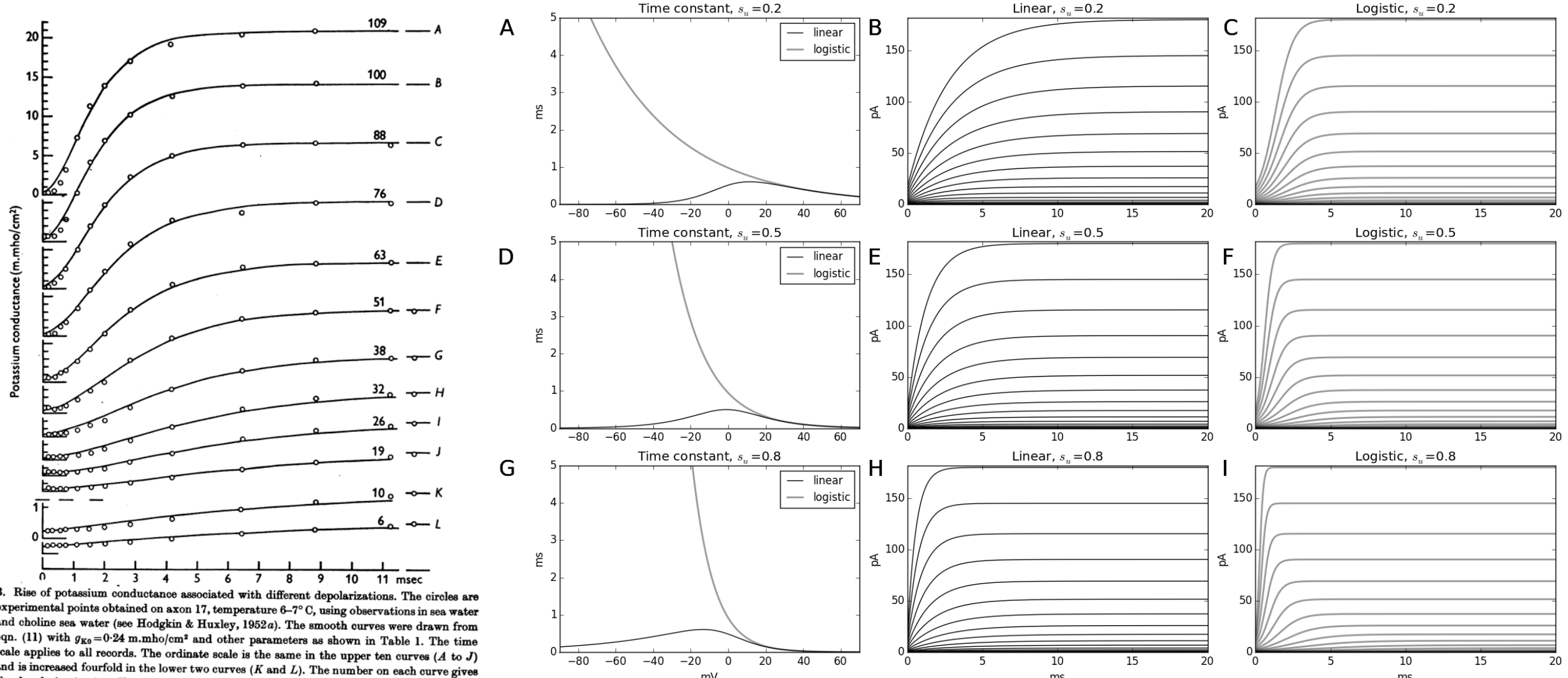


Fig. 3. Rise of potassium conductance associated with different depolarizations. The circles are experimental points obtained on axon 17, temperature 6–7°C, using observations in sea water and choline sea water (see Hodgkin & Huxley, 1952a). The smooth curves were drawn from eqn. (11) with $g_{K0} = 0.24 \text{ m.mho/cm}^2$ and other parameters as shown in Table 1. The time scale applies to all records. The ordinate scale is the same in the upper ten curves (A to J) and is increased fourfold in the lower two curves (K and L). The number on each curve gives the depolarization in mV.

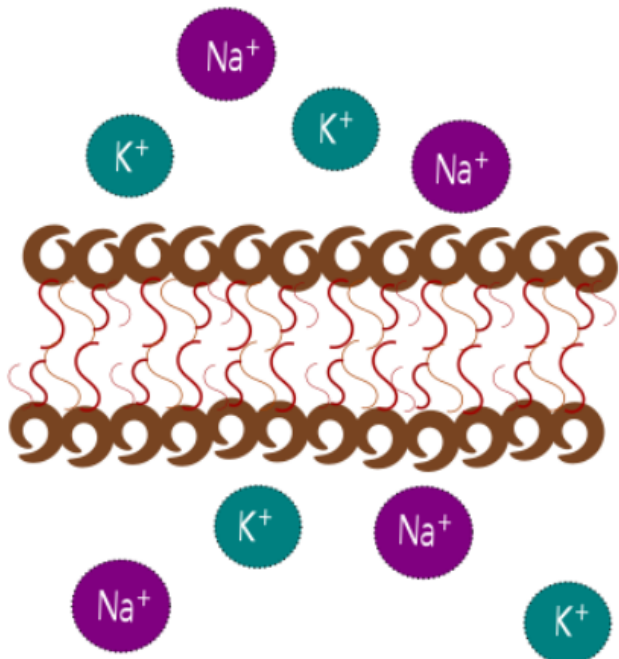
What is the membrane capacitance? ... really



Is there a way to derive an equation that does not depend on such gross analogies?

Membrane potential

$$v = U_i - U_e \quad (1)$$



Assumptions:

1. Charge accumulates around the membrane as a function of the membrane potential

$$Q_{memb} = f(v)$$

2. Total charge around and across the membrane is constant

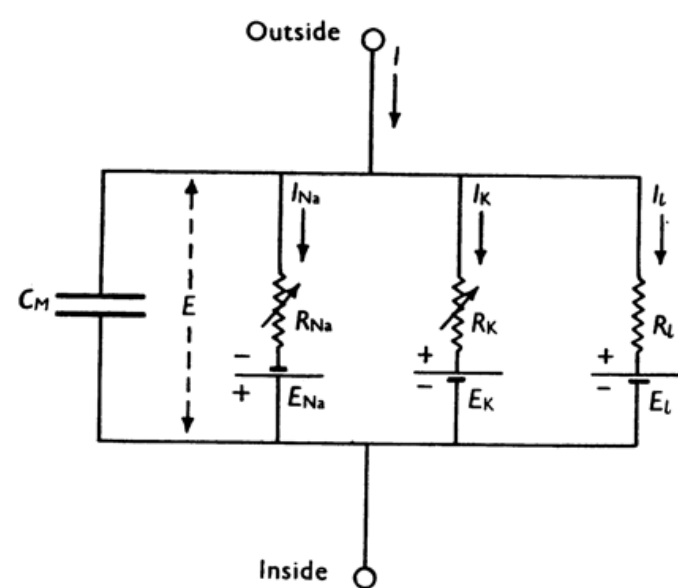
$$\text{const} = Q_{total} = Q_{around} + Q_T$$

Change with respect to time:

$$0 = \partial_t Q_{total} = \partial_t Q_{around} + \partial_t Q_T \quad (2)$$

$$= (\partial_v f)(\partial_t v) + I_T \quad (3)$$

$$(4)$$



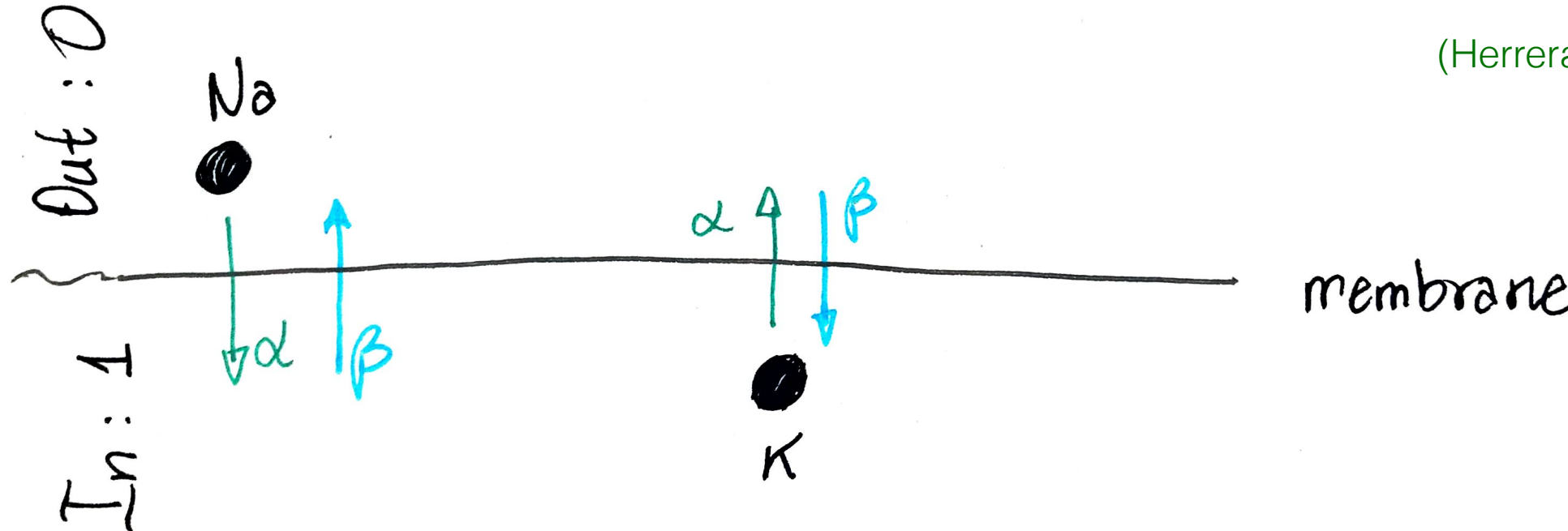
$$0 = C_m \partial_t v + I_{transm}$$

Fig. 1. Electrical circuit representing membrane. $R_{Na} = 1/g_{Na}$; $R_K = 1/g_K$; $R_L = 1/\bar{g}_L$. R_{Na} and R_K vary with time and membrane potential; the other components are constant.

General formula for transmembrane transport

Flux from transmembrane transport: macroscopic perspective

(Herrera-Valdez, 2014)



Forward transport (departure \rightarrow arrival), and backward (arrival \rightarrow departure).
(Principle of detailed balance, Onsager, 1931)

$$\frac{\alpha}{\beta} = \exp\left(-\frac{\Delta G}{kT}\right)$$

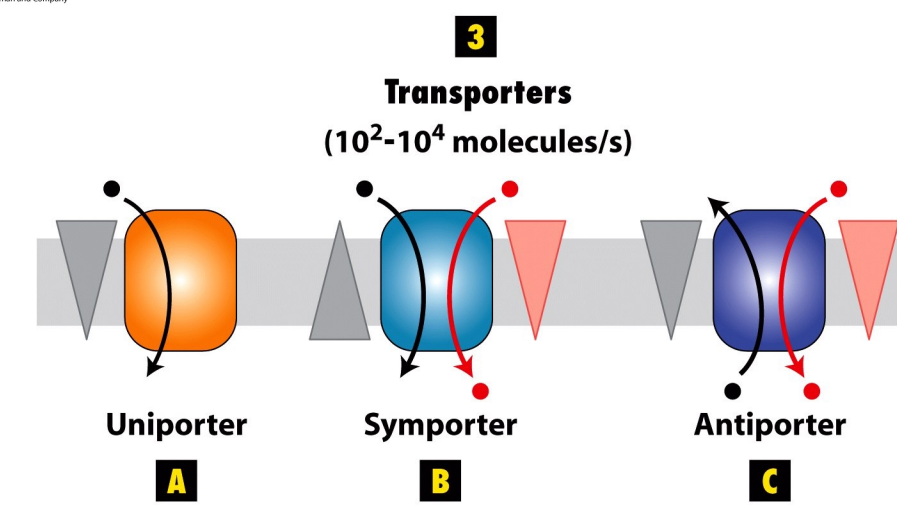
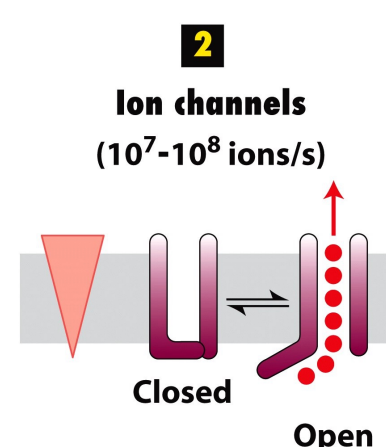
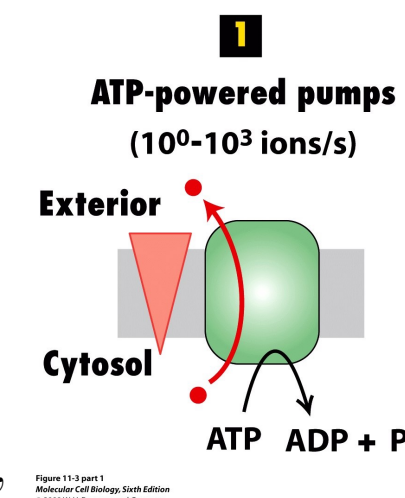
Separation in rates

$$\alpha = r \exp\left(-b \frac{\Delta G}{kT}\right), \quad \beta = r \exp\left((1-b) \frac{\Delta G}{kT}\right),$$

Net flux relative to the departure

$$\alpha - \beta = r \left[\exp\left(-b \frac{\Delta G}{kT}\right) - \exp\left((1-b) \frac{\Delta G}{kT}\right) \right]$$

r in units of molecules/ ($\mu\text{m}^2 \text{ ms}$)



For ions

$$\Delta G_s = qz_s n_s (c_s - d_s) (v_s - v),$$

Example: K⁺ ions moving from inside to outside in physiological conditions

$$[K]_1 > [K]_0$$

$$\Delta G_s = n_s (d_s - c_s) (v_s - v)$$

$$n = 1; c_K = 1; d_K = 0$$

$$v_K \approx -89 < v \approx -60 >$$

$$\Delta G_K = 1(1)(v_K - v) < 0$$

So movement of potassium from inside to outside (but not the other way around $\Delta G_K > 0$) is thermodynamically favorable in physiological conditions

Energy for the transmembrane transport of molecules

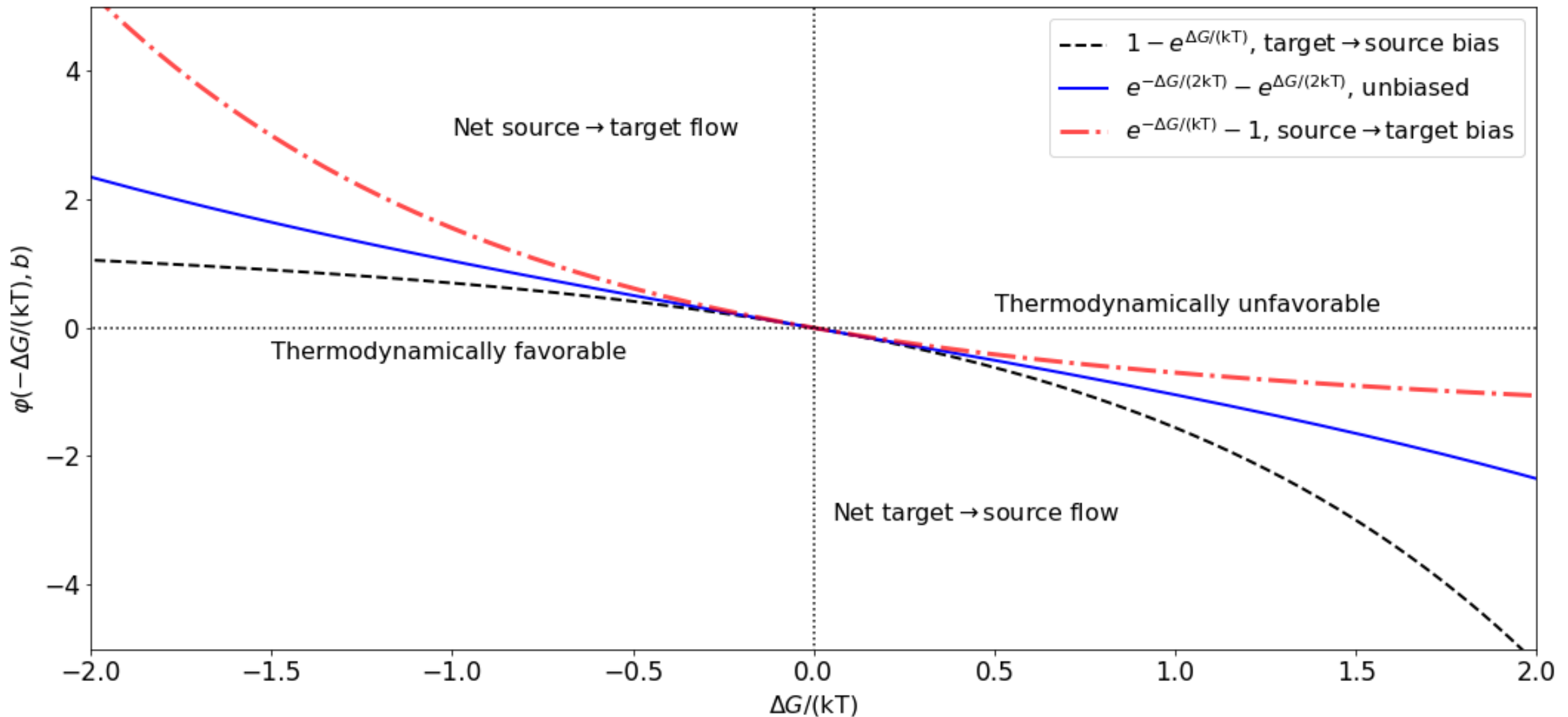
$$\Delta G_s = n_s (c_s - d_s) \left[kT \ln \left(\frac{[s]_0}{[s]_1} \right) - qz_s v \right],$$

For ions

$$\Delta G_s = qz_s n_s (c_s - d_s) (v_s - v),$$

For non-charged molecules

$$\Delta G_s = n_s (c_s - d_s) kT \ln \left(\frac{[s]_0}{[s]_1} \right)$$



Flux and current

Substitution of the formulas for ΔG from equations (4) (5) into equation (10), the flux rate resulting from simultaneously transporting molecules in S across the membrane can be written explicitly

$$\Phi = r \left[\prod_{s \in S} \left(\frac{[s]_0}{[s]_1} \right)^{bn_s(d_s - c_s)} \exp \left(b \frac{\eta v - \delta_{\text{Extra}} v_{\text{Extra}}}{v_T} \right) - \prod_{s \in S} \left(\frac{[s]_0}{[s]_1} \right)^{(b-1)n_s(d_s - c_s)} \exp \left((b-1) \frac{\eta v - \delta_{\text{Extra}} v_{\text{Extra}}}{v_T} \right) \right], \quad (11)$$

where $v_T = kT/q$ and

$$\eta = \sum_{s \in S} n_s (c_s - d_s) z_s \quad (12)$$

represents the net number of charges moved across the membrane.

If the transport is electrogenic, then the product $q\eta$ (in Coulombs) represents the net charge moved across the membrane, relative to the extracellular compartment. Non electrogenic transport yields $\eta = 0$, which means the flow does not depend on the transmembrane potential, and

$$\Phi = r \left[\prod_{s \in S} \left(\frac{[s]_0}{[s]_1} \right)^{bn_s(d_s - c_s)} \exp \left(-b \frac{\delta_{\text{Extra}} v_{\text{Extra}}}{v_T} \right) - \prod_{s \in S} \left(\frac{[s]_0}{[s]_1} \right)^{(b-1)n_s(d_s - c_s)} \exp \left((1-b) \frac{\delta_{\text{Extra}} v_{\text{Extra}}}{v_T} \right) \right]. \quad (13)$$

If only ions are involved in the transport, the flux simplifies to

$$\Phi = r \left\{ \exp \left[b \left(\frac{\eta v - v_o}{v_T} \right) \right] - \exp \left[(b-1) \left(\frac{\eta v - v_o}{v_T} \right) \right] \right\}, \quad (14)$$

where

$$v_o = \delta_{\text{Ext}} v_{\text{Ext}} + \sum_{s \in S} n_s z_s (c_s - d_s) v_s. \quad (15)$$

Flux associated to transmembrane transport for a change in free energy ΔG

$$\varphi = \alpha - \beta = r \left[\exp \left((s-1) \frac{\Delta G}{kT} \right) - \exp \left(s \frac{\Delta G}{kT} \right) \right].$$

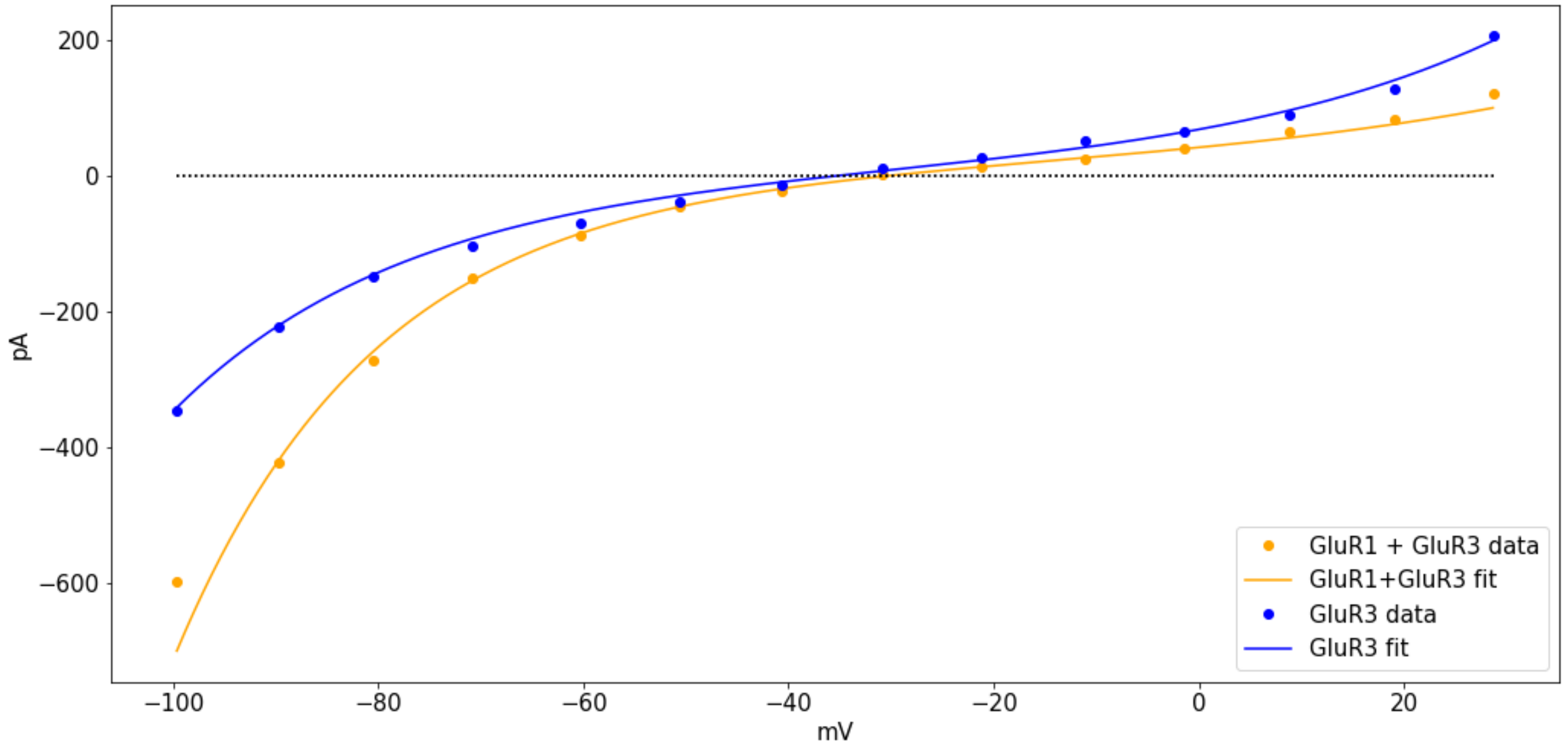
Table 1: Energy required for transmembrane transport mediated by different translocators or channels. The source and target compartments for each ion i are represented by c_i and d_i respectively. The direction of motion of the transport for each ion is indicated by $c_i - d_i$. The reversal potentials are noted in those cases where transport is electrogenic.

Pump or channel	Ion (i)	n_i	c_i	d_i	$c_i - d_i$	$\Delta G_i = n_i z_i q_e (v_i - v)(c_i - d_i)$	η	v_R	$\alpha/\beta = \exp \left(-\frac{\Delta G}{kT} \right) = \exp \left(\frac{\sigma v - v_r}{v_T} \right)$
K ⁺ channel	K ⁺	1	1	0	1	$\Delta G_K = q_e(v_K - v)$	1	v_K	$\exp \left(\frac{v - v_K}{v_T} \right) = \left(\frac{[K]_1}{[K]_0} \right) \exp \left(\frac{v}{v_T} \right)$
Na ⁺ channel	Na ⁺	1	0	1	-1	$\Delta G_{Na} = -q_e(v_{Na} - v)$	-1	$-v_{Na}$	$\exp \left(\frac{v_{Na} - v}{v_T} \right) = \left(\frac{[Na]_0}{[Na]_1} \right) \exp \left(-\frac{v}{v_T} \right)$
Ca ²⁺ channel	Ca ²⁺	1	0	1	-1	$\Delta G_{Ca} = -2q_e(v_{Ca} - v)$	-2	$-2v_{Ca}$	$\exp \left(2 \frac{v_{Ca} - v}{v_T} \right) = \left(\frac{[Ca]_0}{[Ca]_1} \right) \exp \left(-2 \frac{v}{v_T} \right)$
Cl ⁻ channel	Cl ⁻	1	0	1	-1	$\Delta G_{Cl} = q_e(v_{Cl} - v)$	1	v_{Cl}	$\exp \left(\frac{v - v_{Cl}}{v_T} \right) = \left(\frac{[Cl]_1}{[Cl]_0} \right) \exp \left(\frac{v}{v_T} \right)$
Ca ²⁺ ATPase	Ca ²⁺	1	1	0	1	$\Delta G_{Ca} = 2q_e(v_{Ca} - v)$	2	$2v_{Ca} + v_{ATP}$	$\exp \left(\frac{2v - 2v_{Ca} - v_{ATP}}{v_T} \right) = \left(\frac{[Ca]_1}{[Ca]_0} \right) \exp \left(\frac{2v - v_{ATP}}{v_T} \right)$
Na ⁺ -K ⁺ ATPase	Na ⁺	3	1	0	1	$\Delta G_{Na} = 3q_e(v_{Na} - v)$	1	$3v_{Na} - 2v_K + v_{ATP}$	$\exp \left(\frac{v - 3v_{Na} + 2v_K - v_{ATP}}{v_T} \right) = \left(\frac{[Na]_1}{[Na]_0} \right)^3 \left(\frac{[K]_0}{[K]_1} \right)^2 \exp \left(\frac{v - v_{ATP}}{v_T} \right)$
	K ⁺	2	0	1	-1	$\Delta G_K = -2q_e(v_K - v)$			
Na ⁺ -Ca ²⁺ exchanger	Na ⁺	3	0	1	-1	$\Delta G_{Na} = -3q_e(v_{Na} - v)$	-1	$-3v_{Na} + 2v_{Ca}$	$\exp \left(\frac{v - 2v_{Ca} + 3v_{Na}}{v_T} \right) = \left(\frac{[Na]_0}{[Na]_1} \right)^3 \left(\frac{[Ca]_1}{[Ca]_0} \right) \exp \left(\frac{v}{v_T} \right)$
	Ca ²⁺	1	1	0	1	$\Delta G_{Ca} = 2q_e(v_{Ca} - v)$			
Na ⁺ -H ⁺ exchanger	Na ⁺	1	0	1	-1	$\Delta G_{Na} = -q_e(v_{Na} - v)$	0	$v_H - v_{Na}$	$\exp \left(\frac{v_{Na} - v_H}{v_T} \right) = \left(\frac{[Na]_0}{[Na]_1} \right) \left(\frac{[H]_1}{[H]_0} \right)$
	H ⁺	1	1	0	1	$\Delta G_H = q_e(v_H - v)$			
K ⁺ -Cl ⁻ symporter	K ⁺	1	1	0	1	$\Delta G_K = q_e(v_K - v)$	0	$v_K - v_{Cl}$	$\exp \left(\frac{v_{Cl} - v_K}{v_T} \right) = \left(\frac{[Cl]_1}{[Cl]_0} \right) \left(\frac{[K]_1}{[K]_0} \right)$
	Cl ⁻	1	1	0	1	$\Delta G_{Cl} = -q_e(v_{Cl} - v)$			
Na ⁺ -K ⁺ -Cl ⁻ symporter	Na ⁺	1	0	1	-1	$\Delta G_{Na} = -q_e(v_{Na} - v)$			
	K ⁺	1	0	1	-1	$\Delta G_K = -q_e(v_K - v)$	0	$2v_{Cl} - v_{Na} - v_K$	$\exp \left(\frac{v_{Na} + v_K - 2v_{Cl}}{v_T} \right) = \left(\frac{[Na]_0}{[Na]_1} \right) \left(\frac{[K]_0}{[K]_1} \right) \left(\frac{[Cl]_0}{[Cl]_1} \right)^2$
	Cl ⁻	2	0	1	-1	$\Delta G_{Cl} = 2q_e(v_{Cl} - v)$			

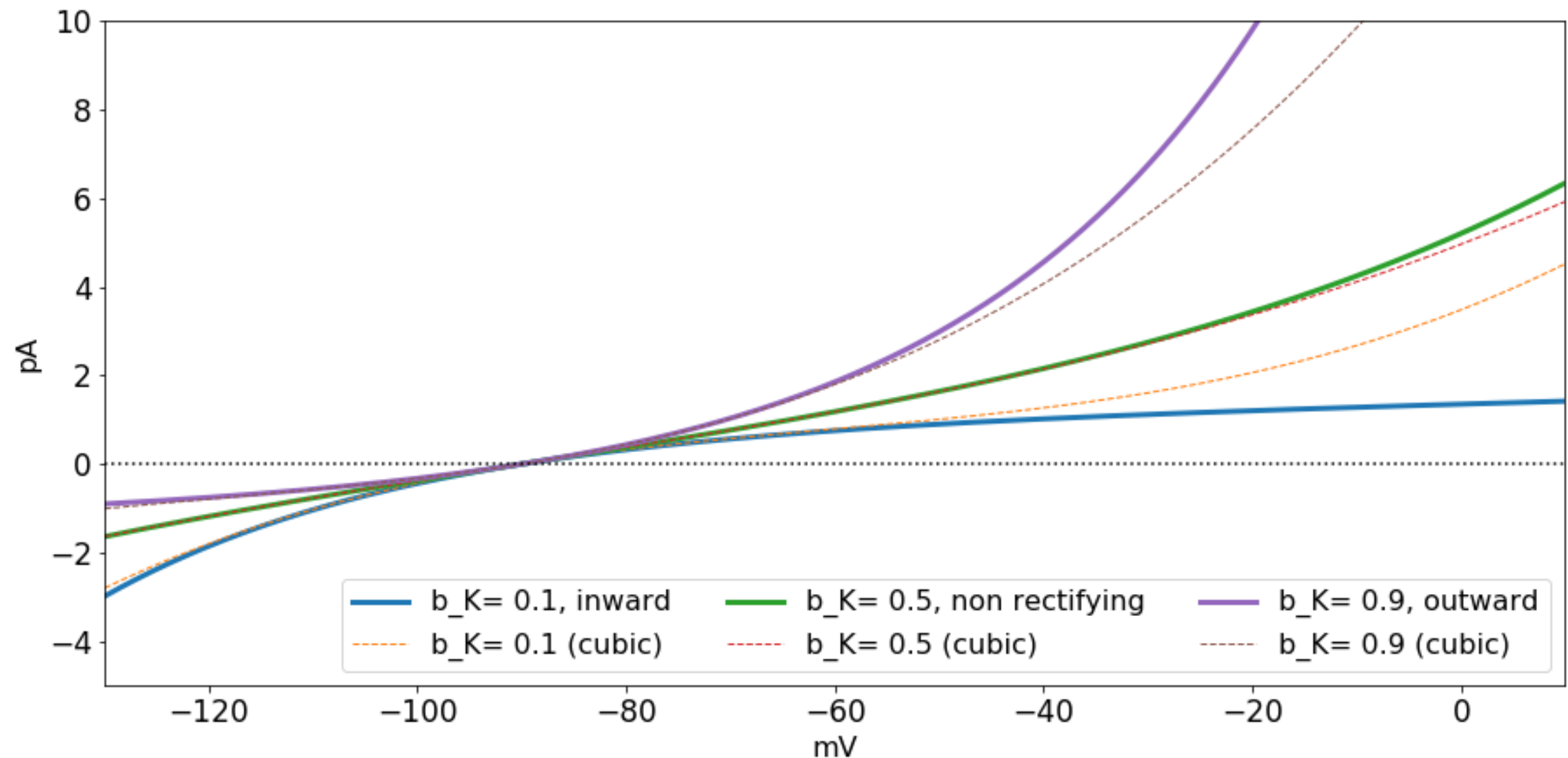
The flux φ can then be converted to a current density multiplying by the net charge transported across the membrane. As a result,

$$\psi(v; v_R, \eta, s, a) = \eta q \varphi = \eta a \left[\exp \left((s-1) \frac{v_R - \eta v}{v_T} \right) - \exp \left(s \frac{v_R - \eta v}{v_T} \right) \right], \quad (1)$$

Currents mediated by glutamate receptors formed by different subunits show different levels of rectification



K currents, possibly including rectification



If only ions are involved in the transport, the flux simplifies to

$$\Phi = r \left\{ \exp \left[b \left(\frac{\eta v - v_o}{v_T} \right) \right] - \exp \left[(b-1) \left(\frac{\eta v - v_o}{v_T} \right) \right] \right\}, \quad (14)$$

where

$$v_o = \delta_{\text{Ext}} v_{\text{Ext}} + \sum_{s \in S} n_s z_s (c_s - d_s) v_s. \quad (15)$$

Lower order approximations to the generic formulation and conductance based models. Conductance-based currents (Hodgkin and Huxley, 1952) are linear approximations of the generic current from equation (16), around the reversal potential v_o/η . To see this, use Taylor's theorem (Courant and John, 2012; Spivak, 2018) to rewrite the generic current from equation (16) as a series around v_o

$$i = q\eta r \left[\left(\frac{\eta v - v_o}{v_T} \right) + \left(b - \frac{1}{2} \right) \left(\frac{\eta v - v_o}{v_T} \right)^2 + \left(\frac{3b^2 - 3b + 1}{3!} \right) \left(\frac{\eta v - v_o}{v_T} \right)^3 + \dots \right]. \quad (17)$$

Truncation of the series to first order gives

$$i \approx g \left(v - \frac{v_o}{\eta} \right), \quad (18)$$

where $g = \eta^2 qr / v_T$ is in units of $\text{nS}/\mu\text{m}^2$, which has the functional form of the conductance-based current used in the Hodgkin and Huxley (1952) model. For instance, the linear approximation for the current through an open sodium channels around v_{Na} in equation (18) gives $g_{\text{Na}} = qr_{\text{Na}} / v_T$, and $v_o = \eta_{\text{Na}} v_{\text{Na}}$, with $\eta_{\text{Na}} = -1$, so that $i_{\text{Na}} \approx g_{\text{Na}}(v - v_{\text{Na}})$.

The flux φ can be converted to a current density multiplying by the net charge transported across the membrane. As a result,

$$\psi(v; v_R, \eta, s, a) = \eta q \varphi = \eta a \left[\exp\left((s-1)\frac{v_R - \eta v}{v_T}\right) - \exp\left(s\frac{v_R - \eta v}{v_T}\right) \right] \quad (1)$$

.

Transmembrane potential dynamics

To show the application of the formulations discussed earlier, let us build a generic model of transmembrane potential dynamics with currents generated by N different electrogenic transport mechanisms. For simplification purposes, consider only one such mechanism, labeled as l , with $p_l N_l$ active sites, where N_l is the number of membrane sites where the l th transport mechanism is found, and p_l is the proportion of active sites (might be voltage or ligand dependent). Then the total current mediated by the l th mechanism in a patch of membrane can be written as $\bar{a}_l p_l \varphi_l(v)$ with $\bar{a}_l = qN_l r_l$ (in $\text{pA}/\mu\text{m}^2$), and

$$\varphi_l(v) = \exp\left[b_l\left(\frac{\eta_l v - v_l}{v_T}\right)\right] - \exp\left[(b_l - 1)\left(\frac{\eta_l v - v_l}{v_T}\right)\right], \quad (30)$$

where v_l/η_l is the reversal potential for the l th current, $l \in \{1, \dots, N\}$. There is experimental evidence for some ion channels that supports the replacement of \bar{a}_l as a constant (Nonner and Eisenberg, 1998). The time-dependent change in transmembrane potential can be written as

$$\partial_t v = - \sum_{l=1}^N a_l p_l \varphi_l(v), \quad (31)$$

with v is in mV and $a_l = \bar{a}_l/C_M$ in mV/mS (pA/pF) represents the current amplitude for the l th transport mechanism, normalized by the membrane capacitance, for $l \in \{1, \dots, N\}$. Only electrogenic transport mechanisms are included.

Rectification

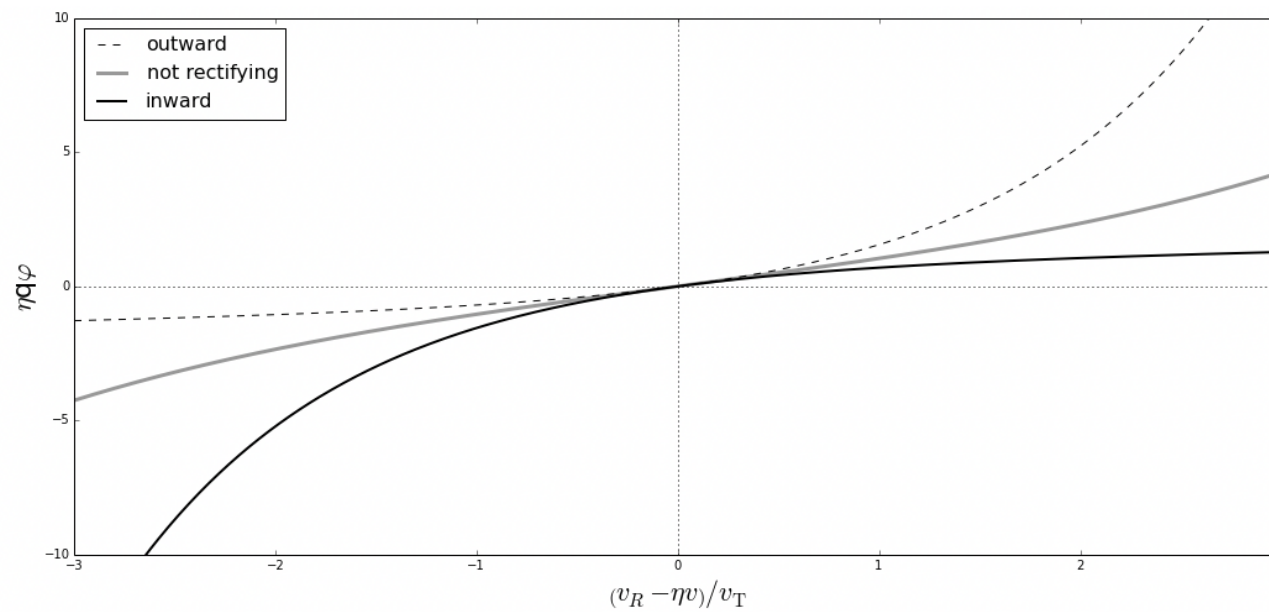
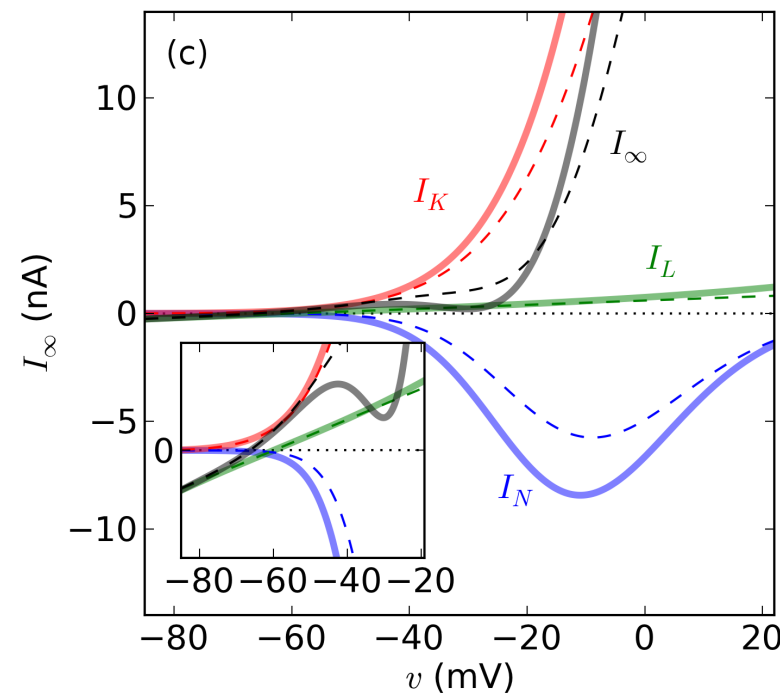


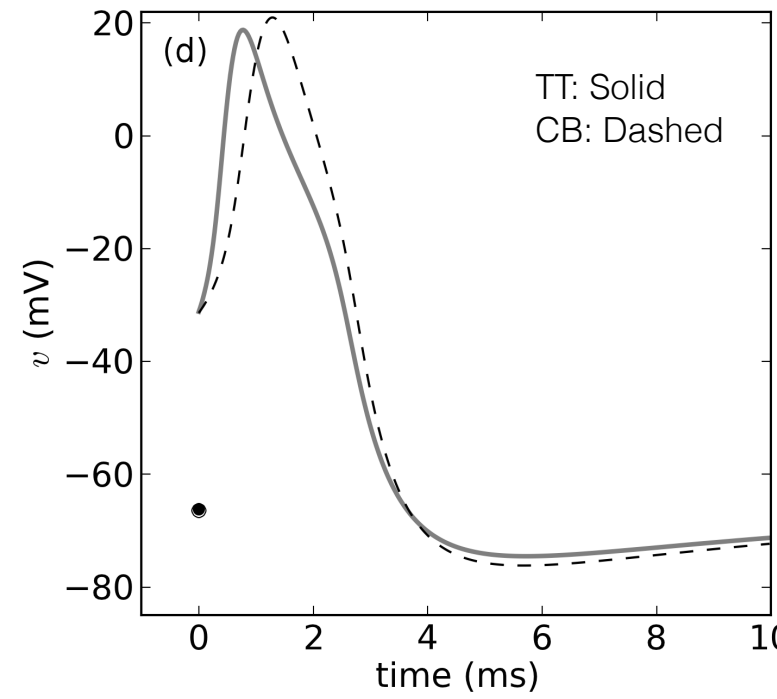
Figure 1: Generic currents from equation (10) showing different levels of rectification similar to those displayed by voltage-dependent K^+ channels. In this instance, $v \in [-180, 20]$ mV, $v_R = -80$ mV, and $\eta = 1$. The rectification is inward ($s = 0.1$, solid black), none ($s = 0.5$, solid gray), or outward ($s = 0.9$, dashed black). See Table 1.

The nonlinear thermodynamical model causes big changes in excitability and dynamics

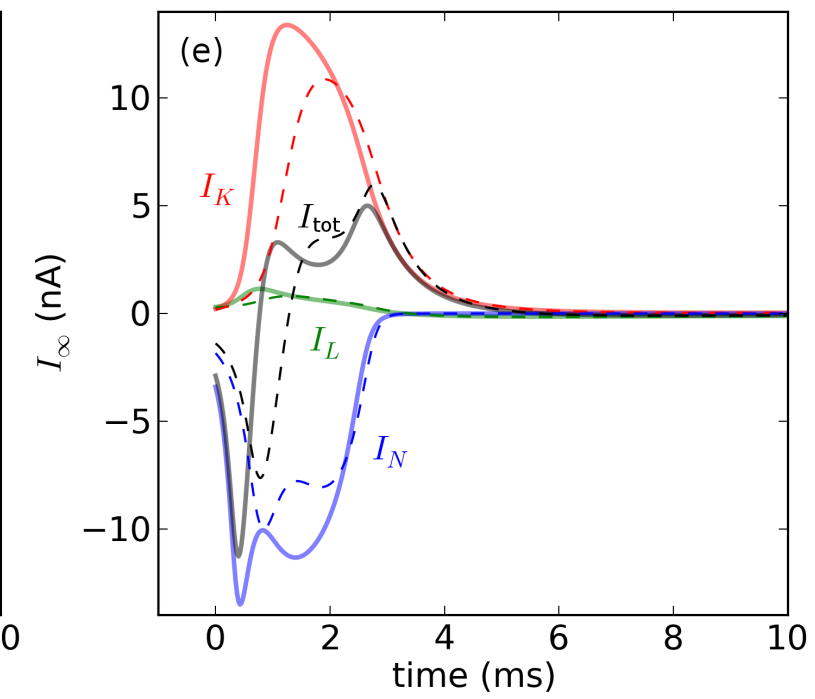
Voltage-gated steady state currents



Neuronal action potential

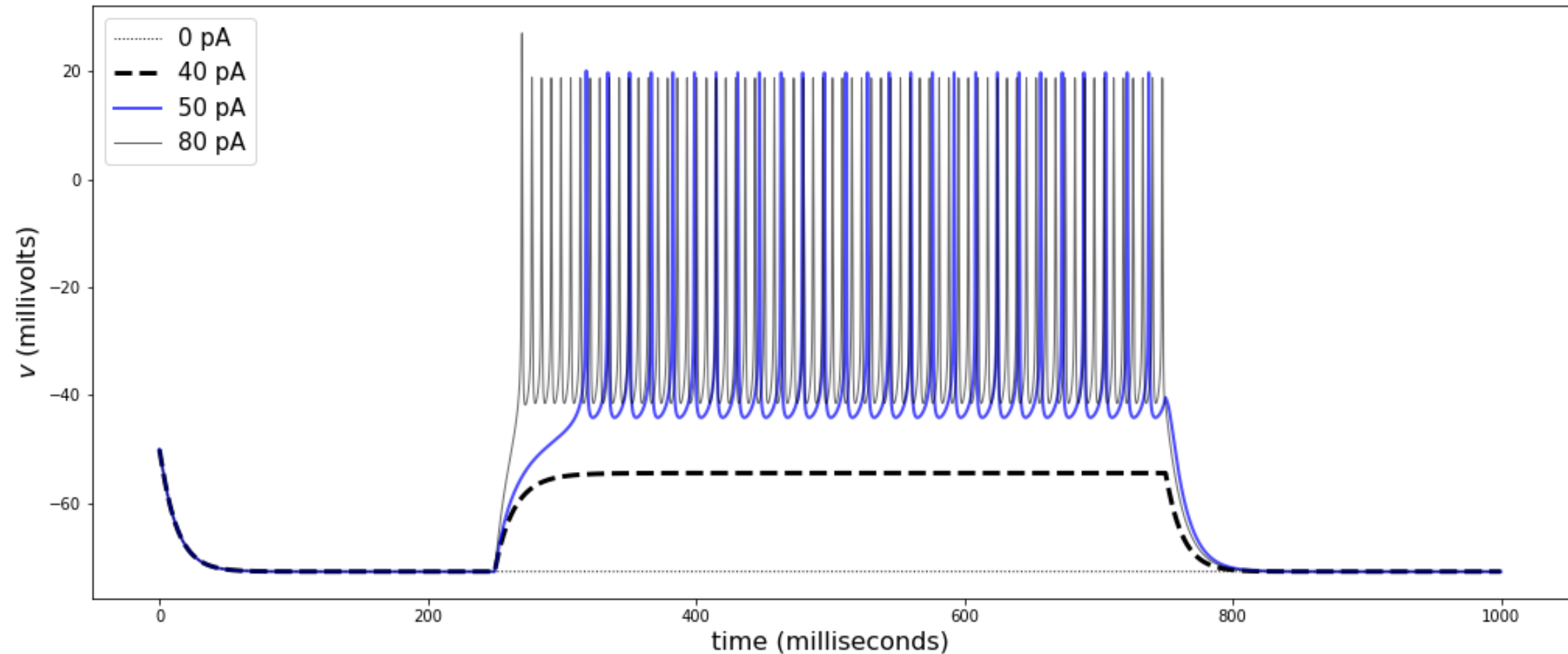


Currents during action potential



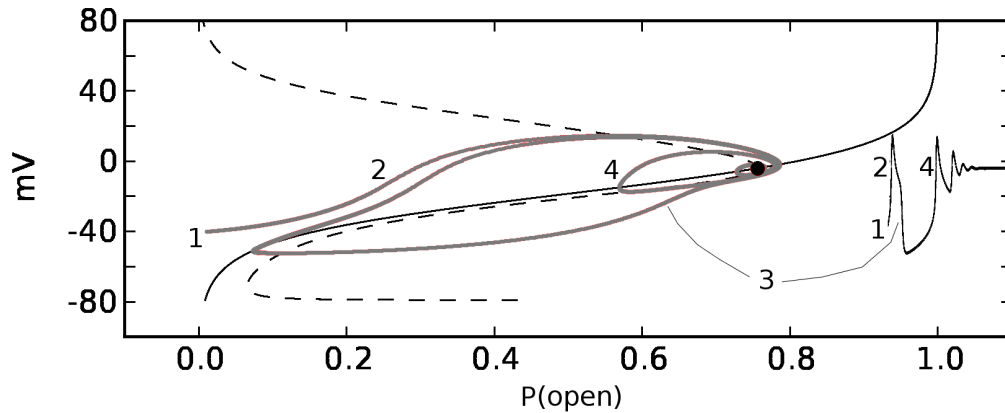
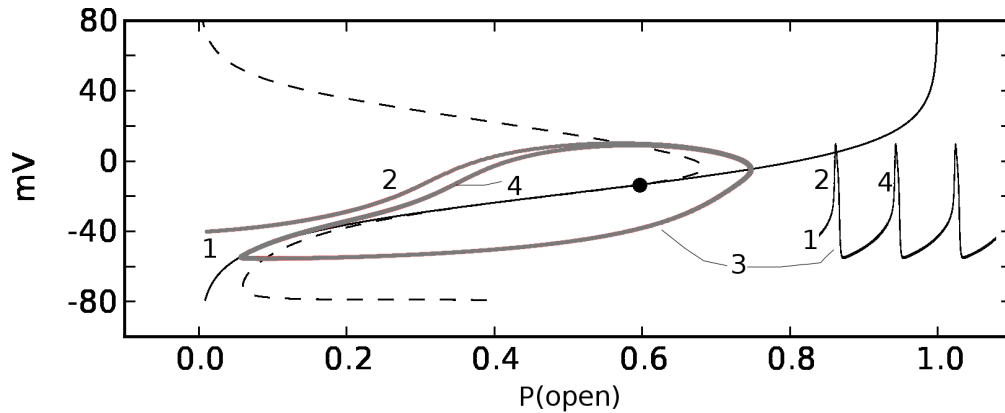
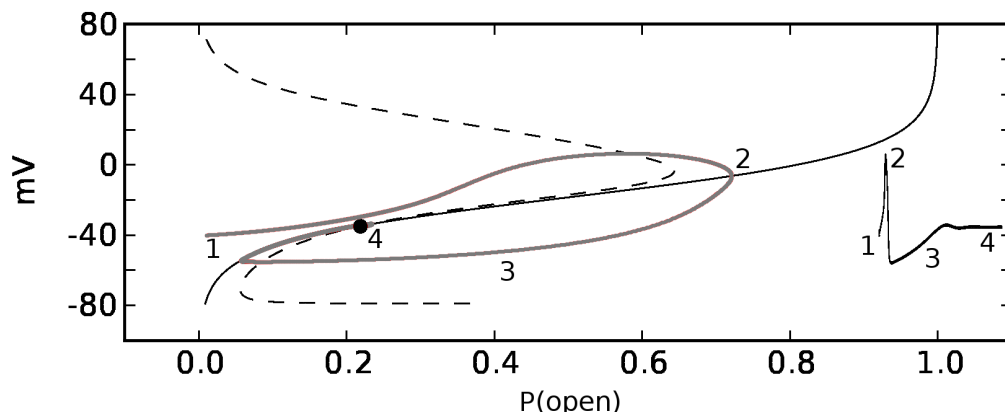
Herrera-Valdez, 2012

Fast spiking interneuron



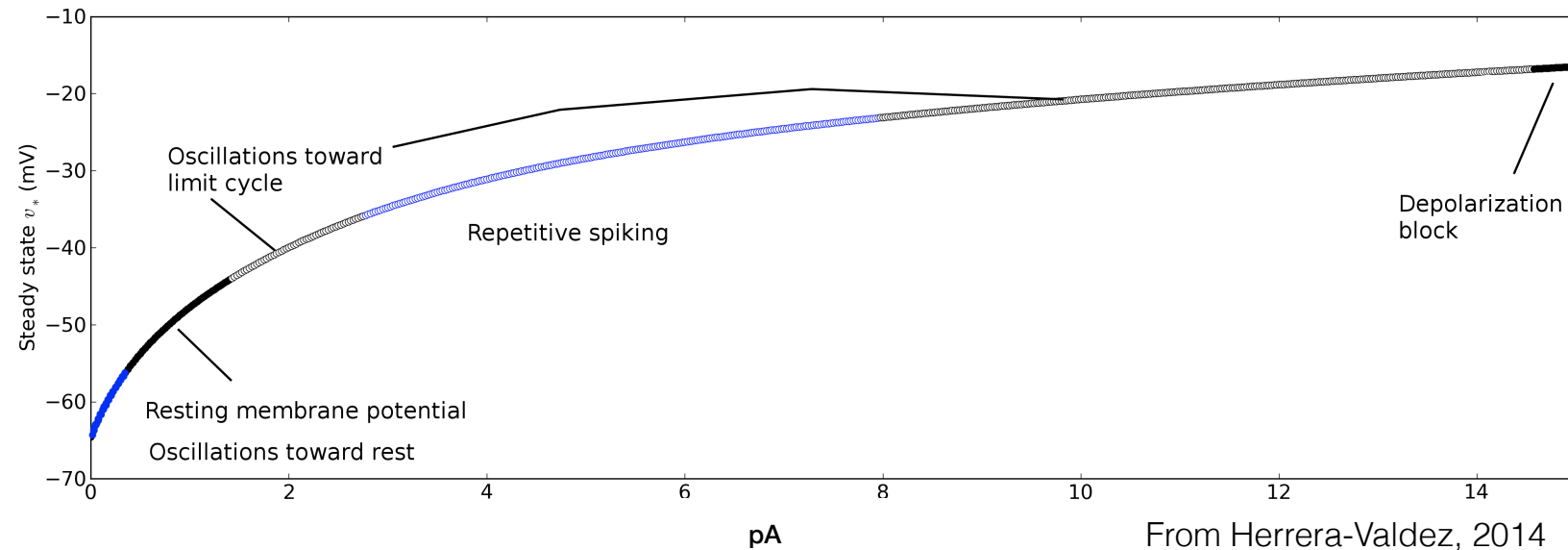
Same neuron, possibly different responses to stimulation

The internal and external context matter



From Herrera-Valdez, 2008

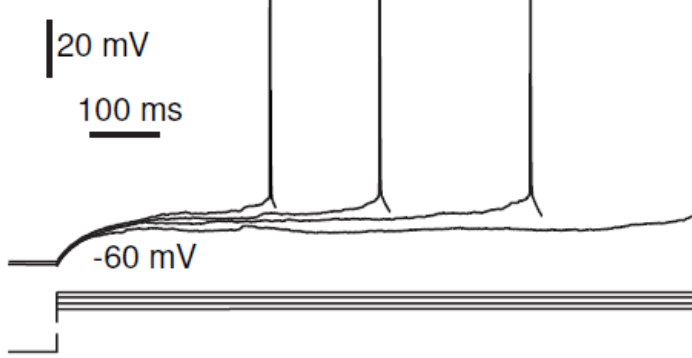
Sequences of bifurcations as a function of input current:
The same neuron can integrate inputs in different ways depending on the external current



From Herrera-Valdez, 2014

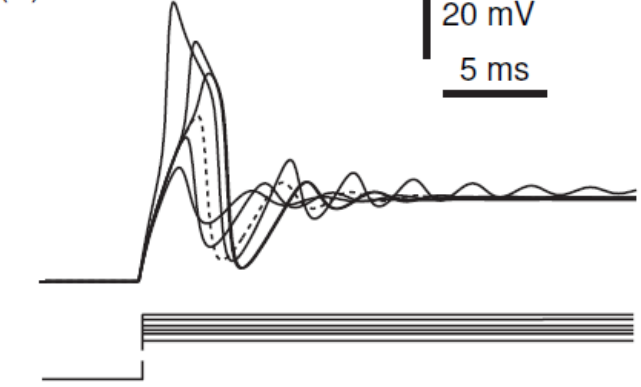
Aggregation

(a) Near asymptotically stable nodes



Resonance

(b) Near asymptotically stable foci



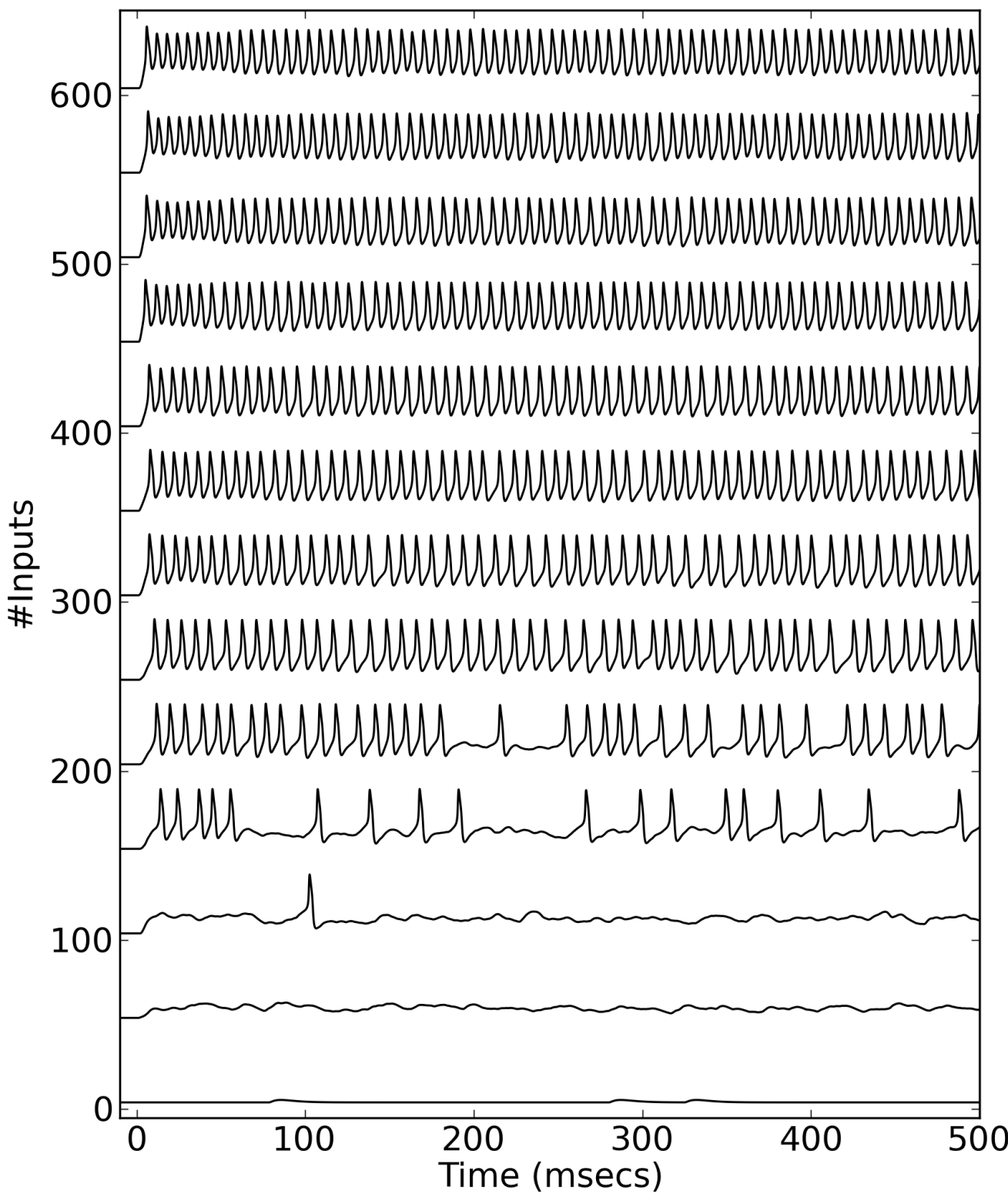
From Izhikevich, 2006

Change in membrane potential: $\partial_t v = f_i(v, w; p) + f_s(v; p) + I_F$

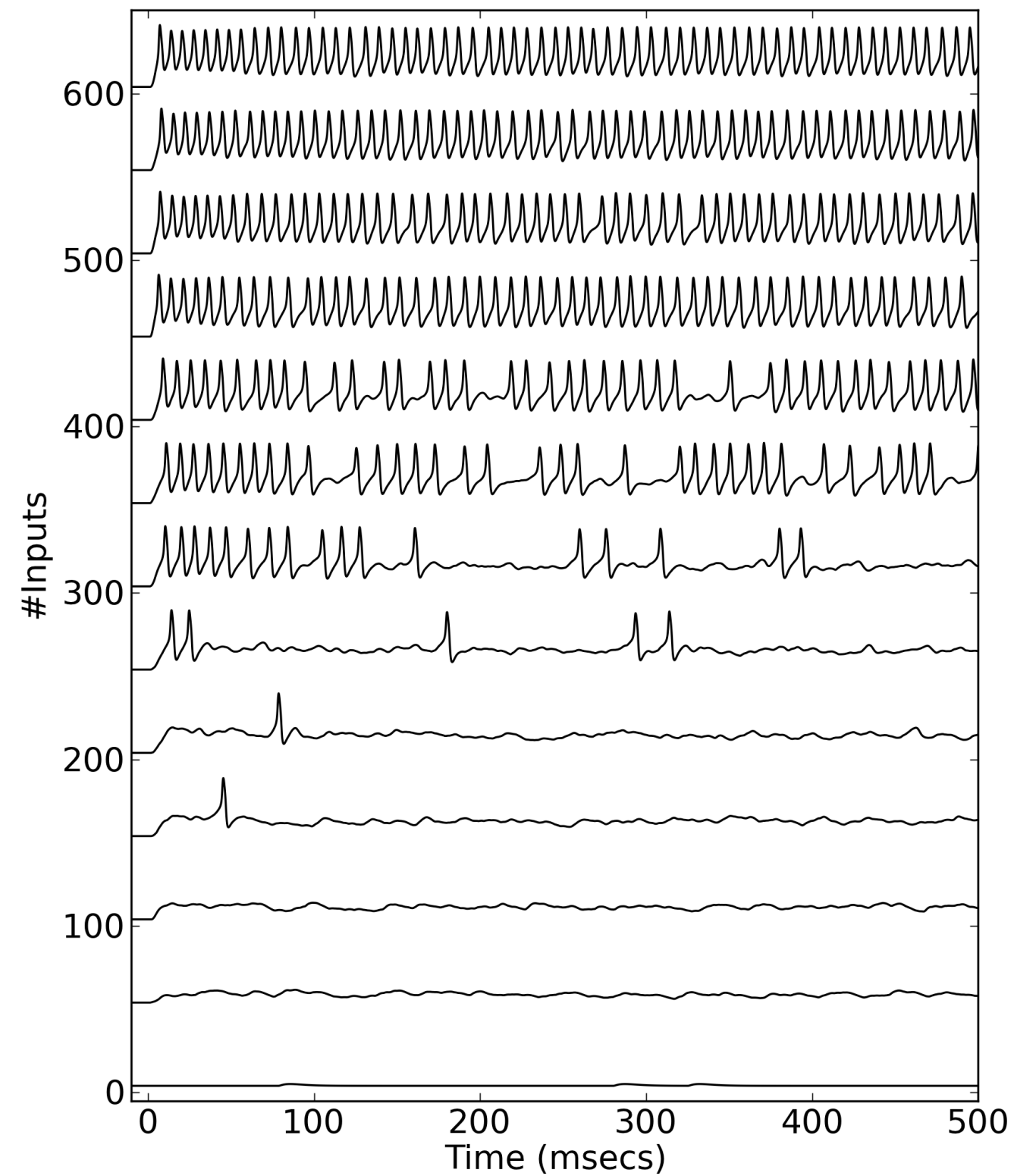
Proportion of open K channels: $\partial_t w = g(v, w; p)$

Spiking activity in response to fast excitatory synaptic input

Generic formulation



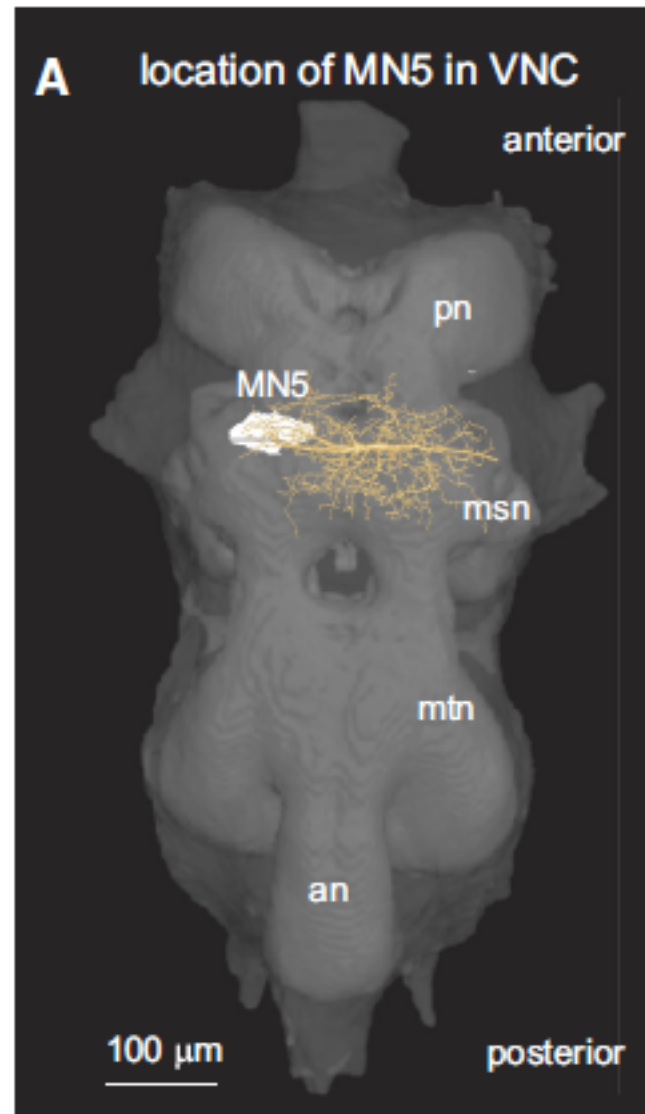
CB



Dynamical Systems

Bifurcation structures accurately describe
the relationship between
the electrophysiological phenotype
and the patterns of expression of
transmembrane proteins mediating transport

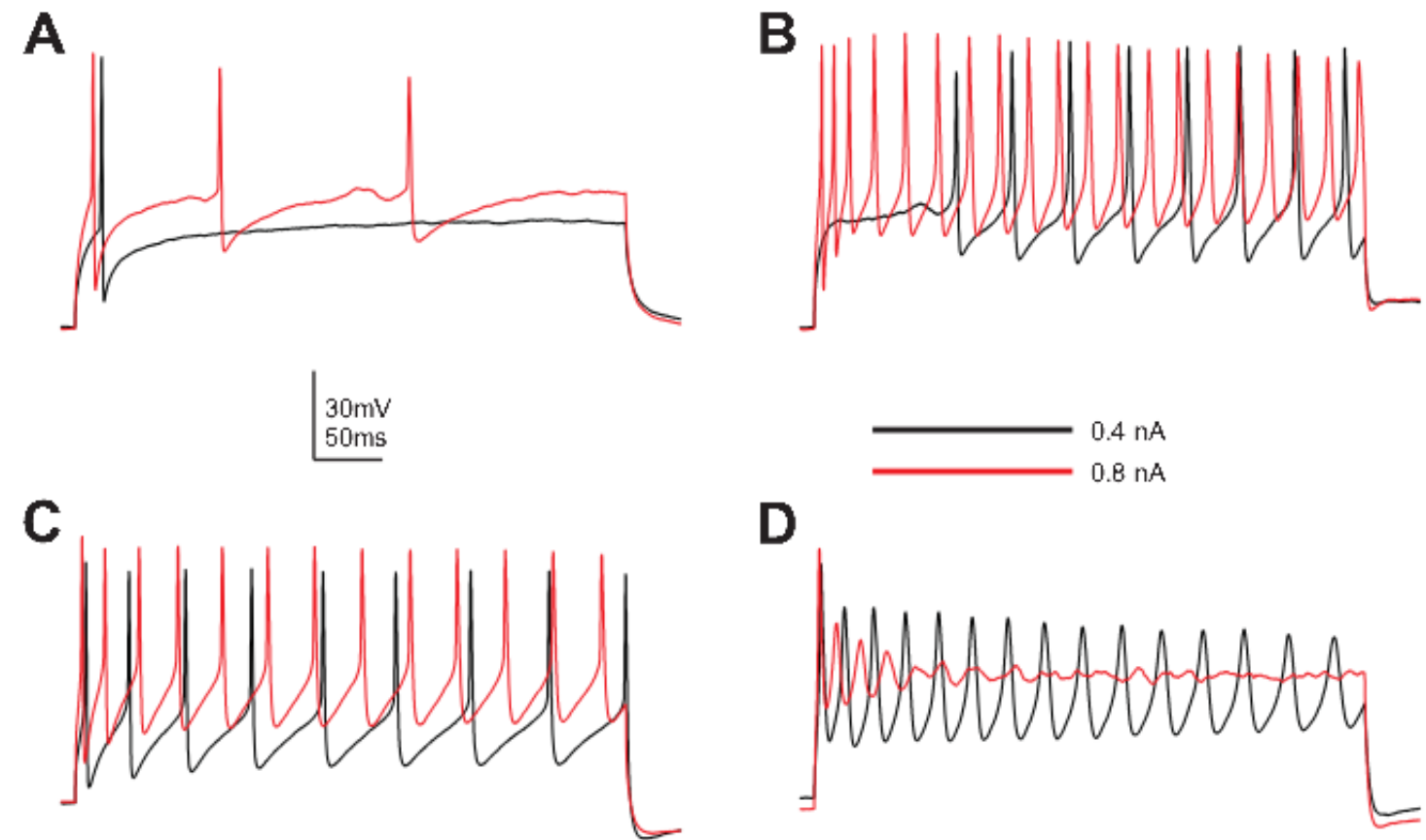
Patch recordings from adult MN5 Drosophila motoneuron



MN5 controls the dorsolateral wing muscle in adult Drosophila.

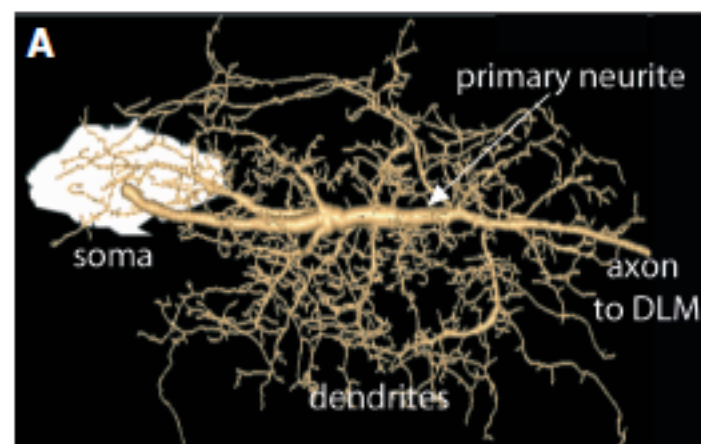
While freely behaving, wing beat can be over 200 Hz

Motoneurones MN1-5 fire at a maximum of 30 Hz



Herrera-Valdez, et al. 2013

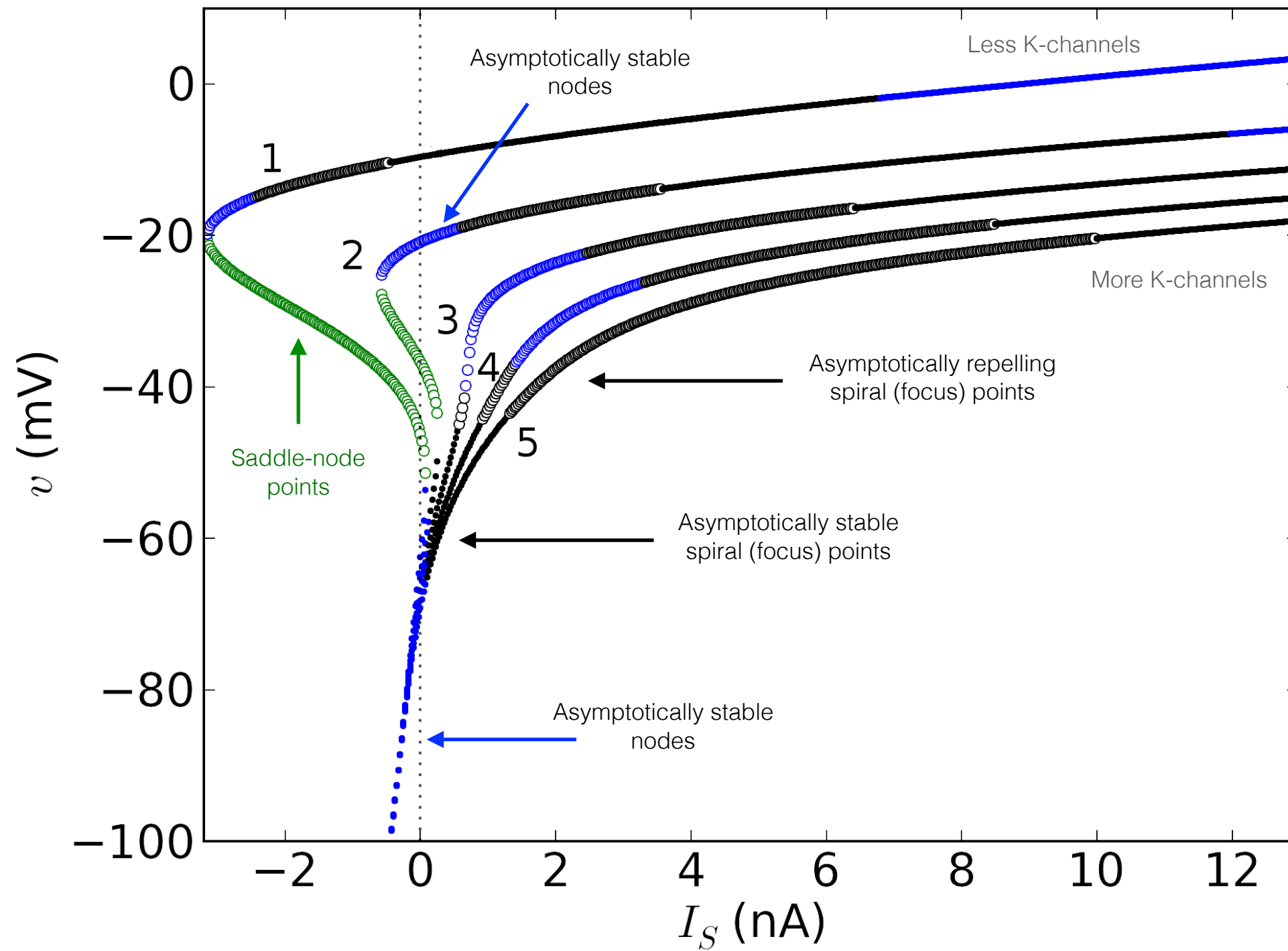
The dynamics (sometimes) suggest resonance as a mechanism for excitability. Central dogma for recruitment: motor neurons are not supposed to resonate with stimulus.



Kuehn & Duch, 2008

Why are the patterns so different?

Bifurcation diagram with respect to the external current, varying the quotient of sodium to potassium channels in the membrane:
A neuron may loose or win the ability to resonate or aggregate its inputs by regulating the expression of channels in its membrane



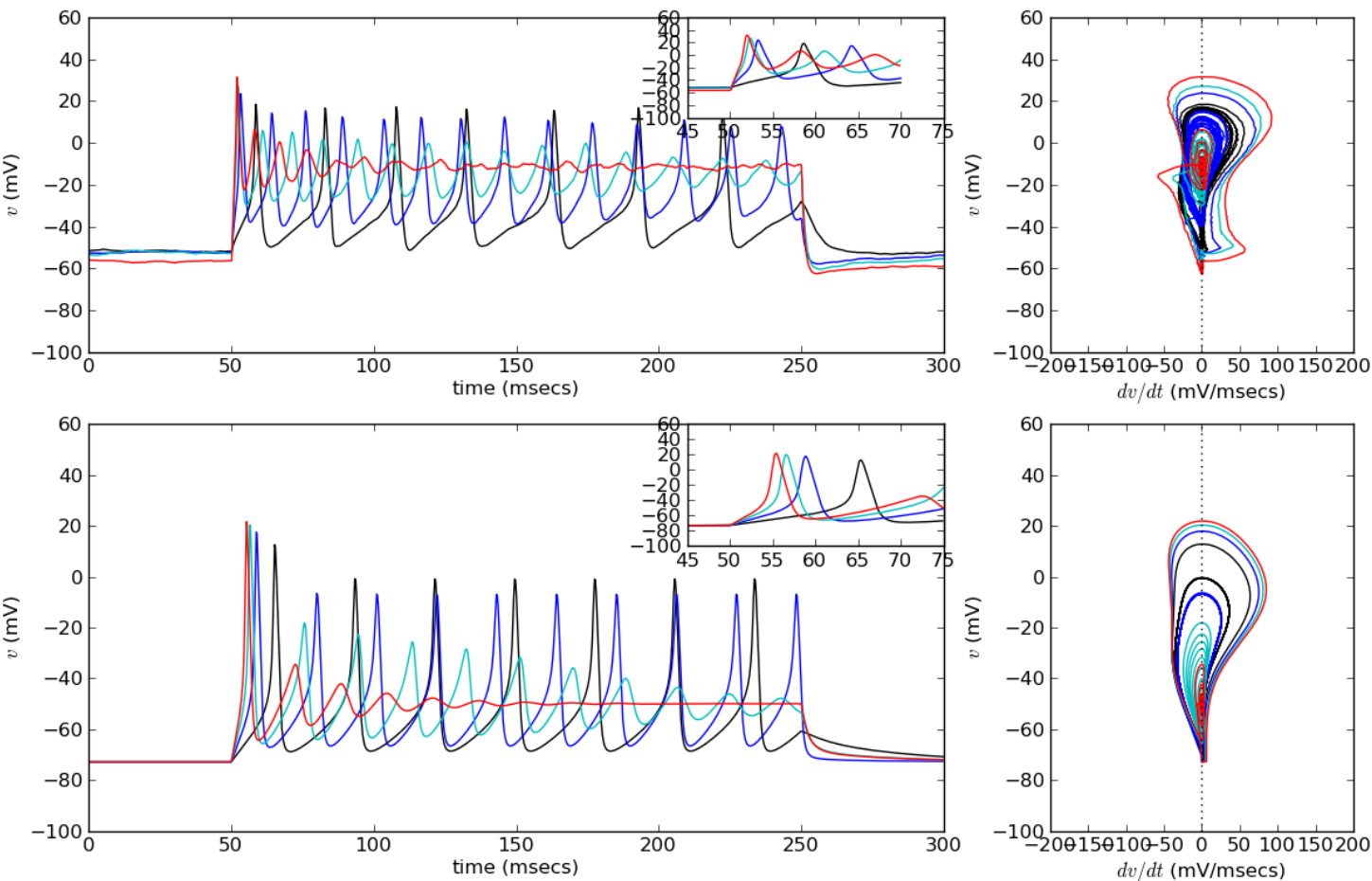
Recording vs model

$$C_m \partial_t v = -I_{\text{Na}}(v, w) - I_K(v, w) - I_{\text{NaK}}(v),$$

$$\partial_t w = w [F_w(v) - w] C_w(v),$$

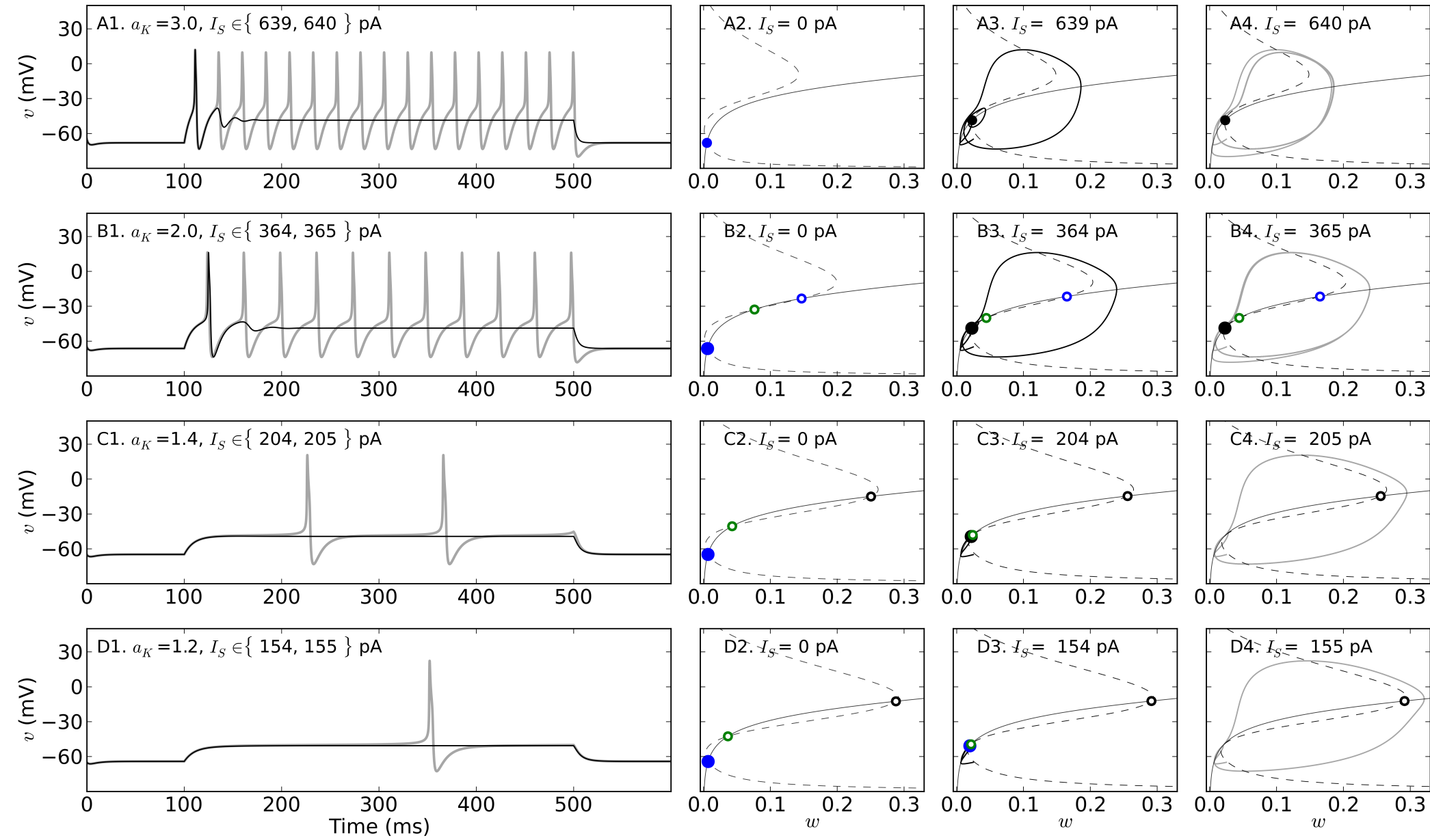
Care was taken to match the membrane capacitance, input resistance, maximum dv/dt , and rheobase.

As a consequence of the fitting process, the model predicts the contribution of the NaK pump (leak current), the maximum contribution of the Na and K channels

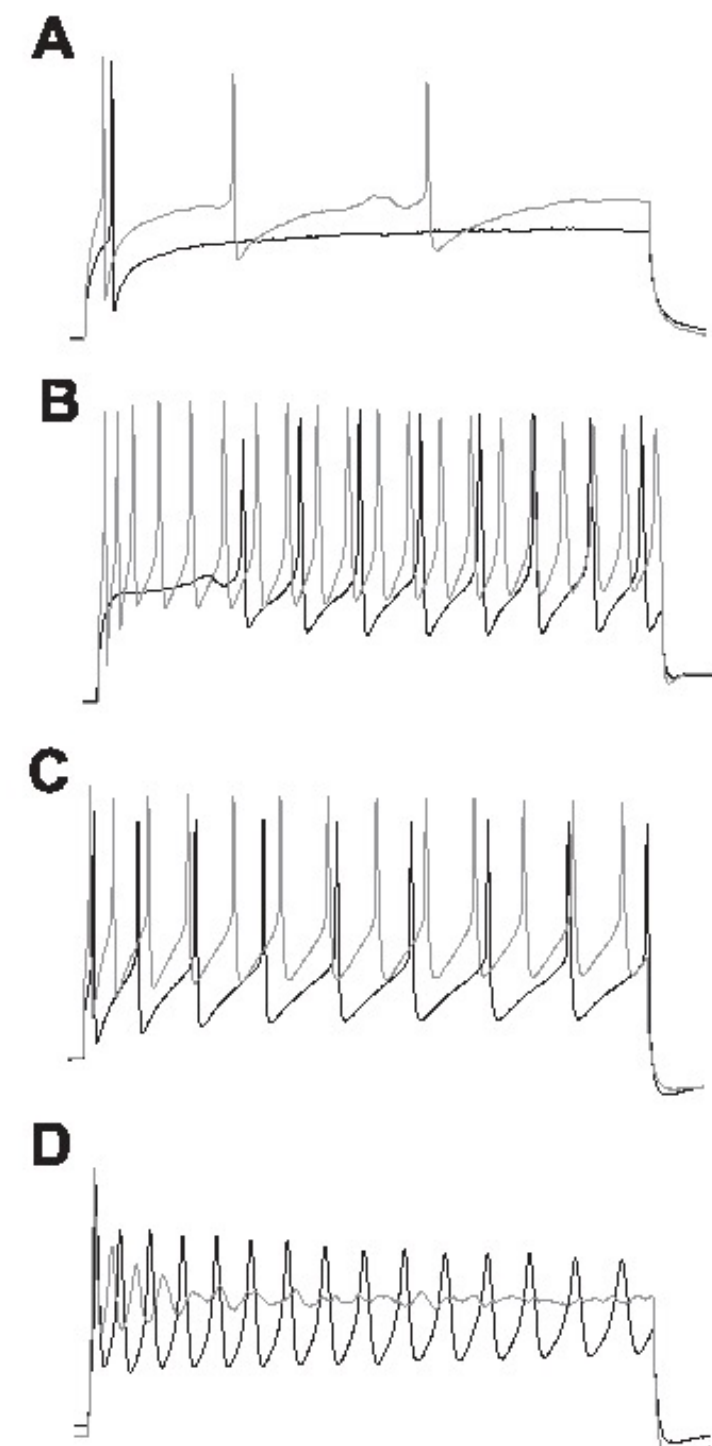
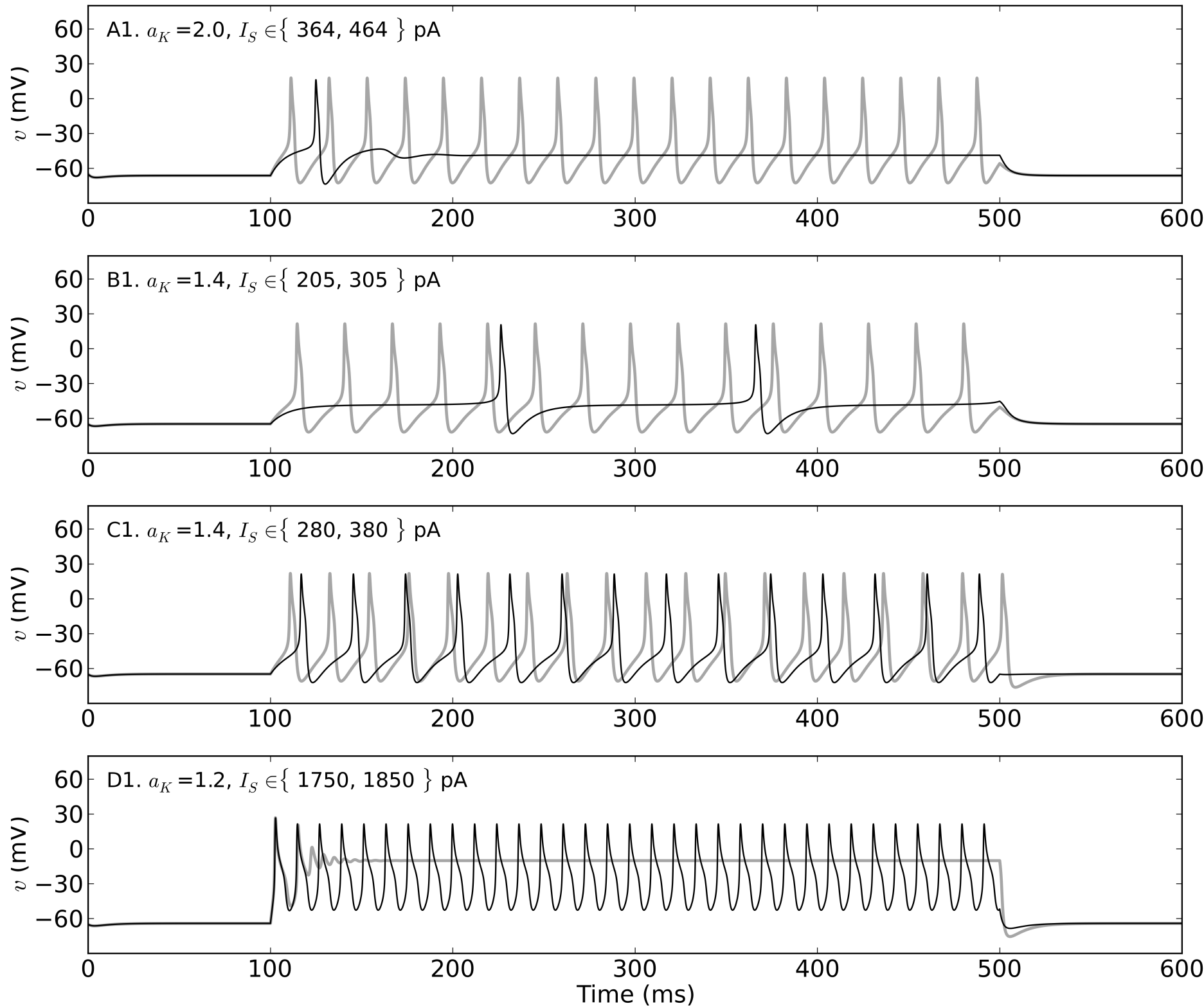


Transmembrane potential dynamics

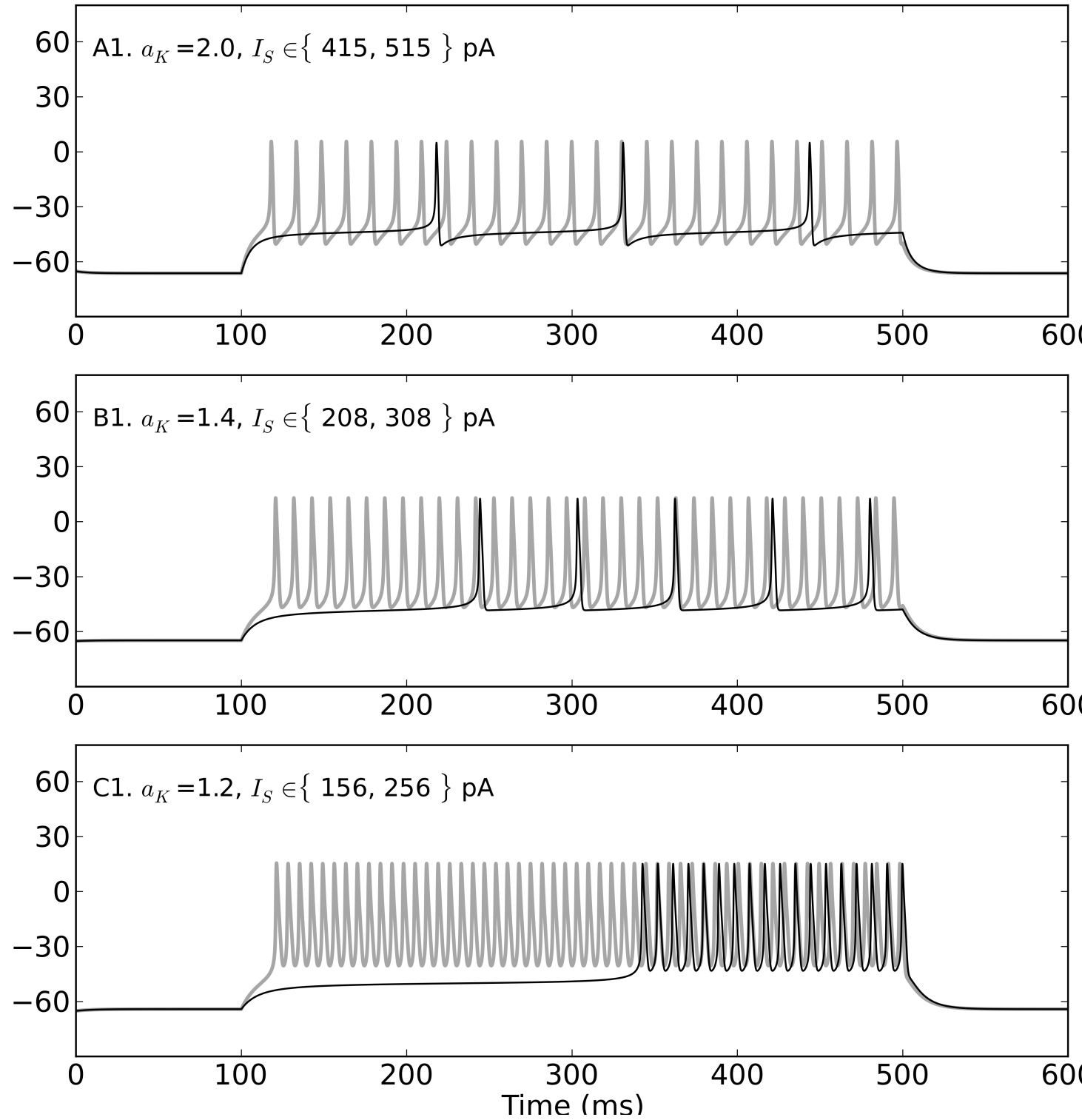
$$C_m \partial_t v = - \sum_l I_l(v), \quad I_l = \bar{a}_l p_l \sigma_l \left[\exp \left((s-1) \frac{\sigma_l v - v_{rl}}{v_T} \right) - \exp \left(s \frac{\sigma_l v - v_{rl}}{v_T} \right) \right]$$



Matching the behaviors of MN5 recordings using the bifurcation structure



Longer delays in comparison to the spiking period



Short term synaptic plasticity

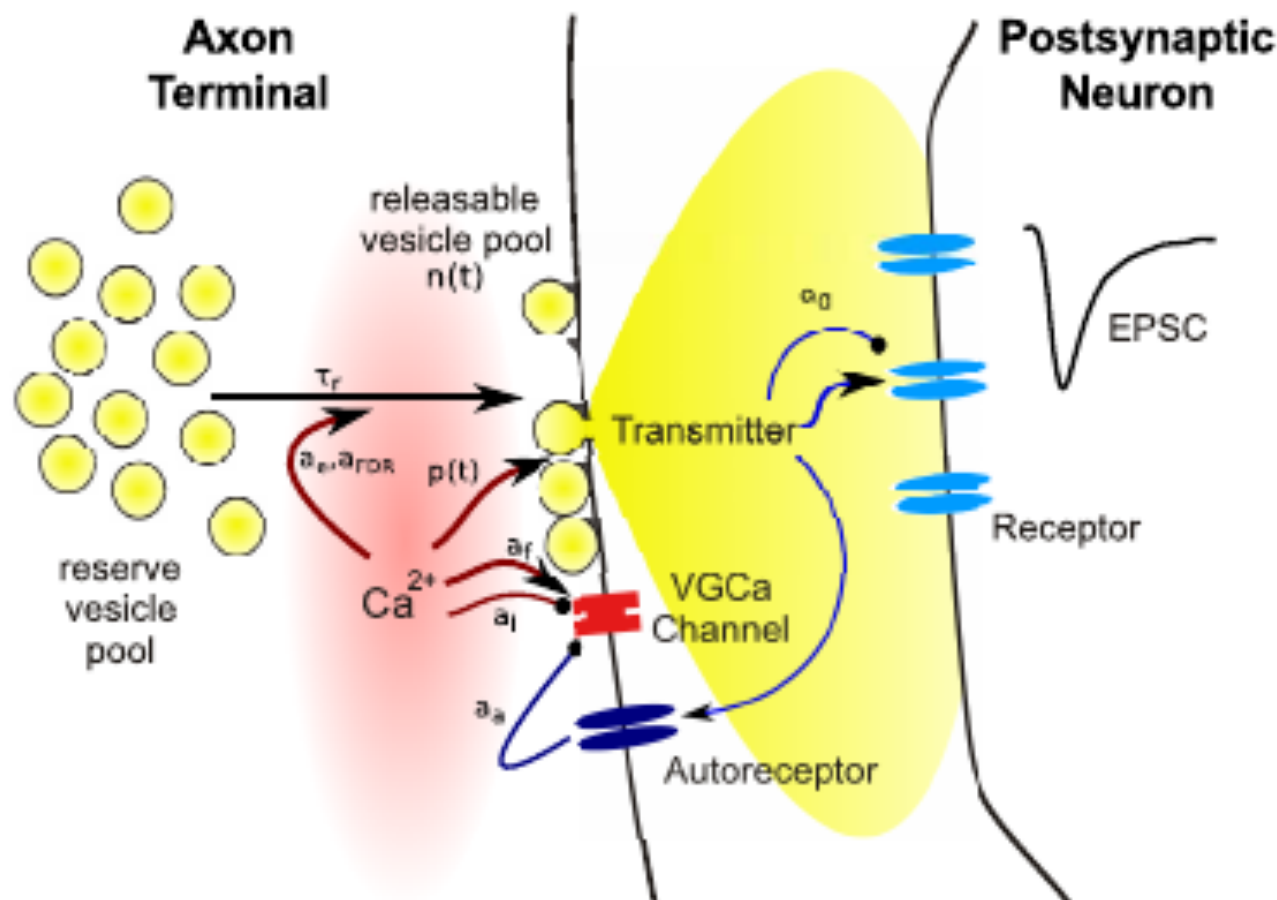


FIGURE 1 | Schematic illustration of the main steps involved in synaptic transmission, and of variables subject to use-dependent modification. Symbols refer to quantities used in the model equations in this review.

Let represent an average $c_a = [Ca]_i$ in axonal terminals forming a synaptic contact. Let p and x represent the probability of release and the density of readily releasable vesicles in the terminal. A simple model for the dynamics of presynaptic release is then

$$\partial_t c_a = \frac{c_{a\infty} - c_a}{\tau_c} - k I_N(v_a) \quad (1)$$

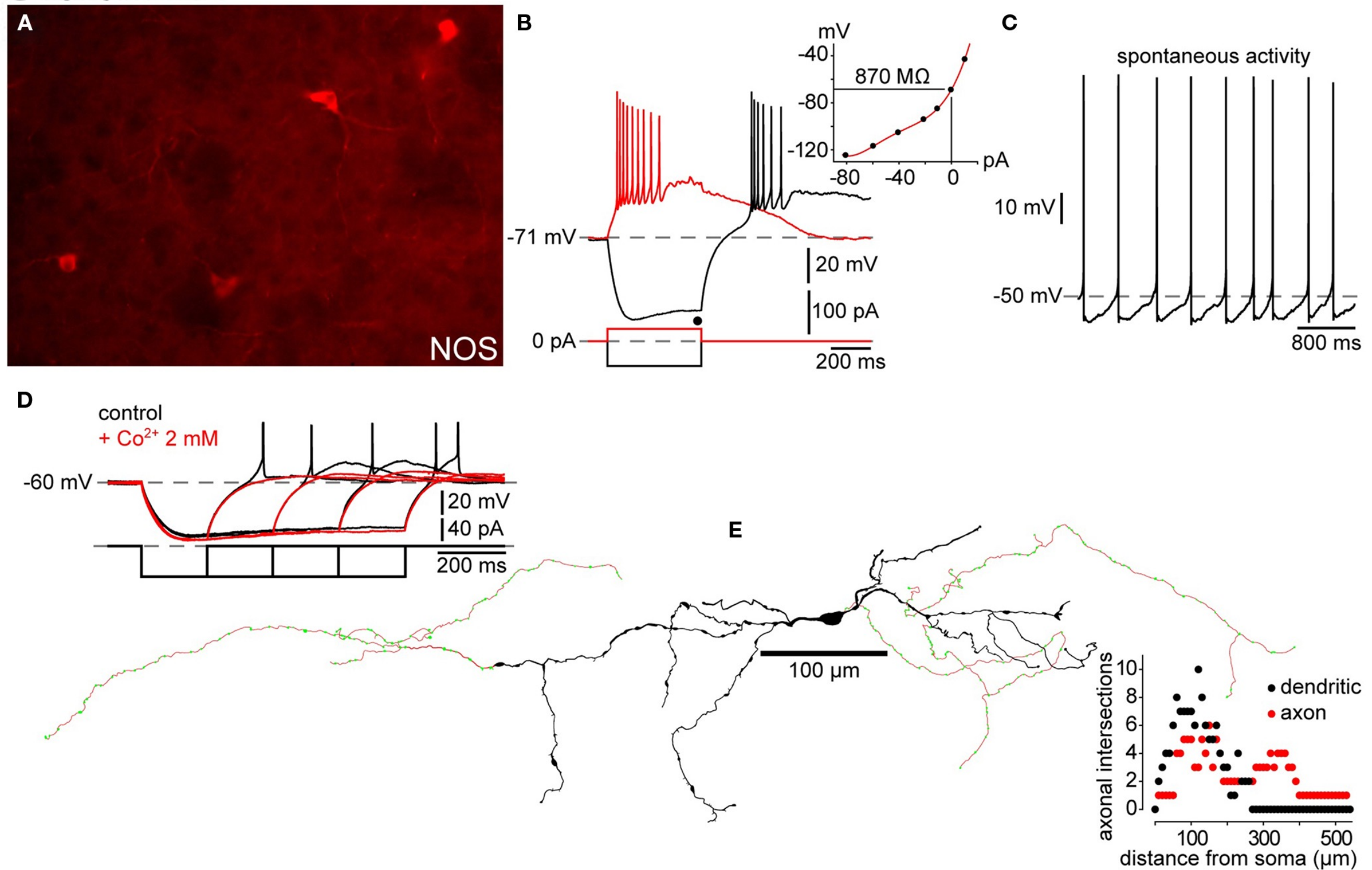
$$p_\infty(c) = \frac{c^l}{c^l + c_m^l} \quad (2)$$

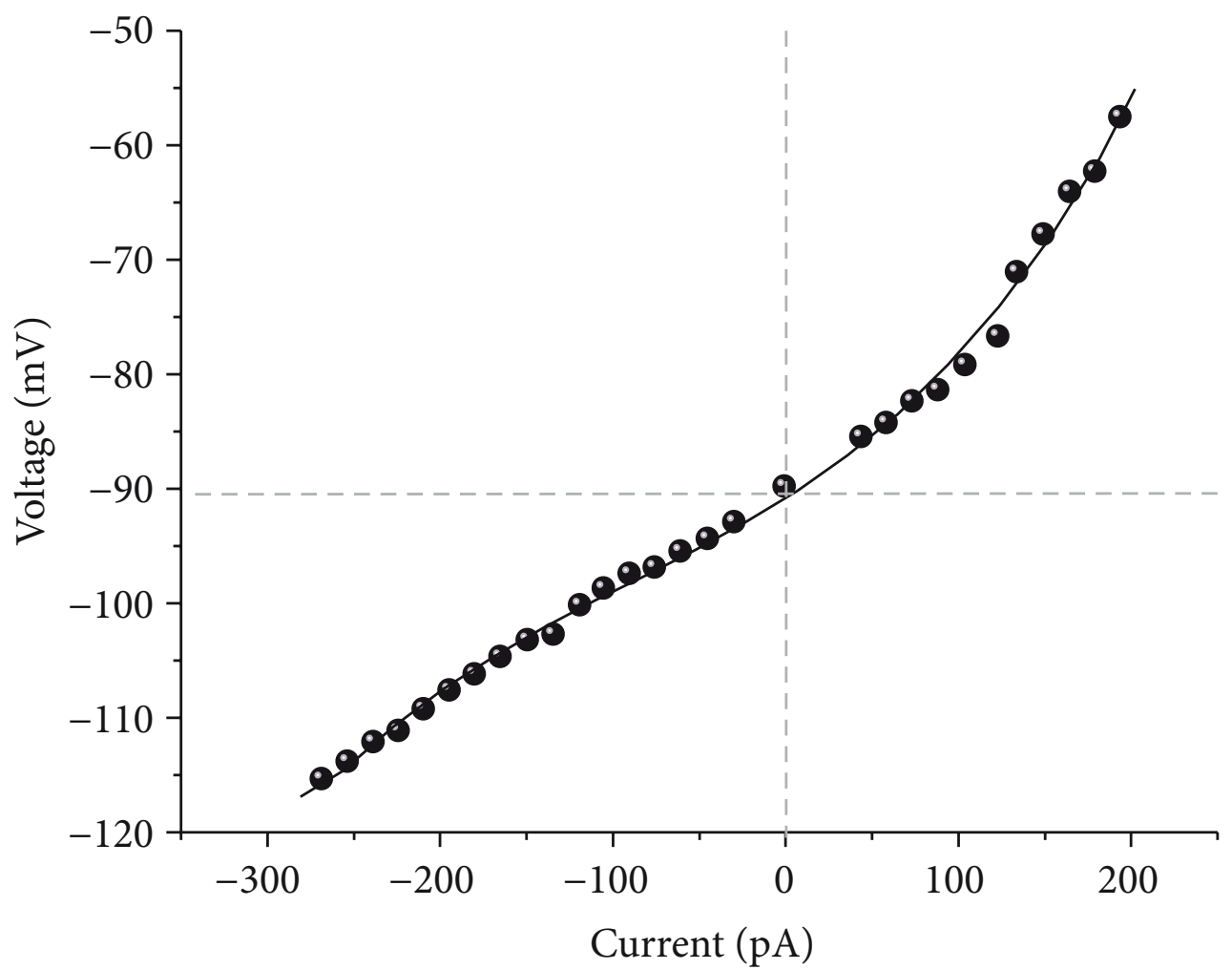
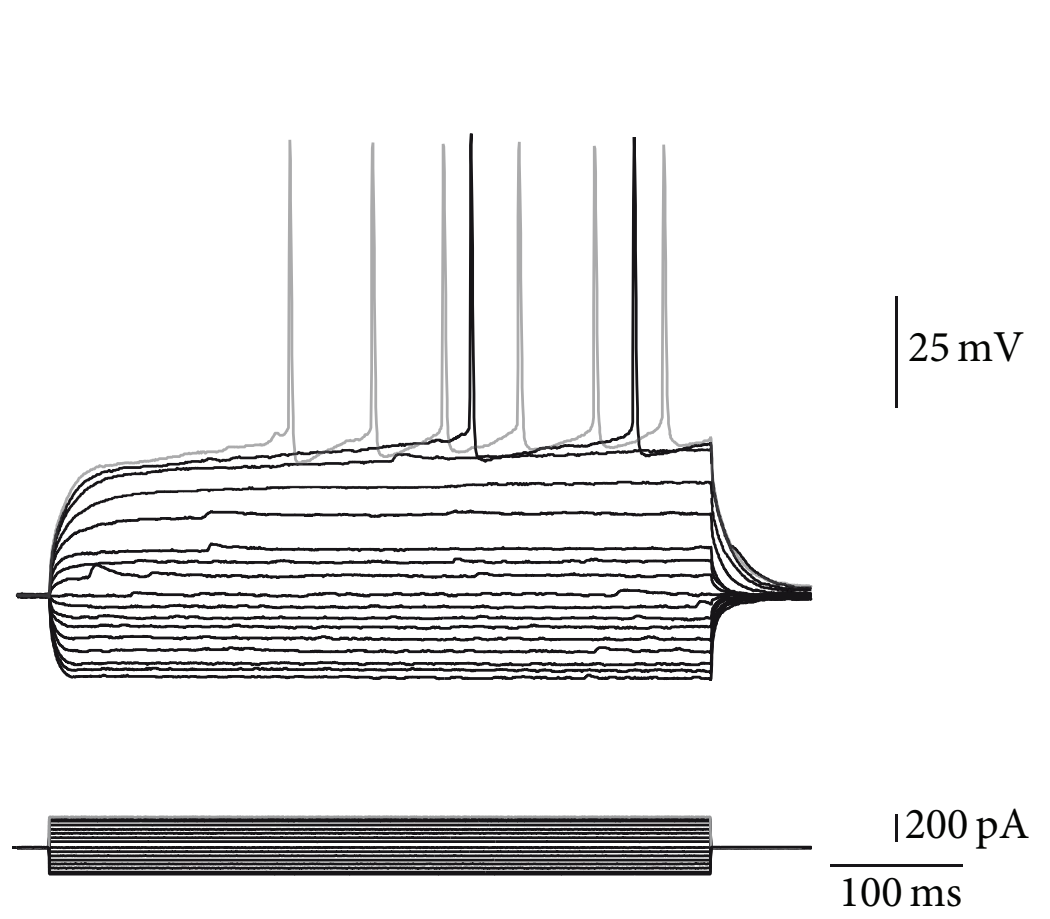
$$\partial_t p = \frac{p_\infty(c) - p}{\tau_p} \quad (3)$$

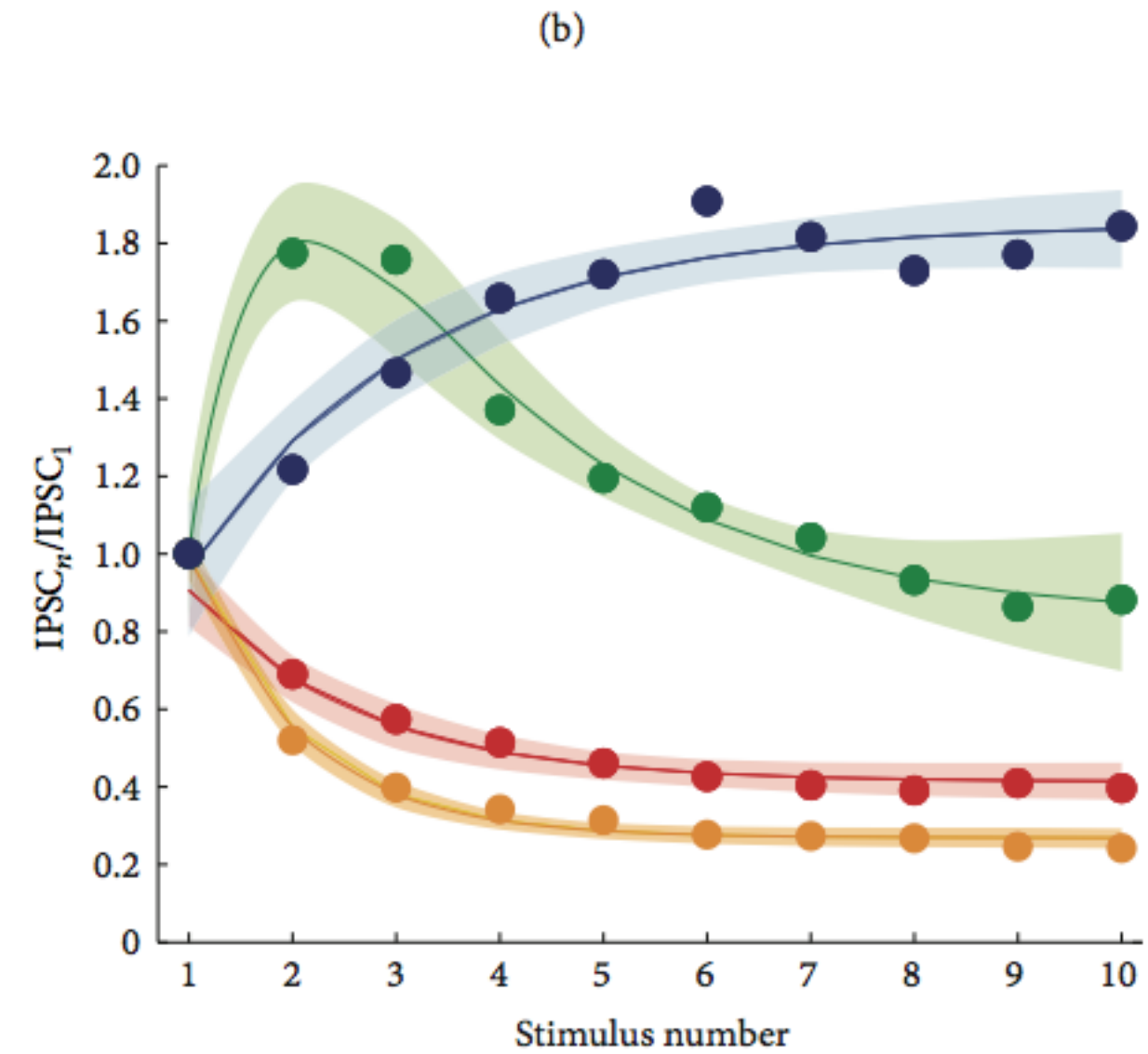
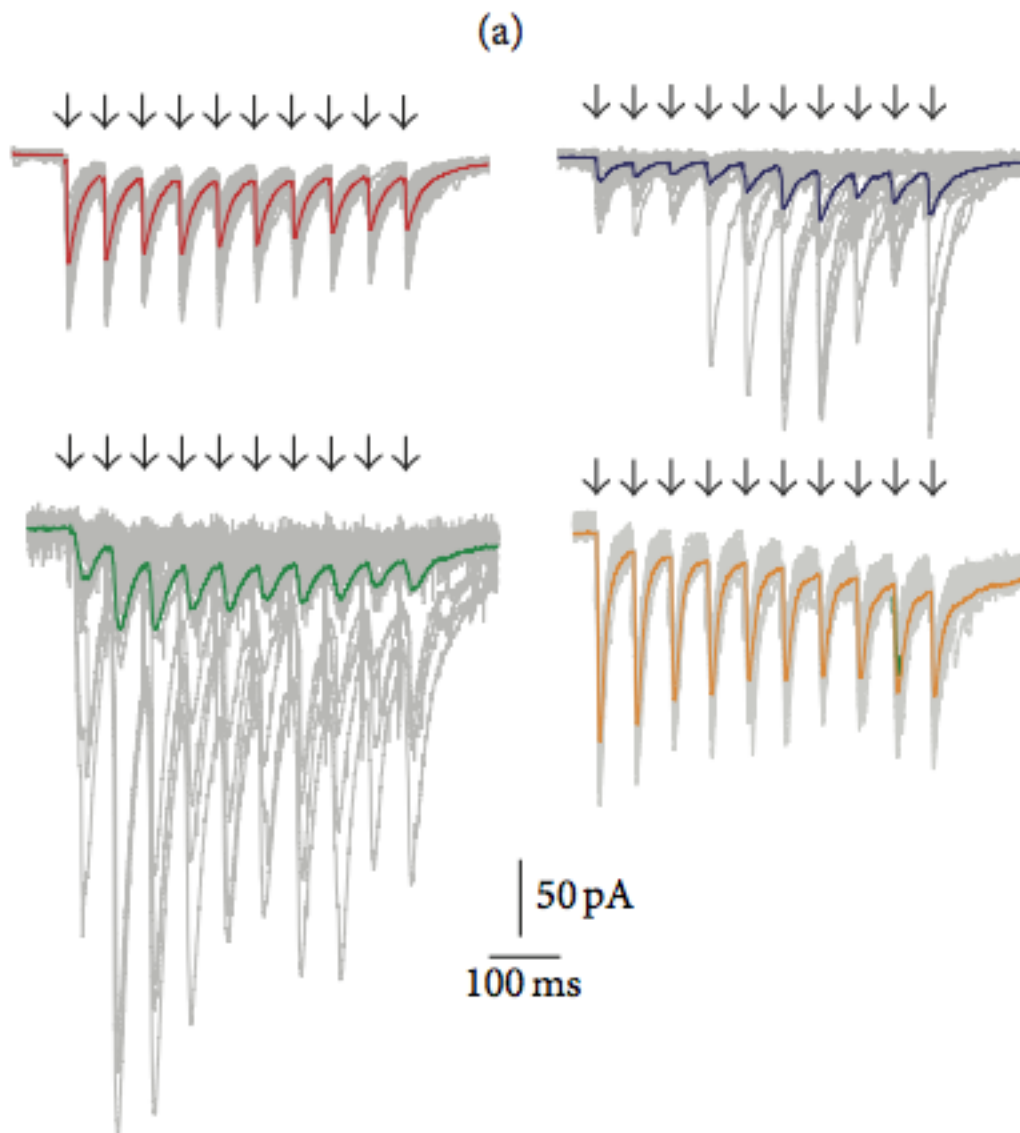
$$\partial_t x = x \frac{x_\infty - x}{\tau_x} - pxh \quad (4)$$

where h is equivalent to the time step in the time series, l is the cooperativity of calcium for the increase in the probability of release.

Long range interneurons enable communication between local networks in the striatum

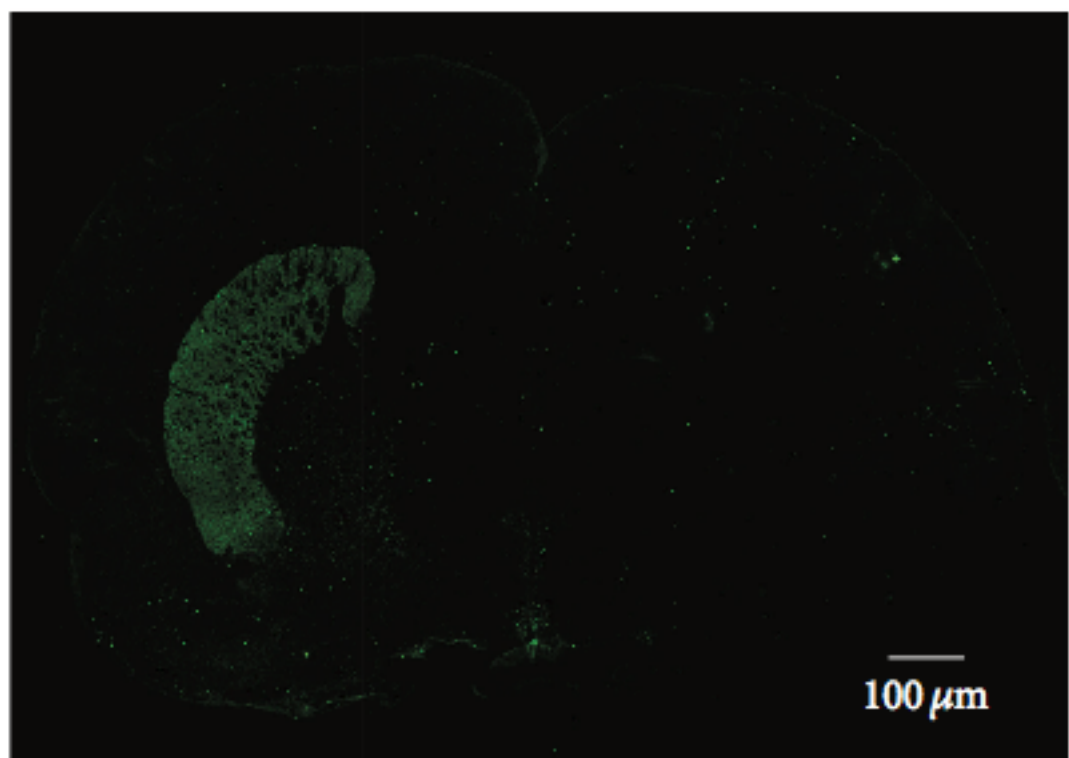




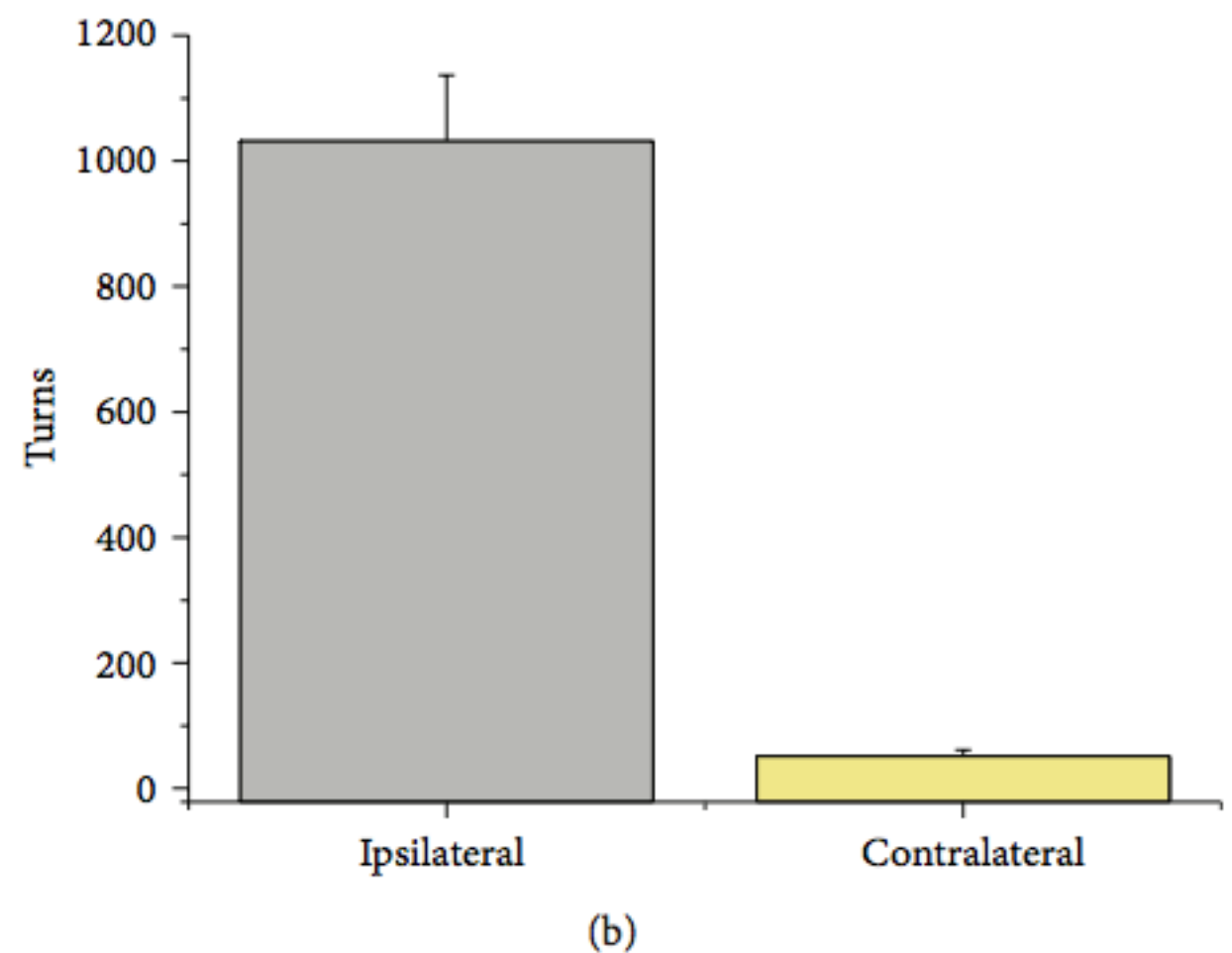


(c)

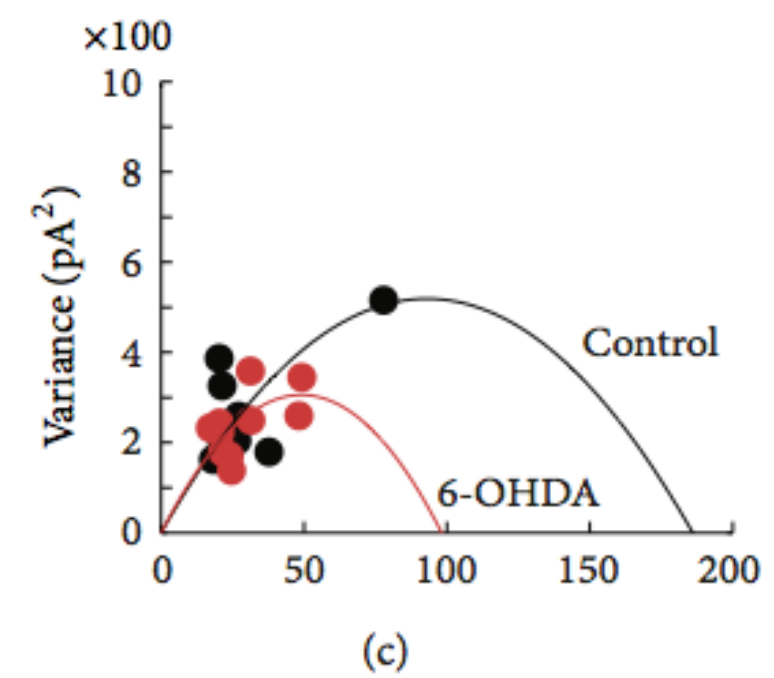
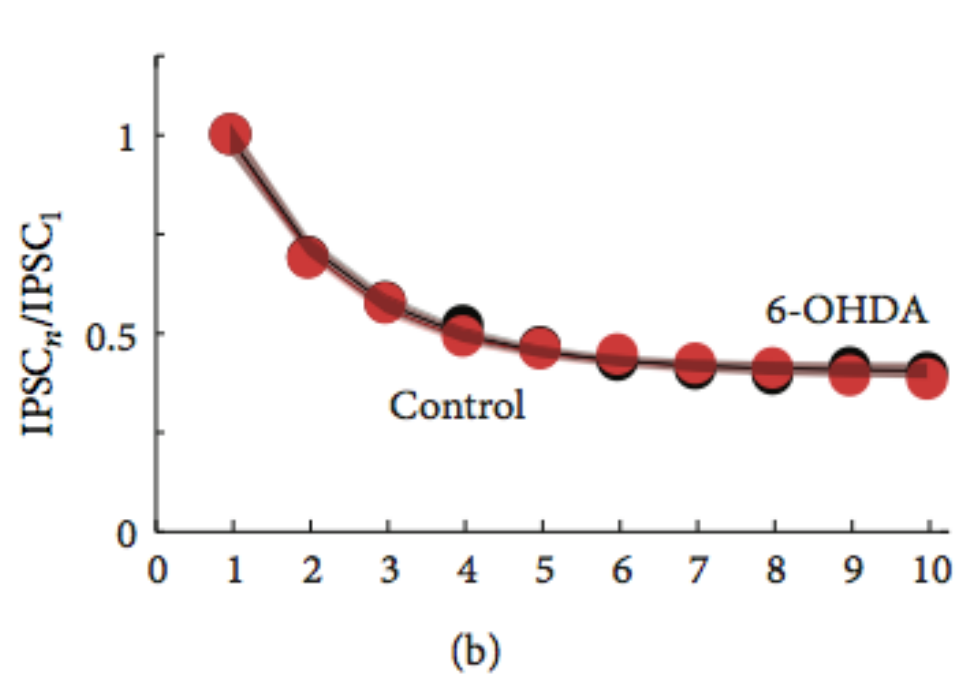
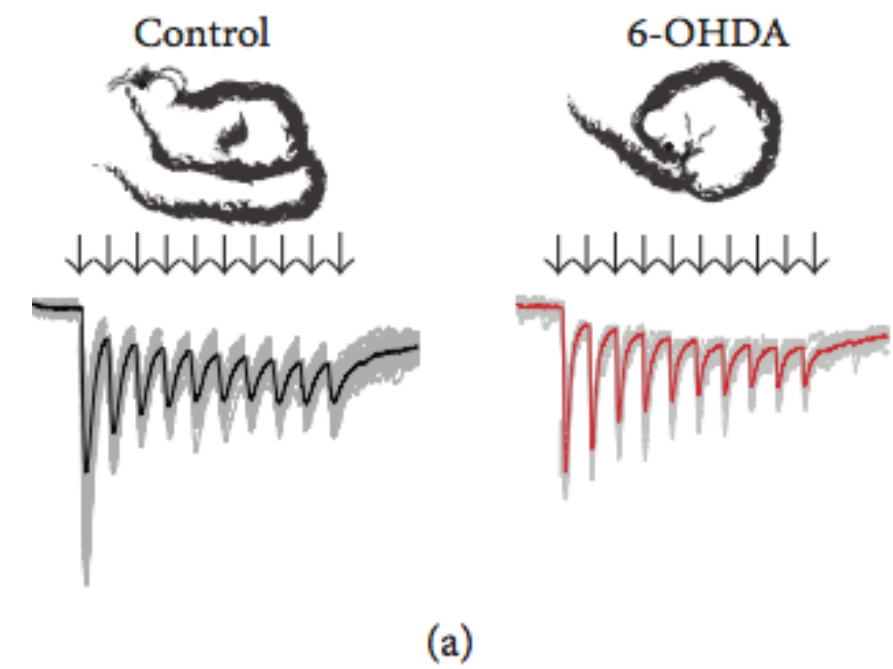
(d)

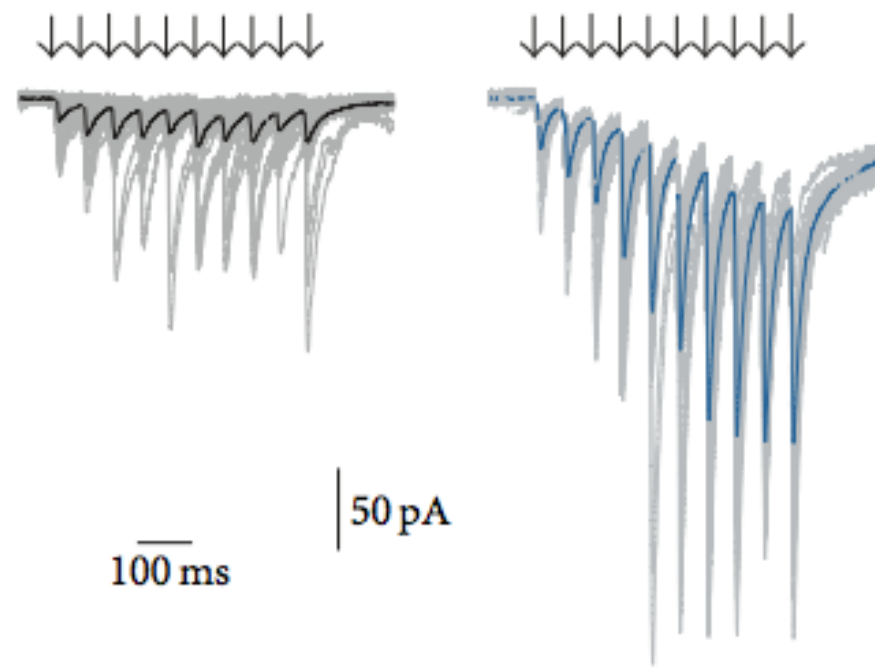


(a)

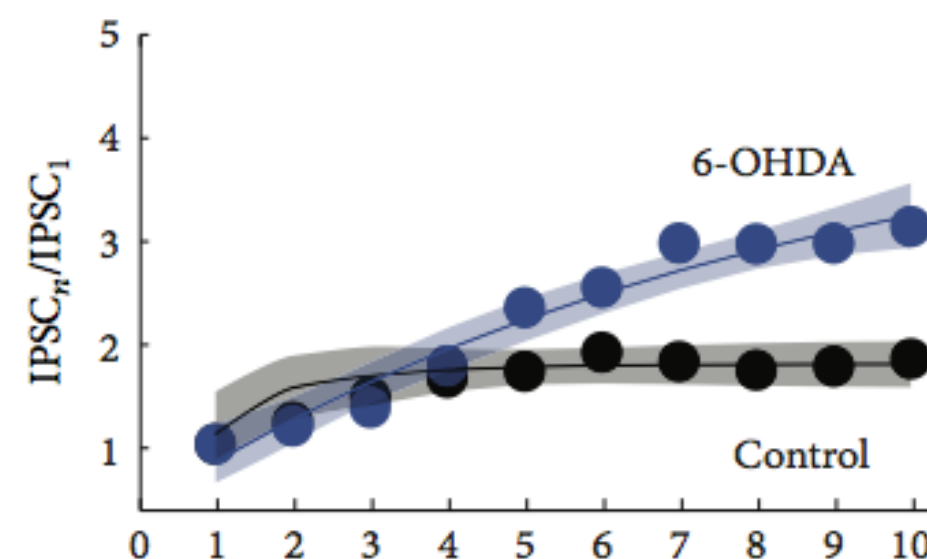


(b)

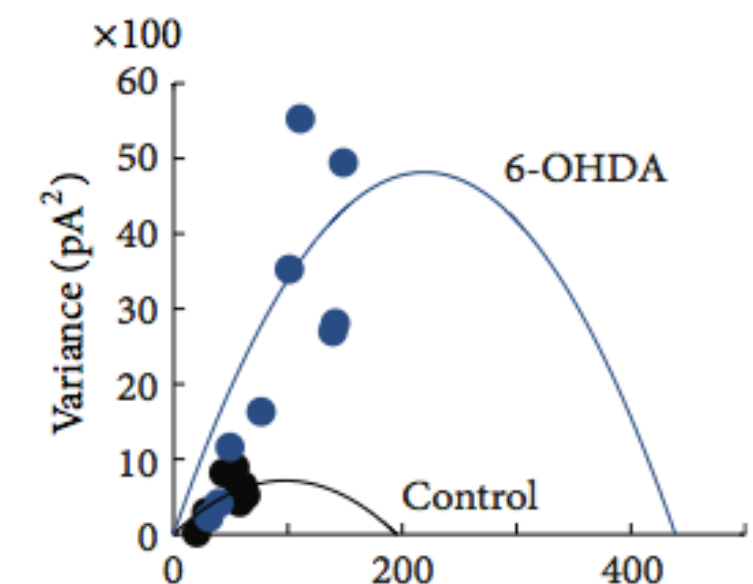




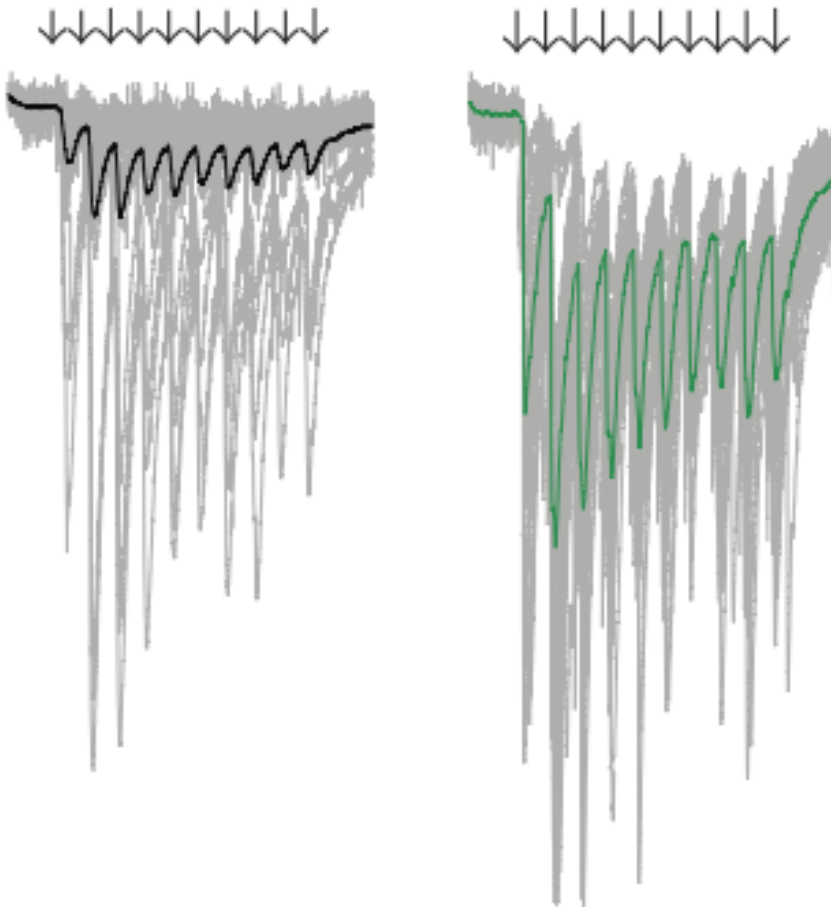
(d)



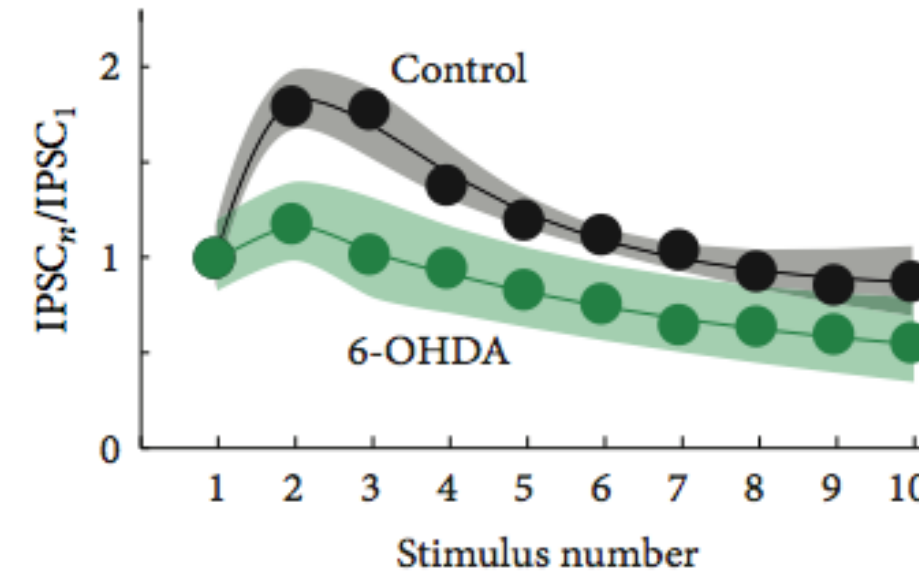
(e)



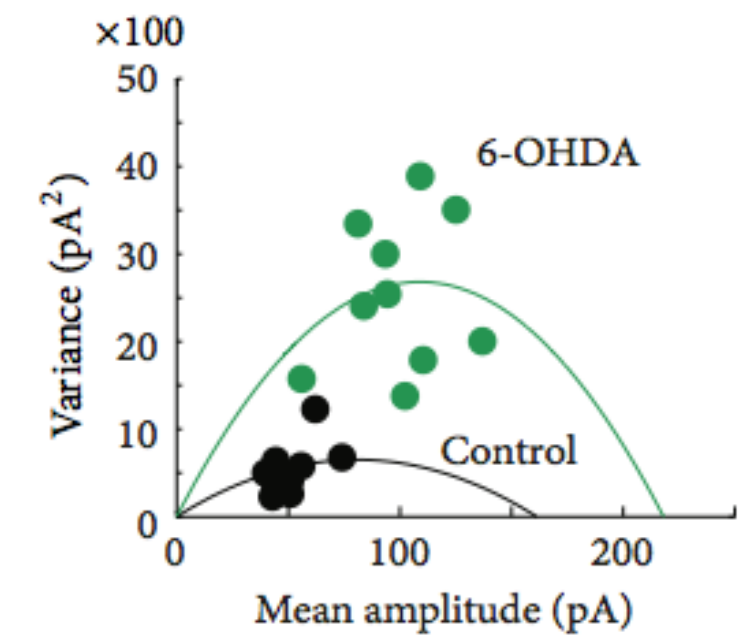
(f)



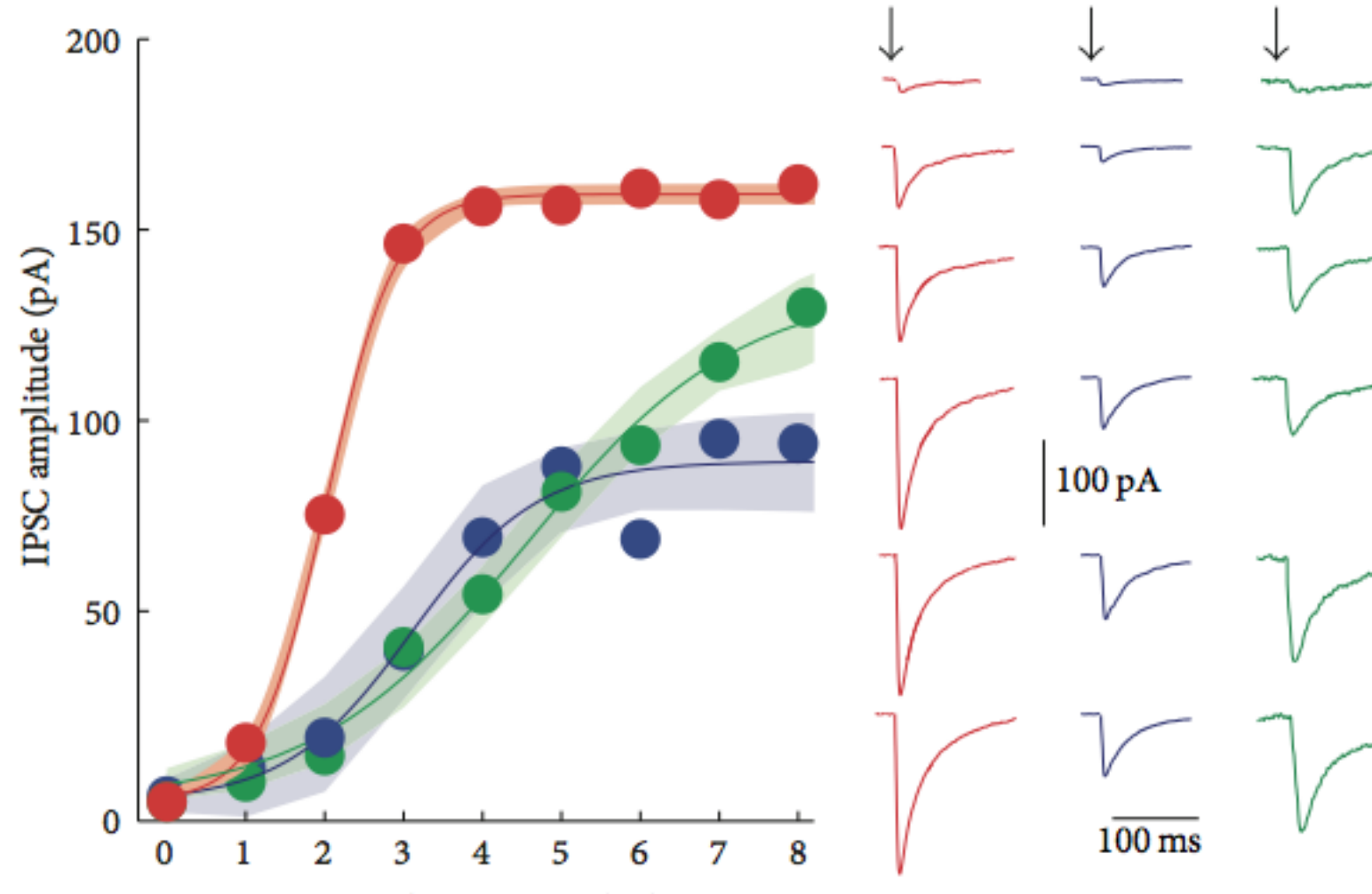
(g)



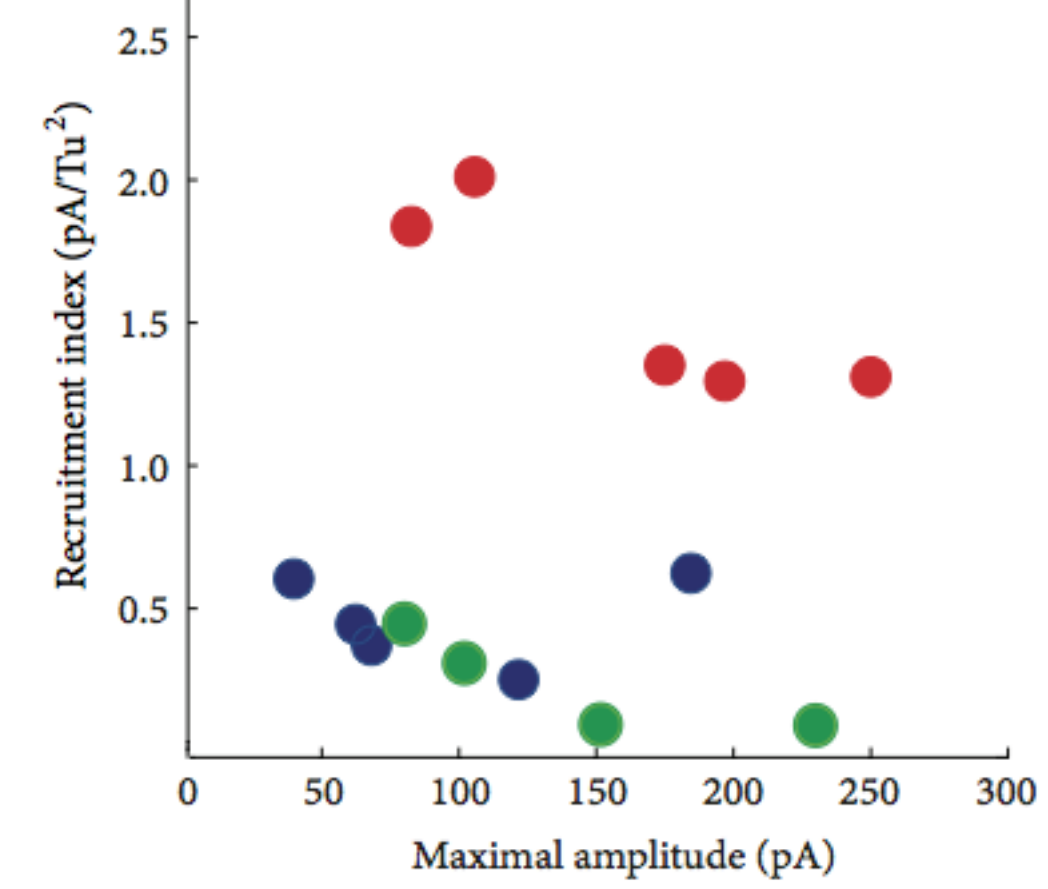
(h)



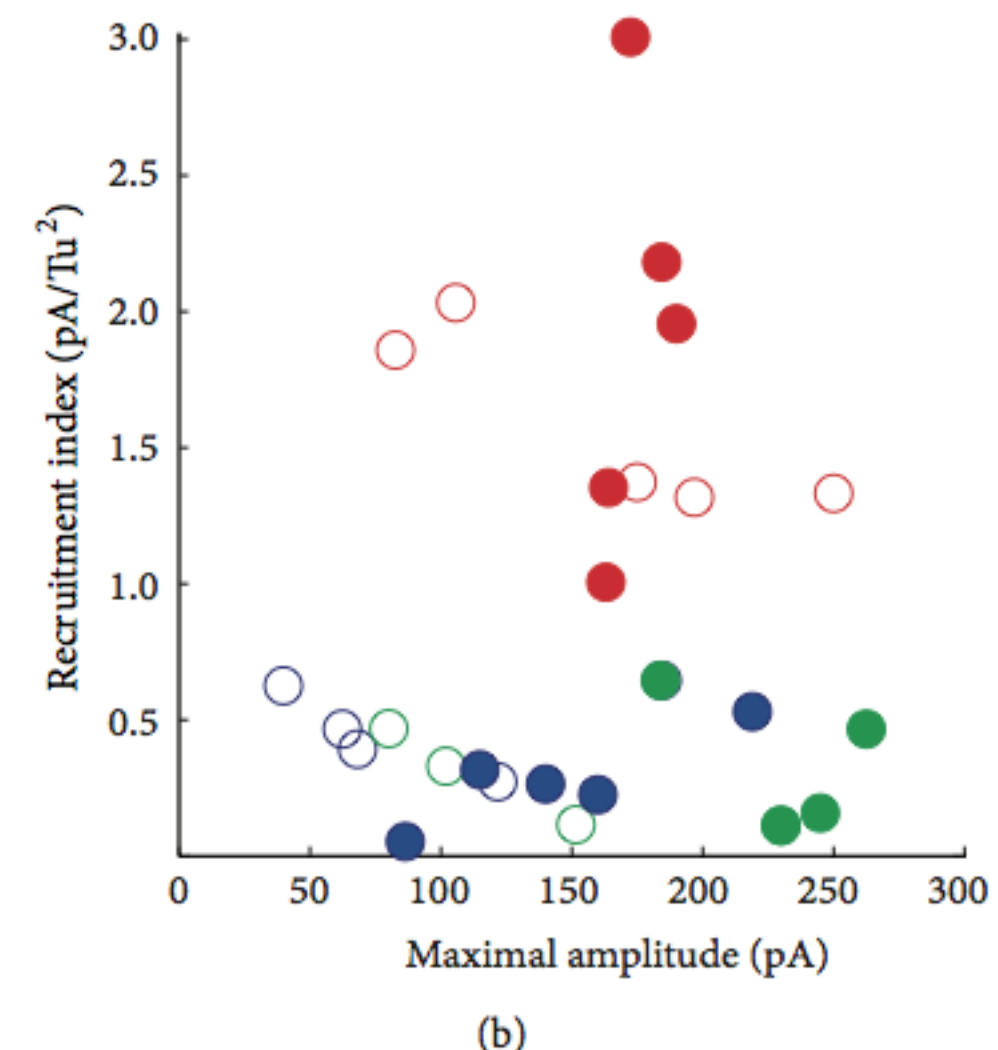
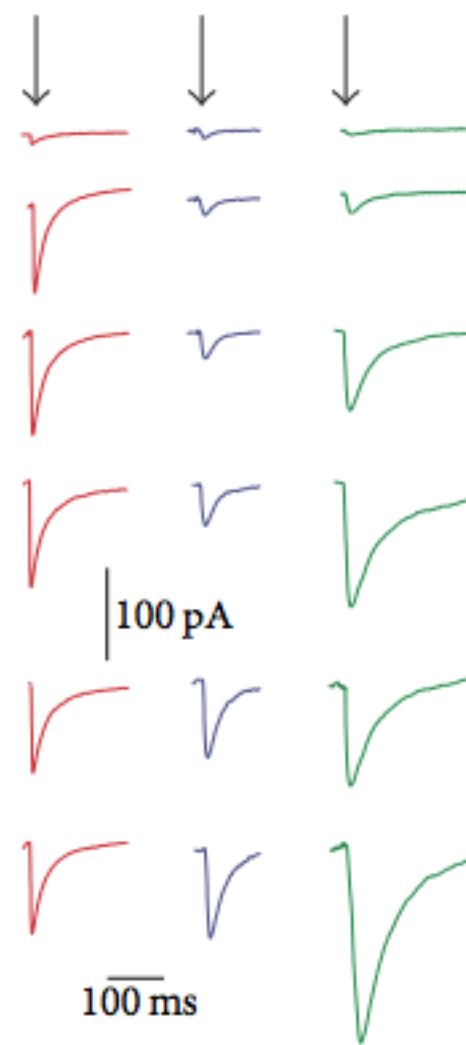
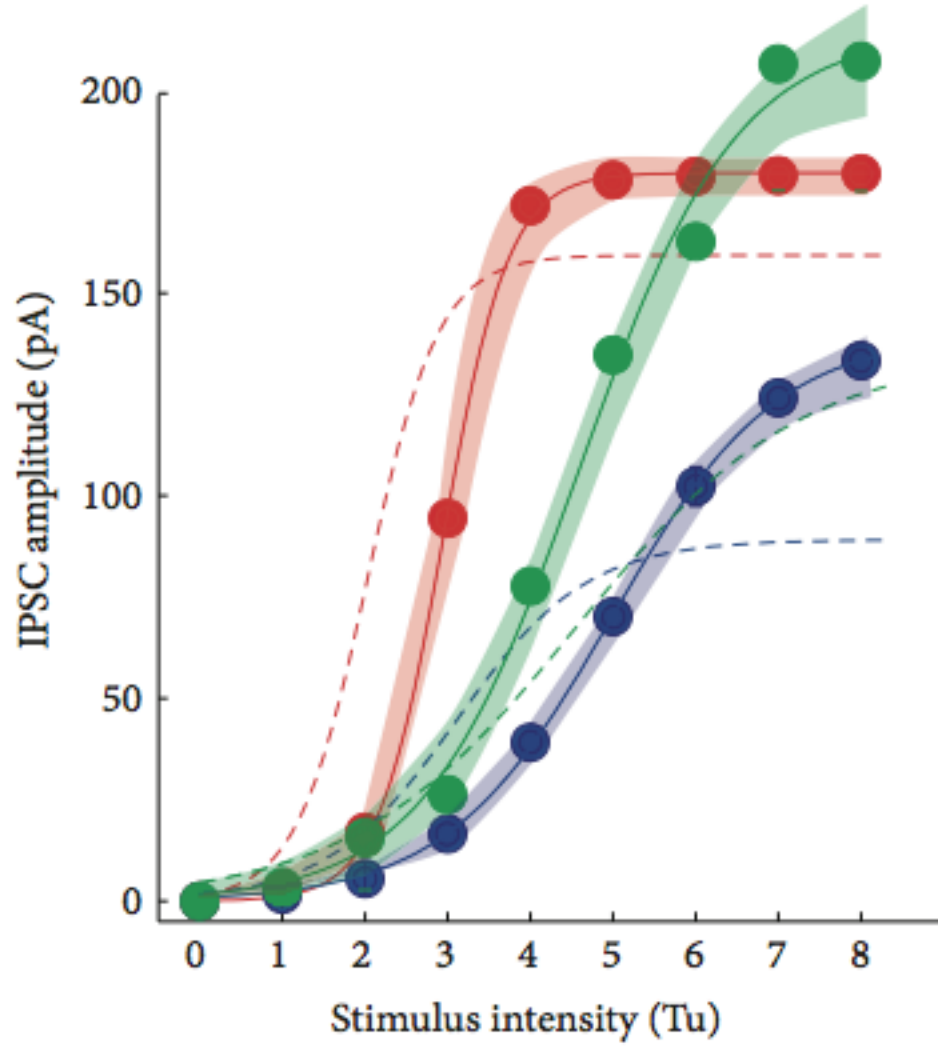
(i)

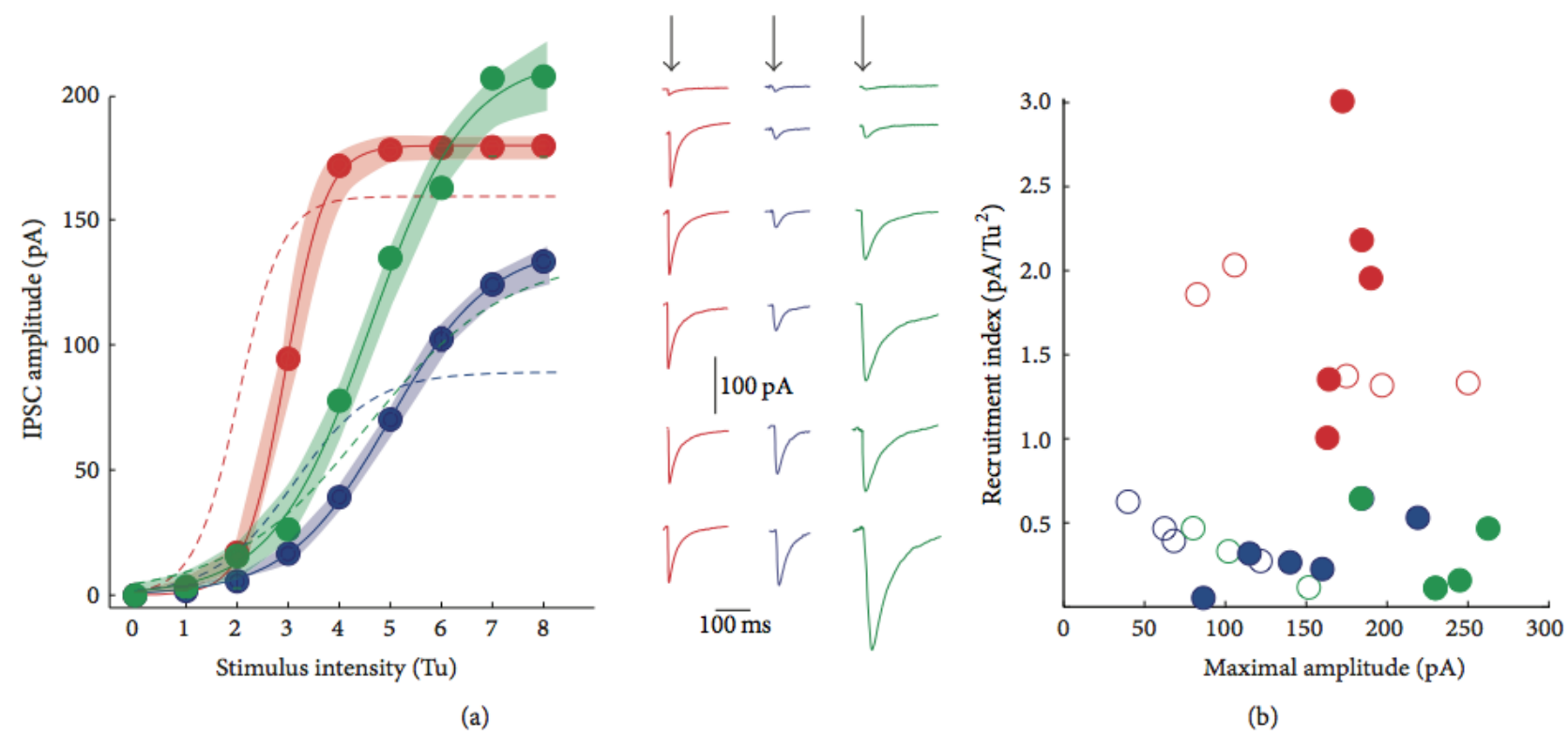
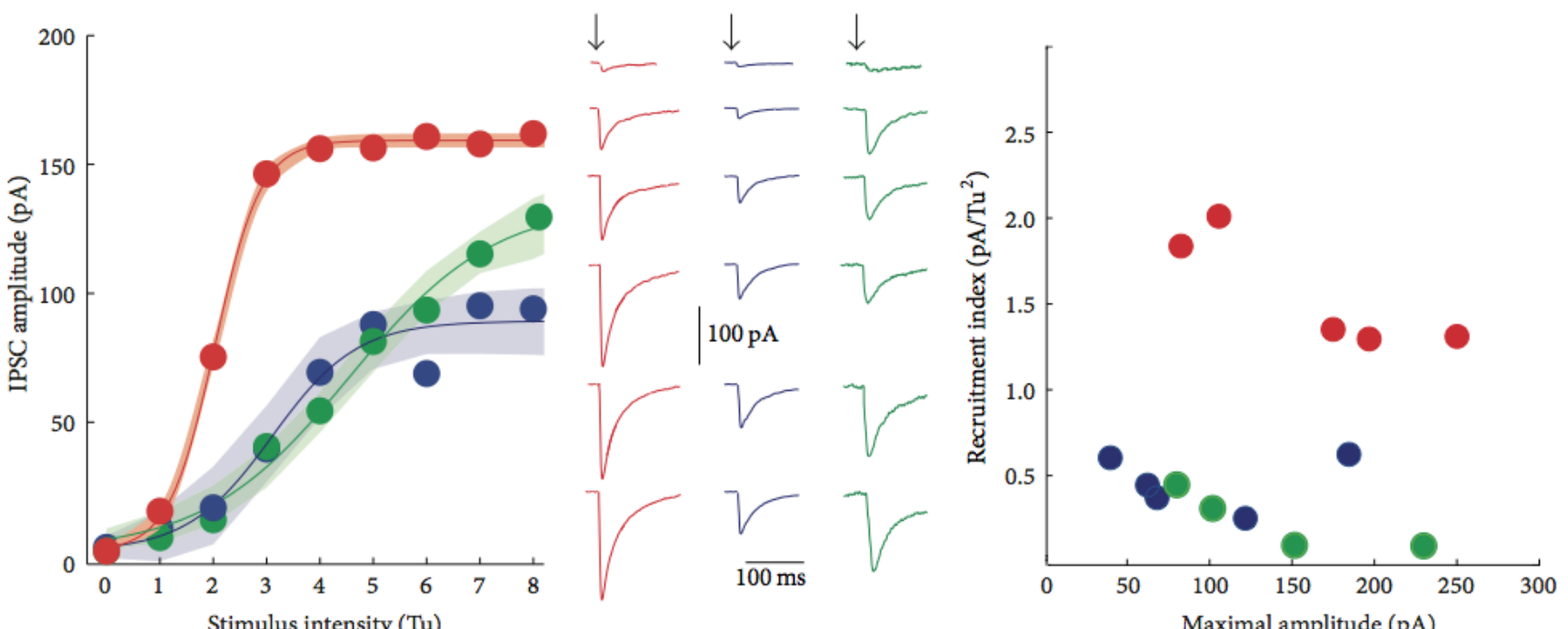


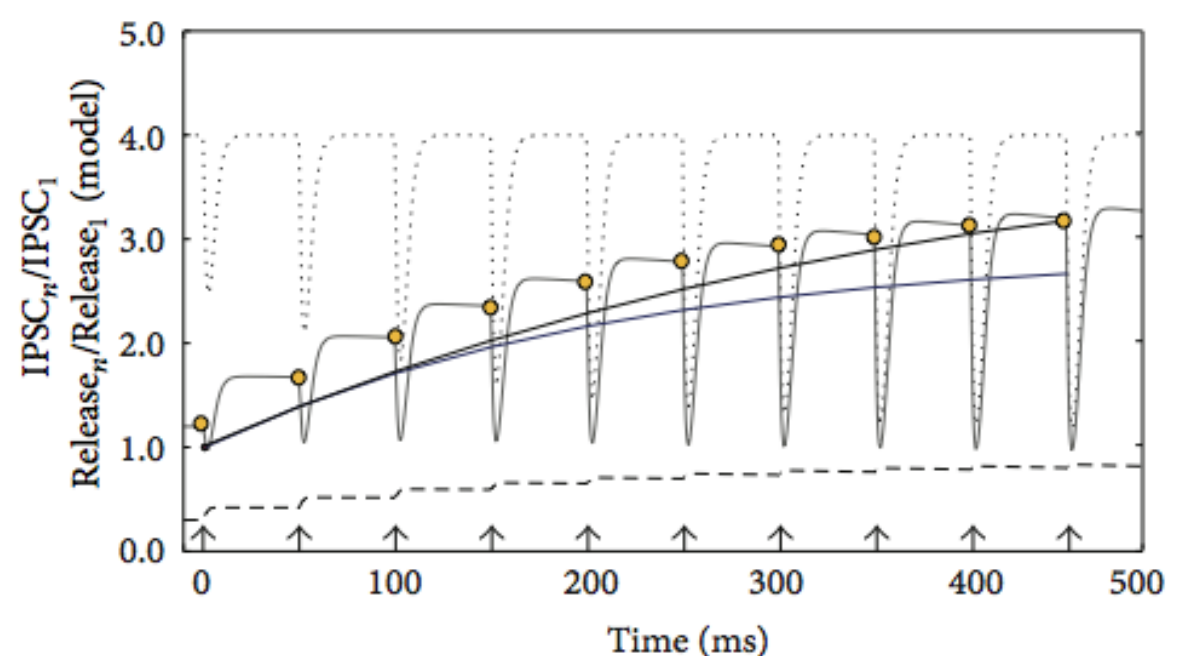
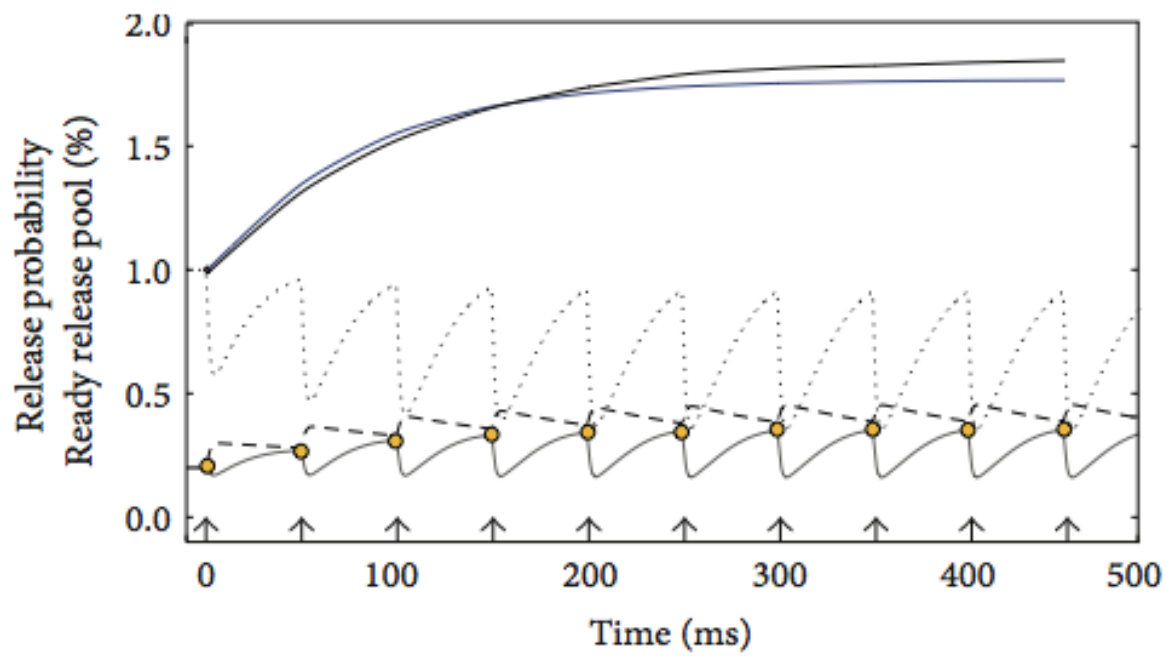
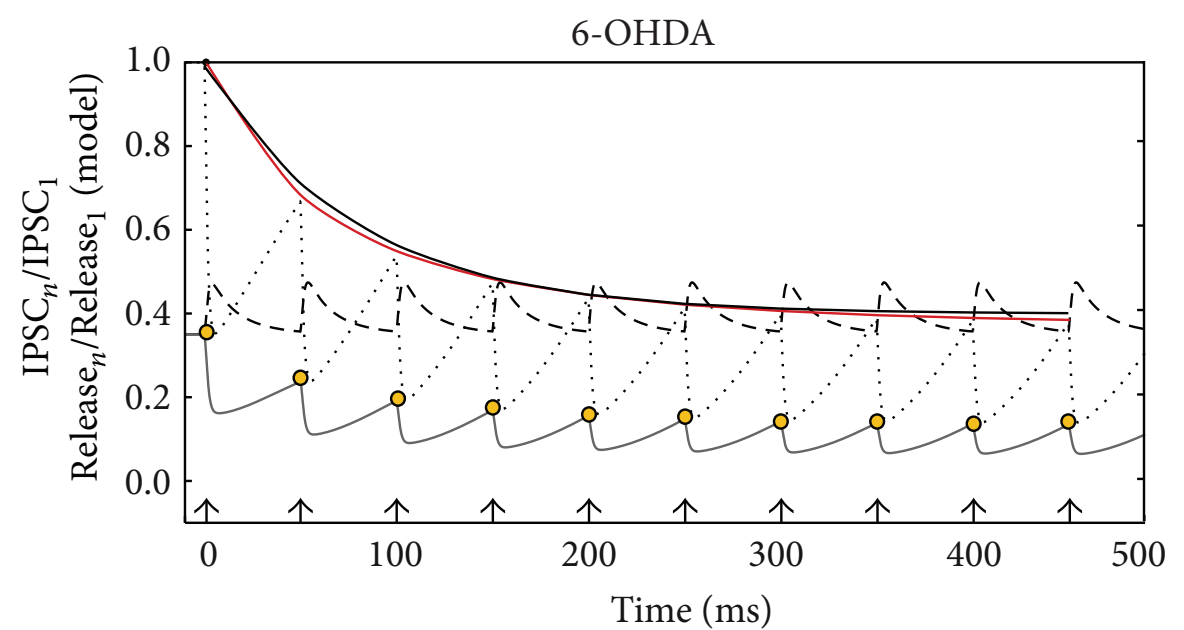
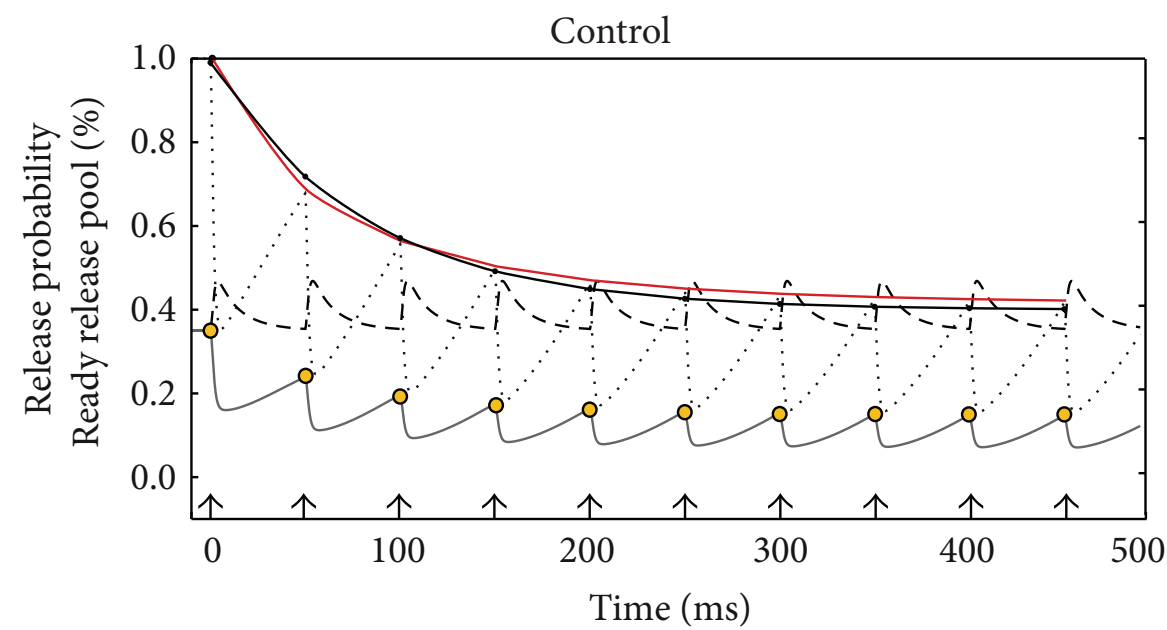
(a)

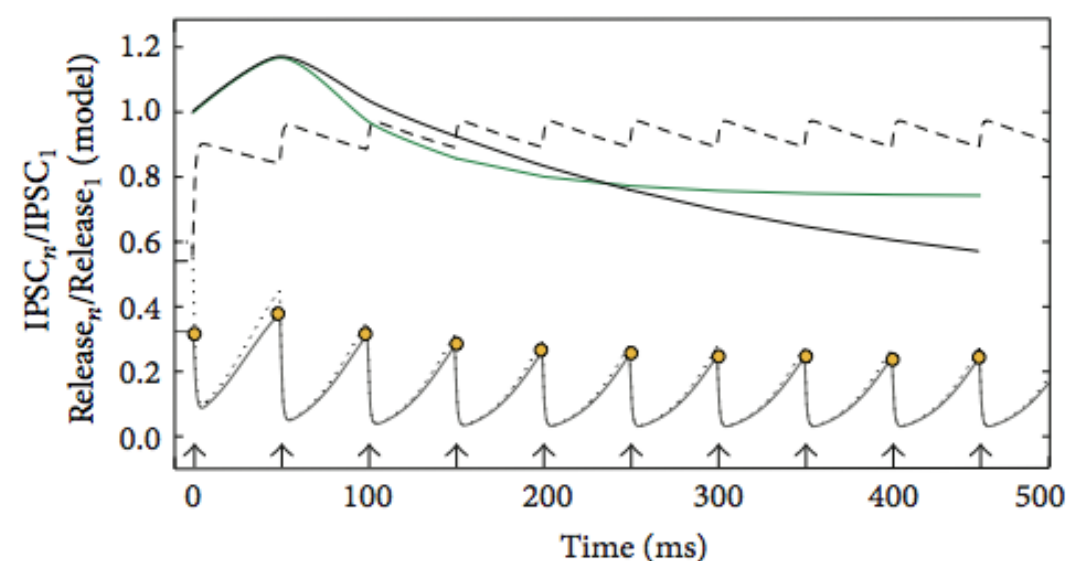
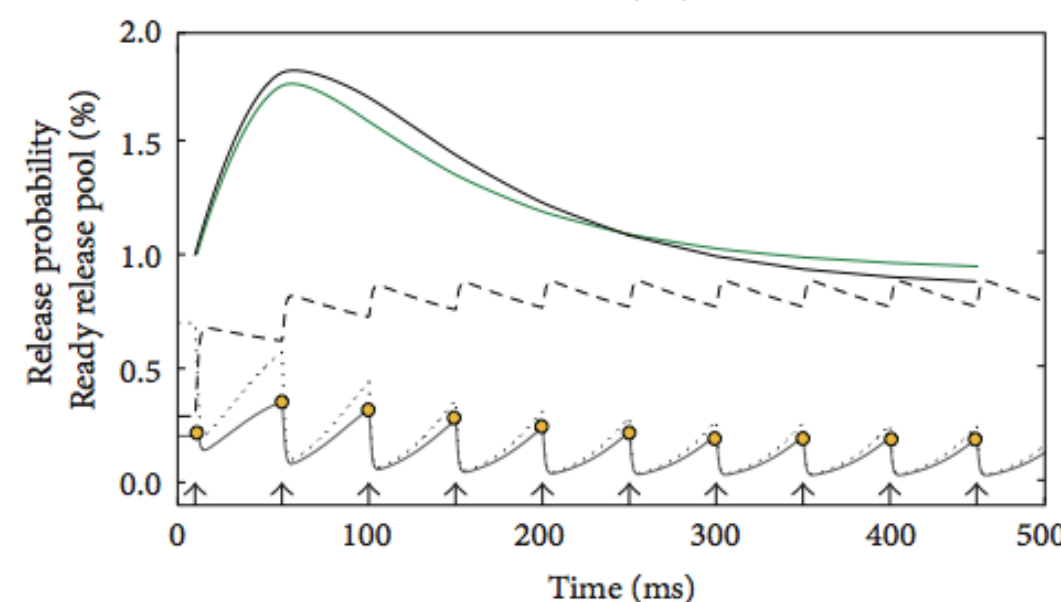
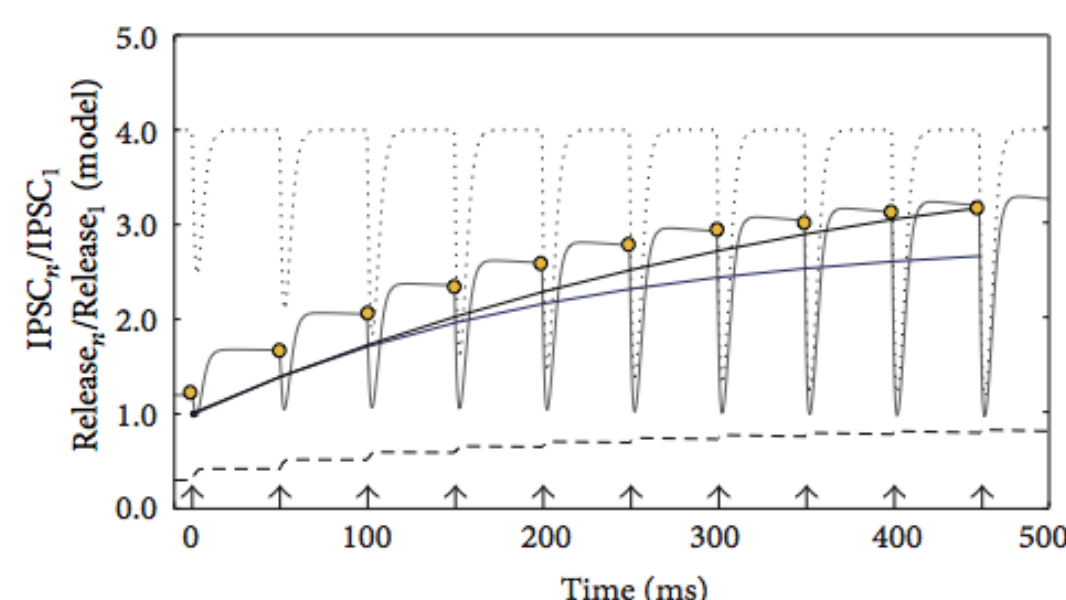
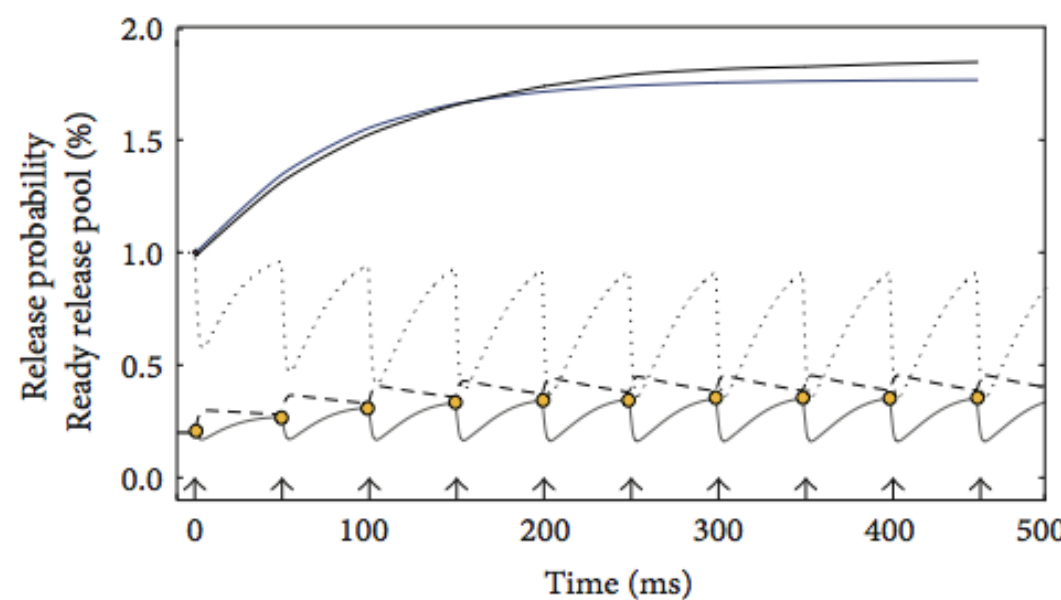
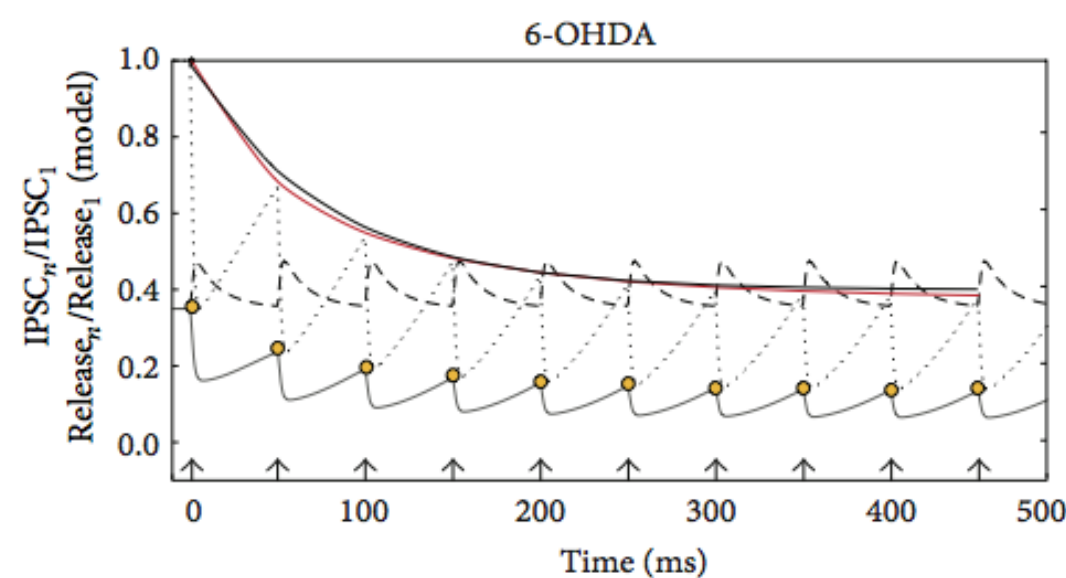
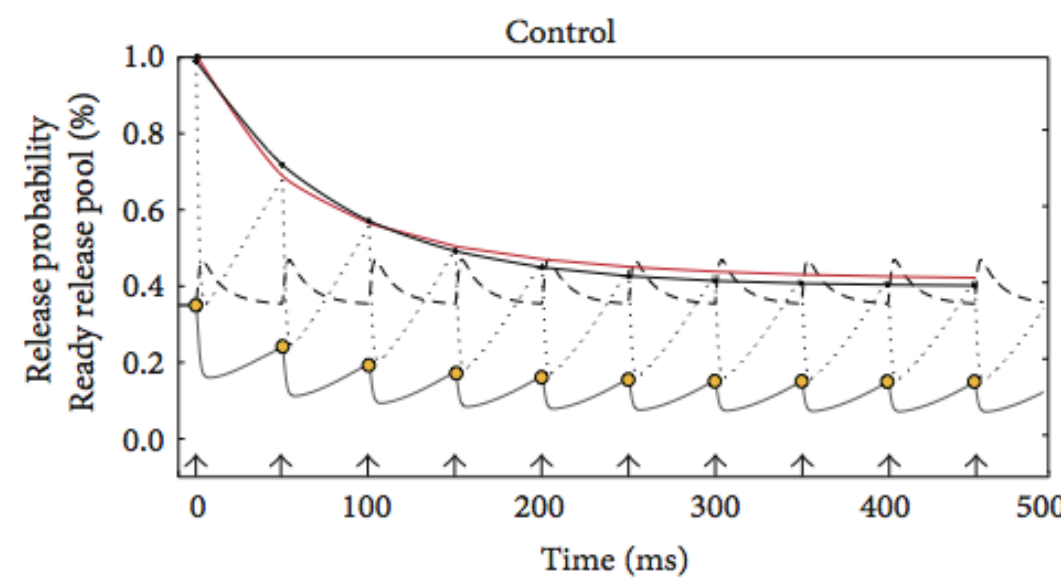


(b)



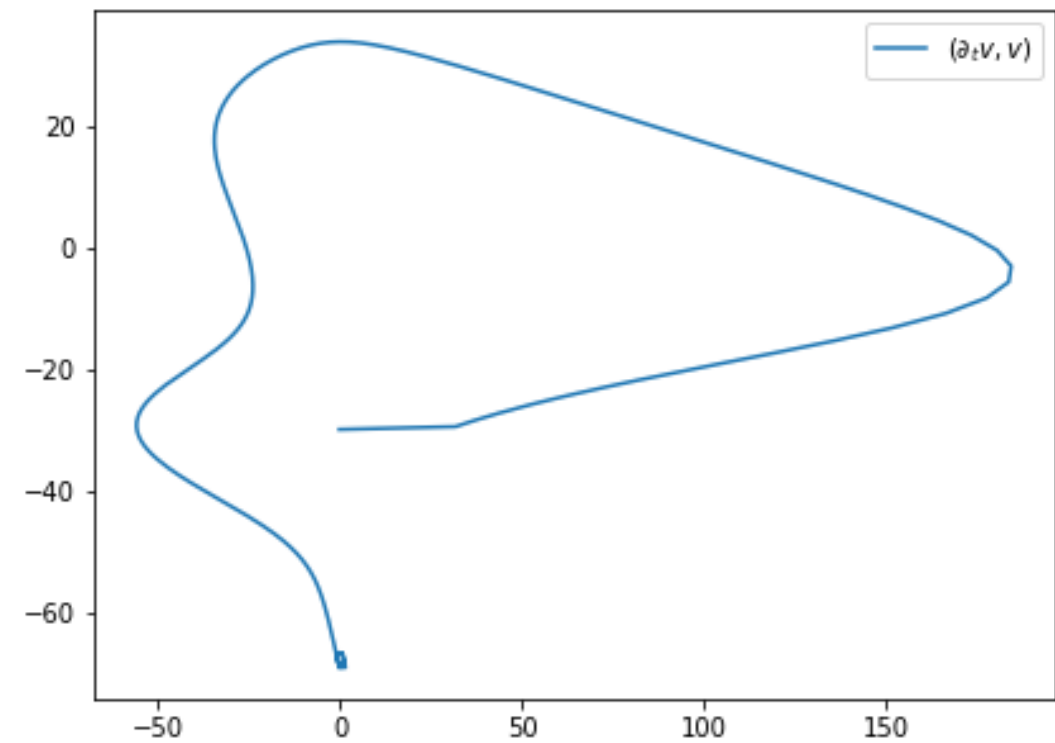
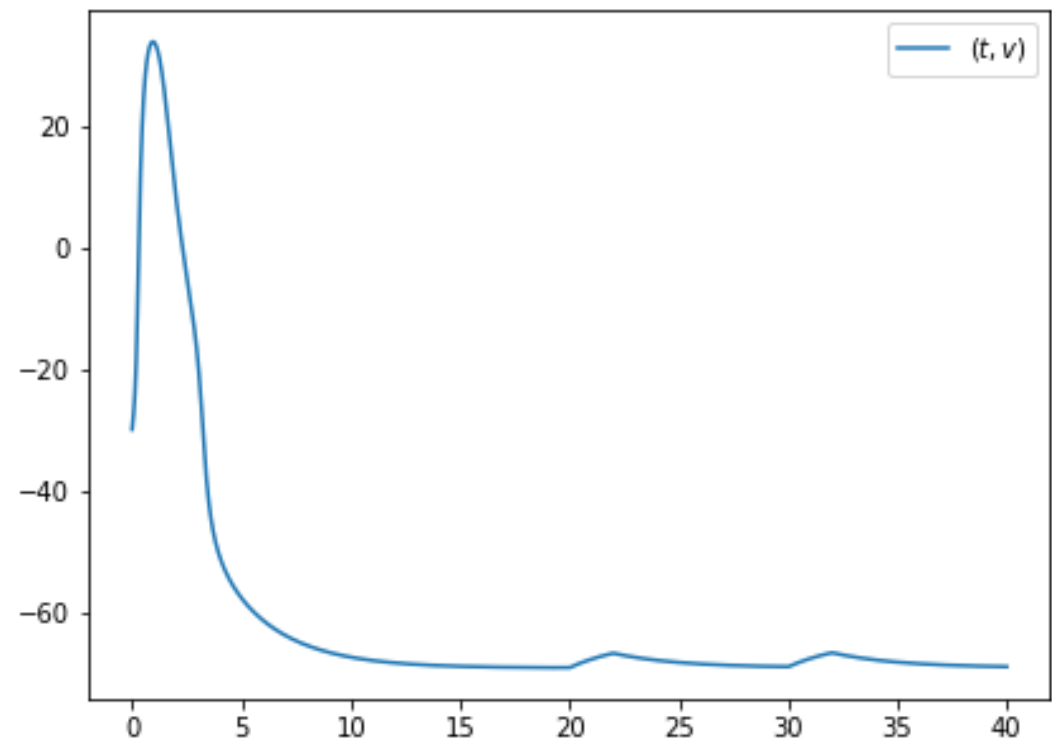


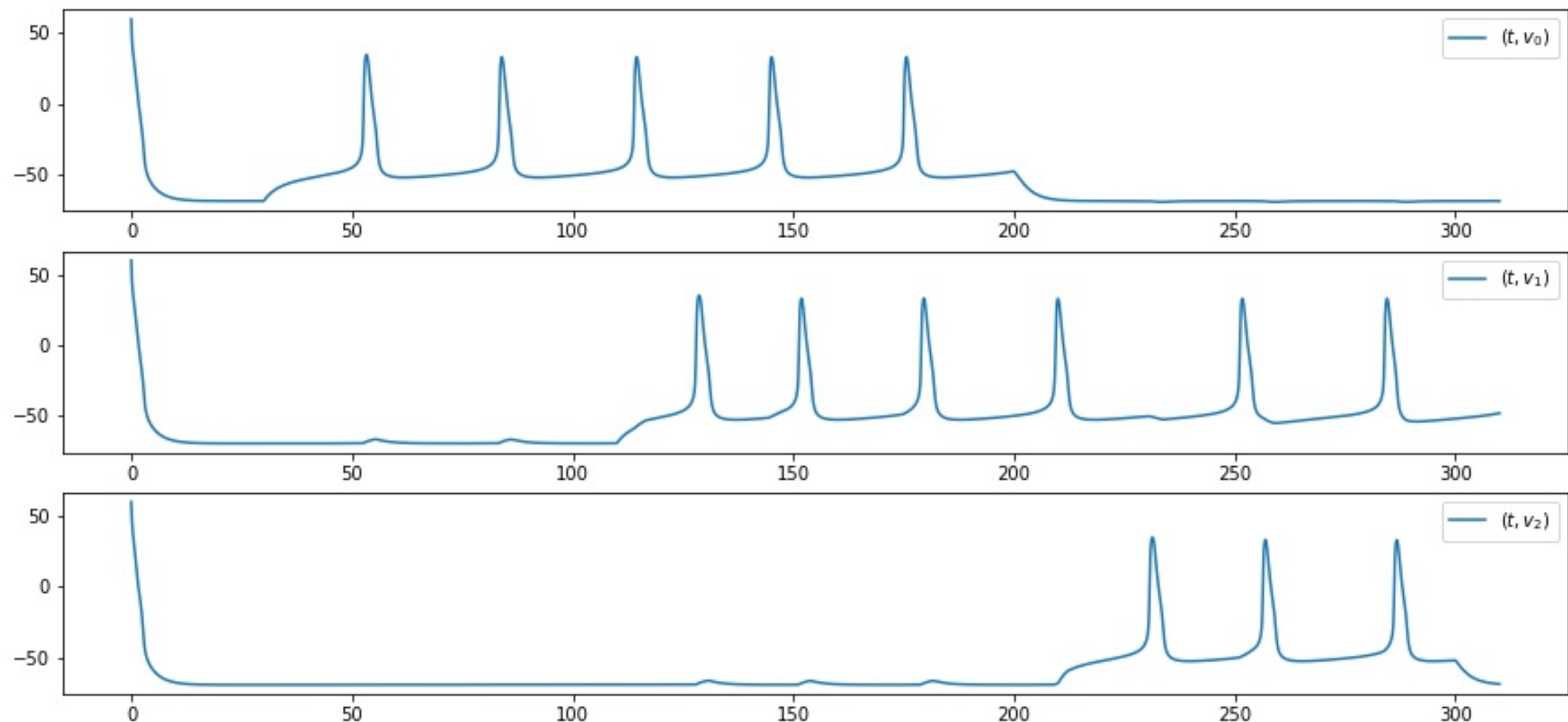


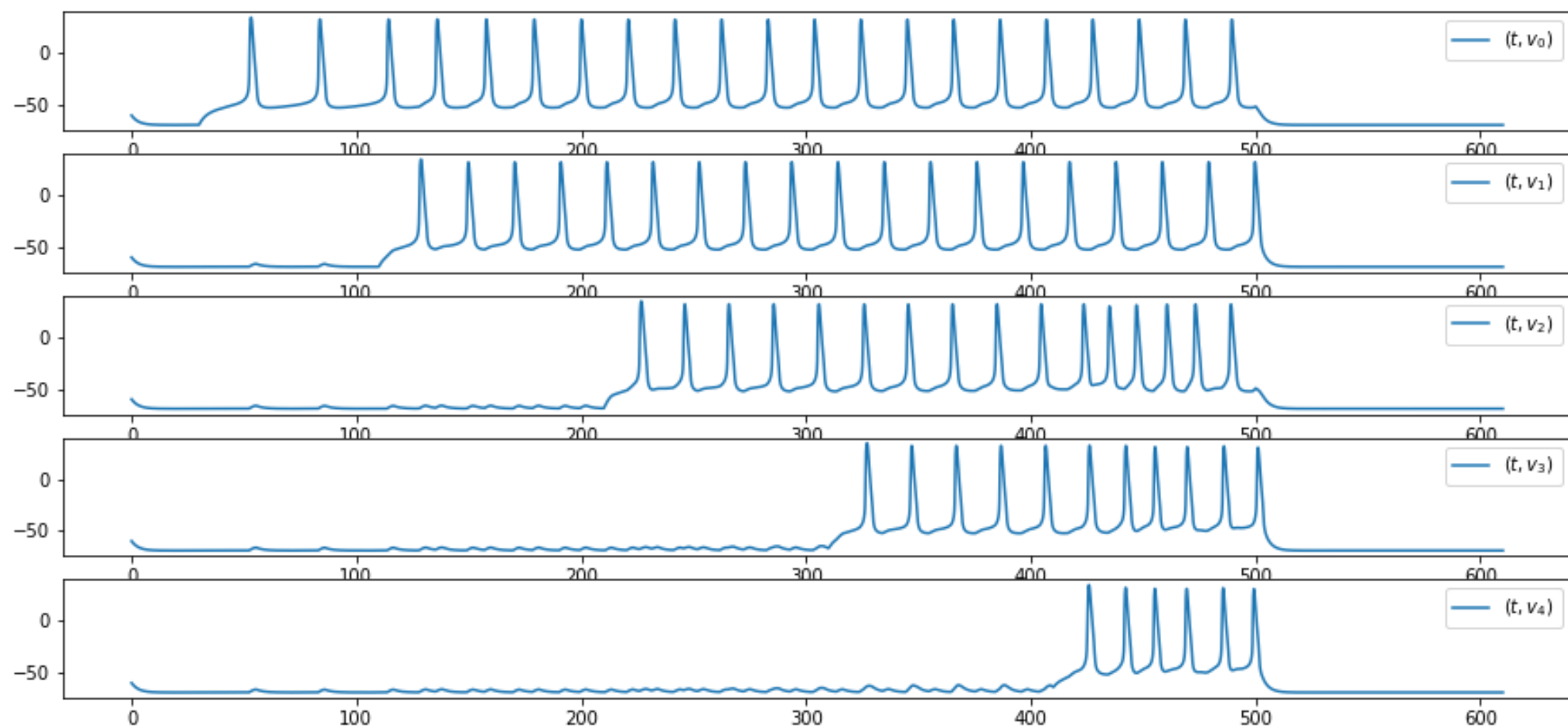
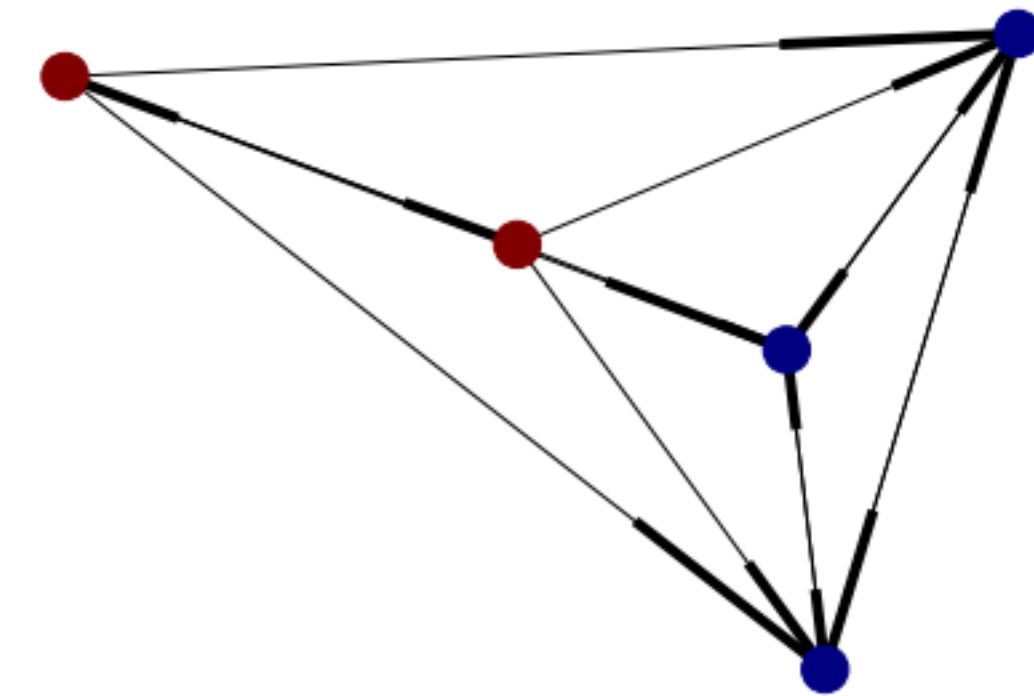


Cellular excitability and activity in neuronal networks:
Changes in joint activity in neurons receiving
common synaptic input

Network dynamics with reduced biophysical models



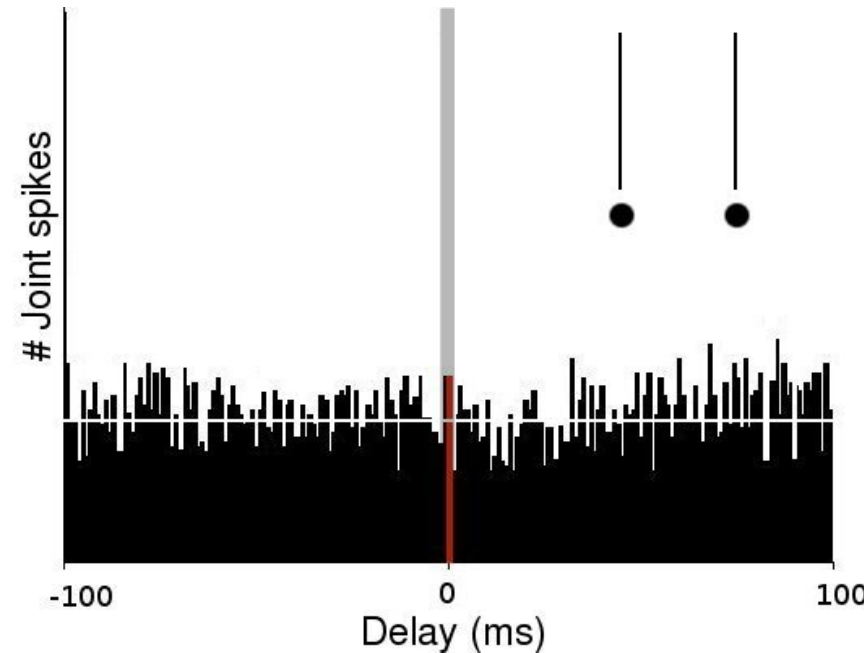




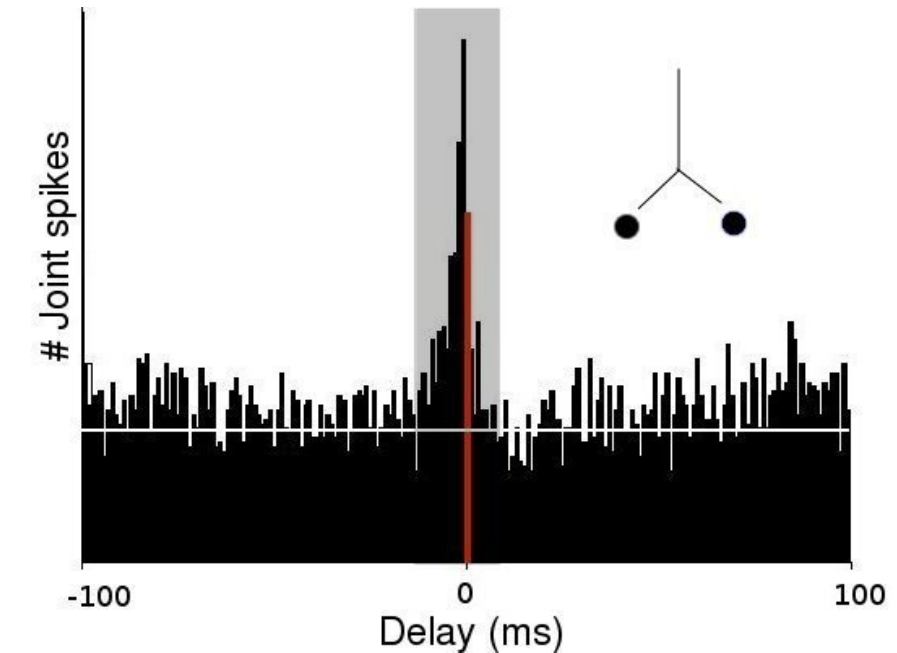
Changes in joint activity in neurons receiving common synaptic input

Thumb-index flexor motor units pairs show nearly coincident spiking, but other finger flexor pairs do not.

d1 vs d2, d3, d4



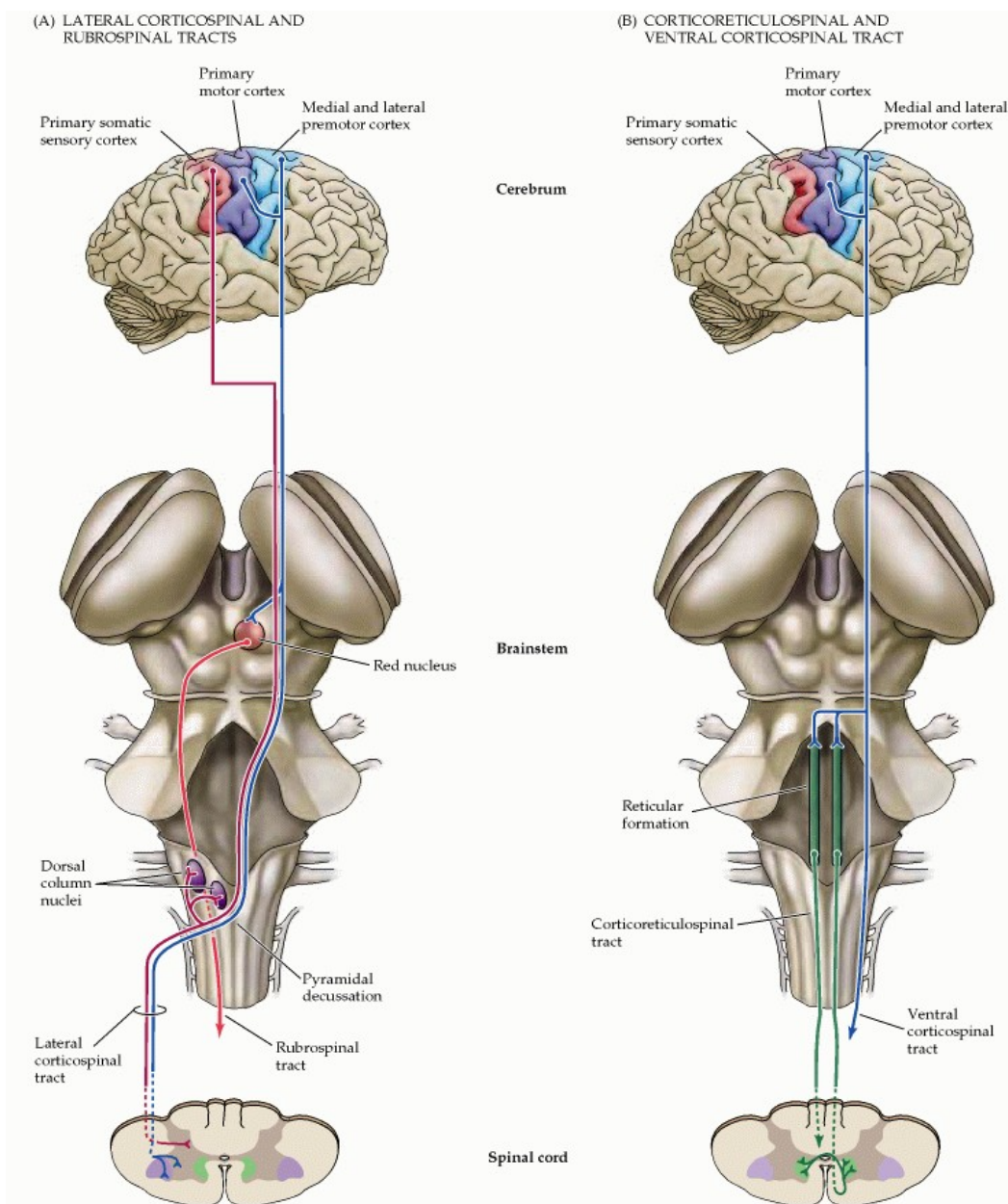
Index vs thumb



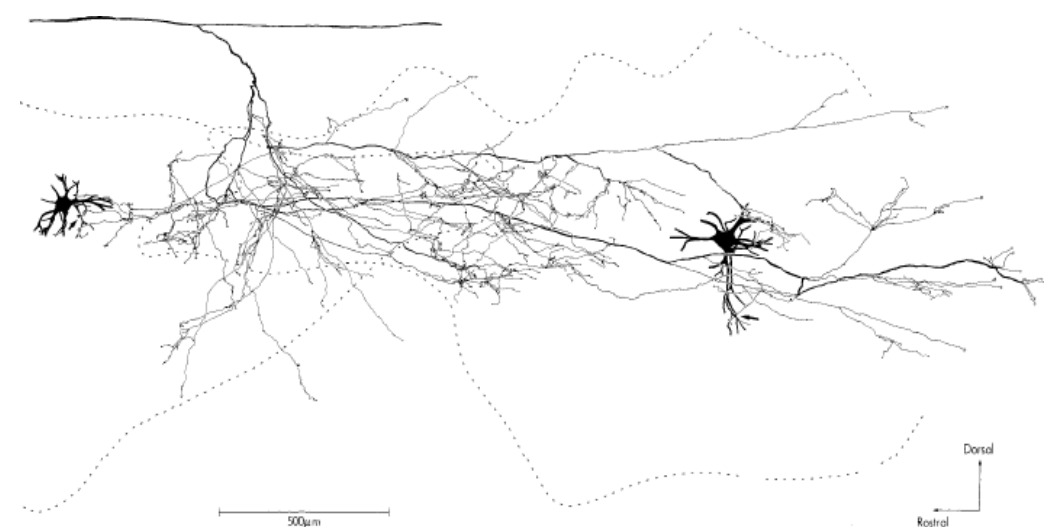
Does nearly-coincident spiking result from the joint occurrence of unitary post-synaptic potentials from common stem presynaptic fibers?

Fuglevand, et al, 2004

Motor pathways in human

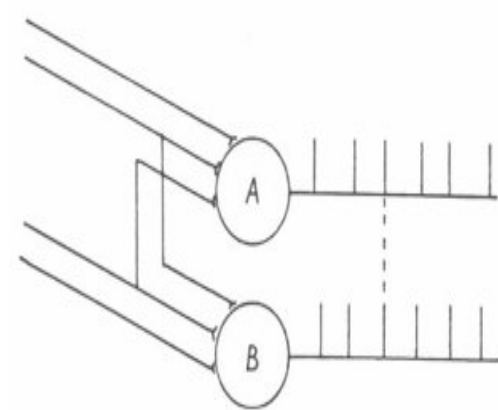


Corticospinal axon collaterals reach multiple levels of the spinal cord

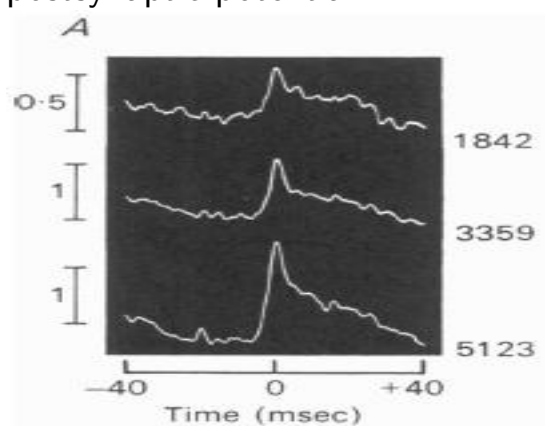


From Laurence, Porter and Redman 1985.

"Short term synchrony":

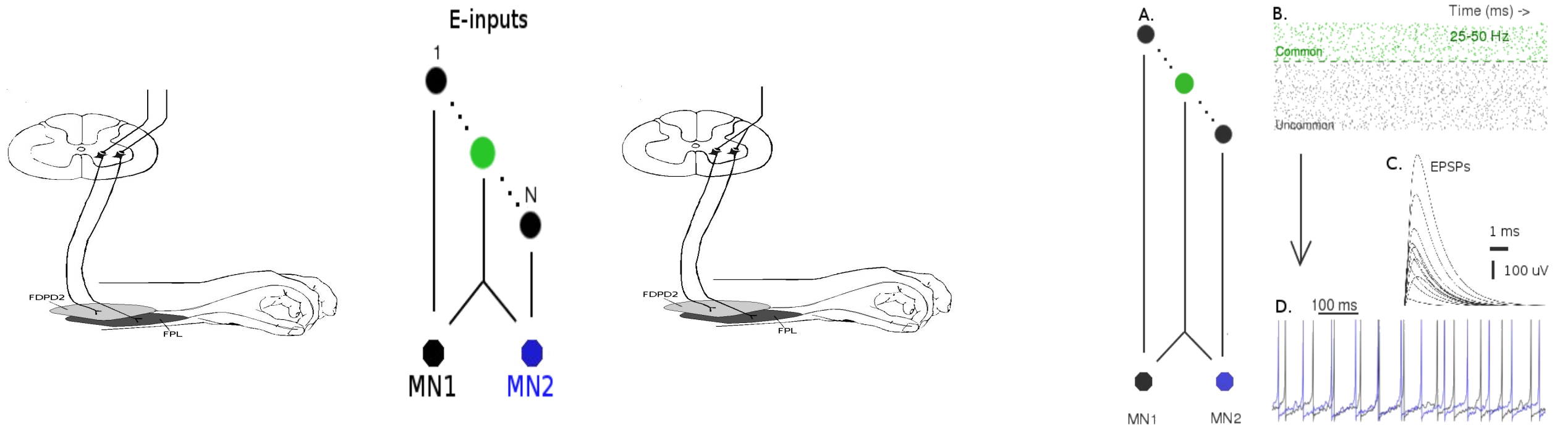


Common average excitatory postsynaptic potential:



"Short-term synchrony results from the joint occurrence of unitary post-synaptic potentials from common stem presynaptic fibers." Sears and Stagg 1976

Model

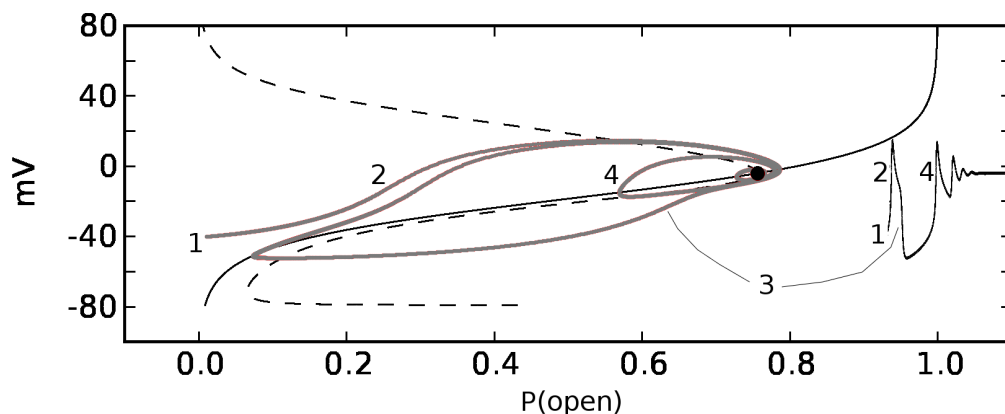
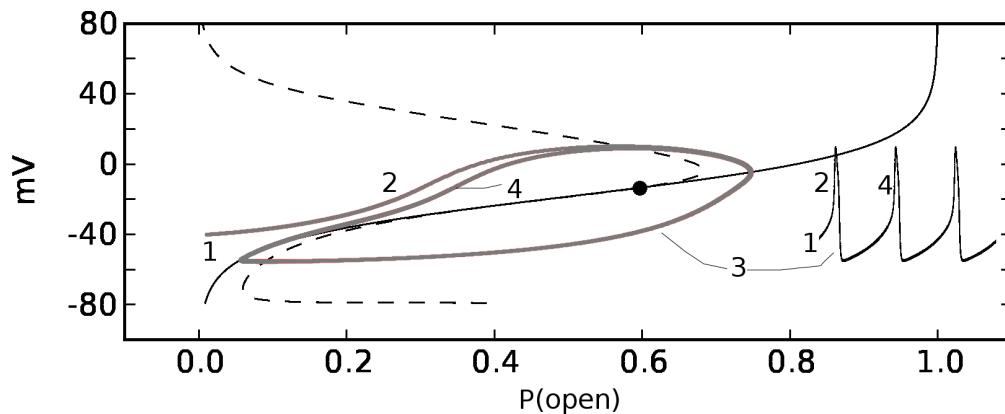
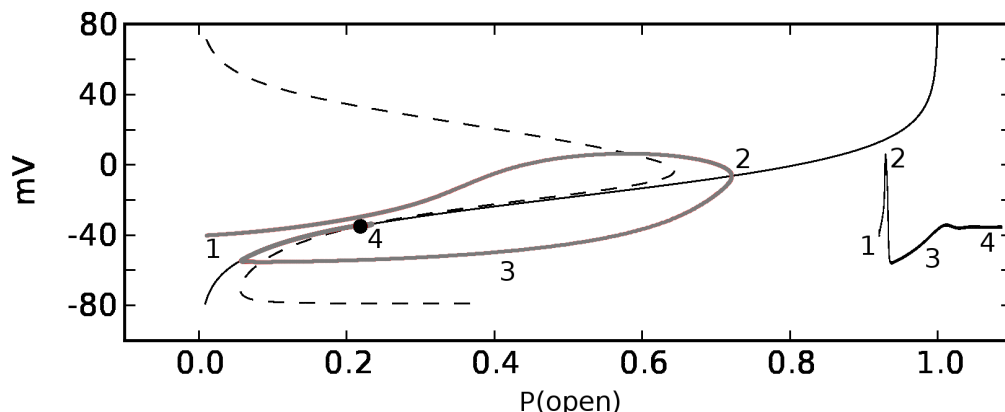


$$C_m \partial_t v = -I_K(w, v; p) - I_{Na}(w, v; p) - I_{NaK}(v; p) - I_E(t, \bar{a}_E, v; q) - I_I(t, \bar{a}_I, v; q) - I_F(t, \bar{a}_F; q),$$

$$\partial_t w = w^k \frac{w_\infty(v; p) - w}{\tau_w(v; p)},$$

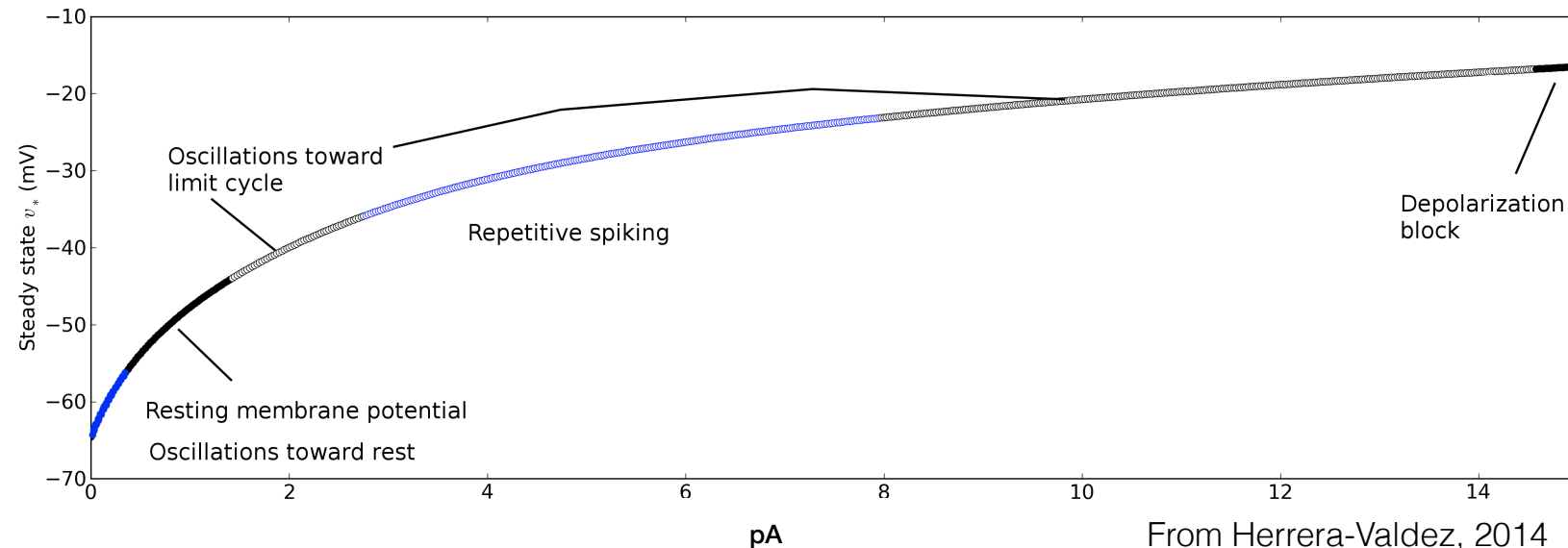
Same neuron, possibly different responses to stimulation

The internal and external context matter



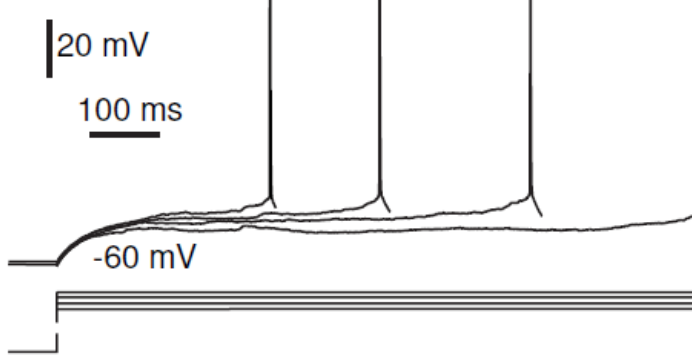
From Herrera-Valdez, 2008

Sequences of bifurcations as a function of input current:
The same neuron can integrate inputs in different ways depending on the external current



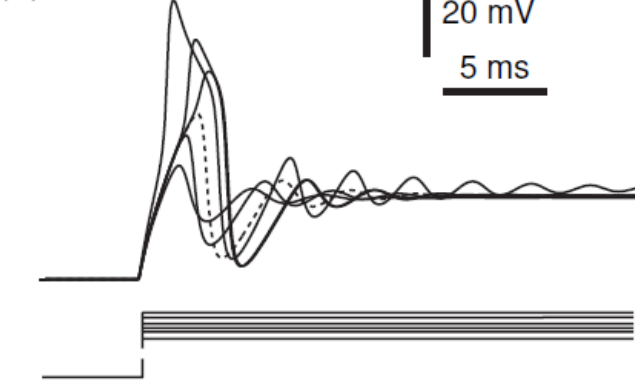
Aggregation

(a) Near asymptotically stable nodes



Resonance

(b) Near asymptotically stable foci

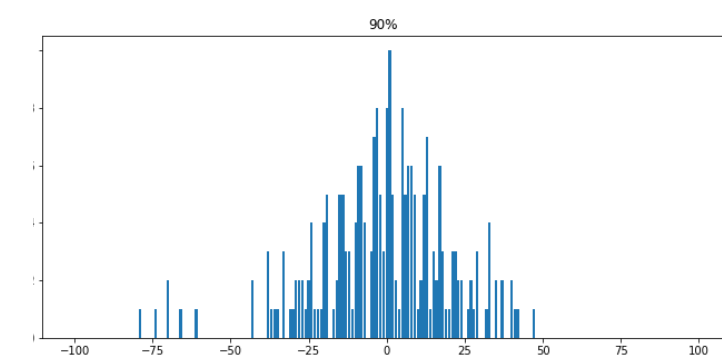
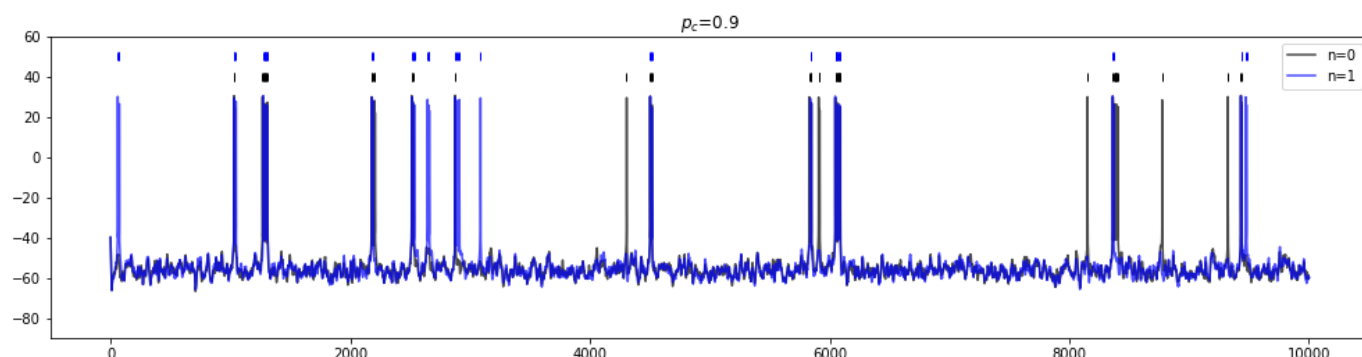
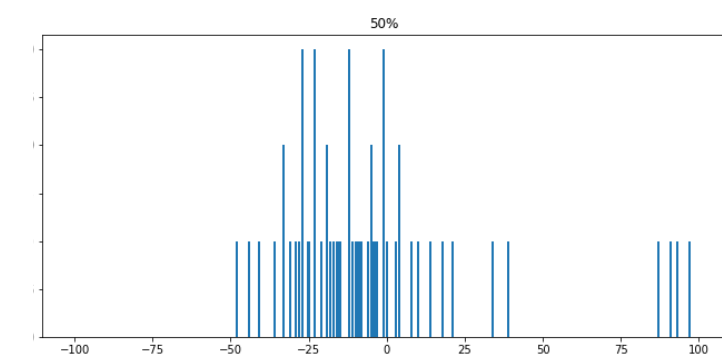
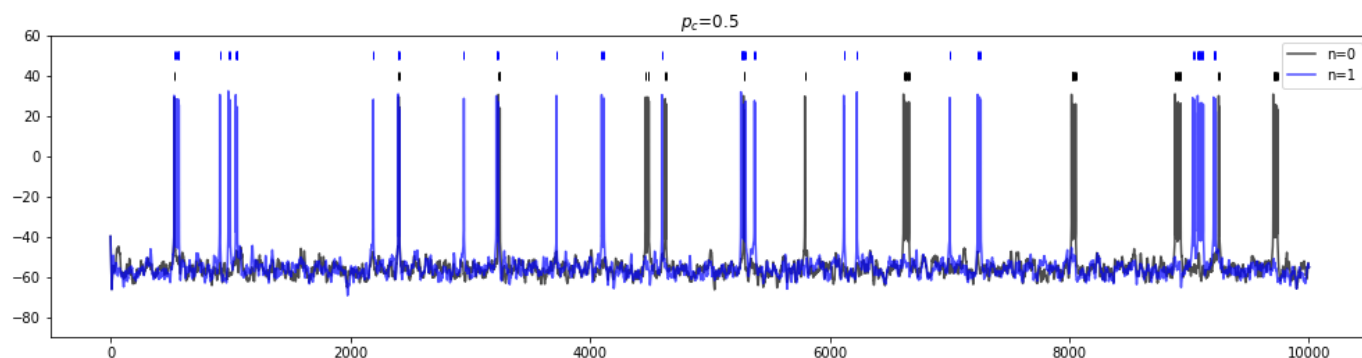
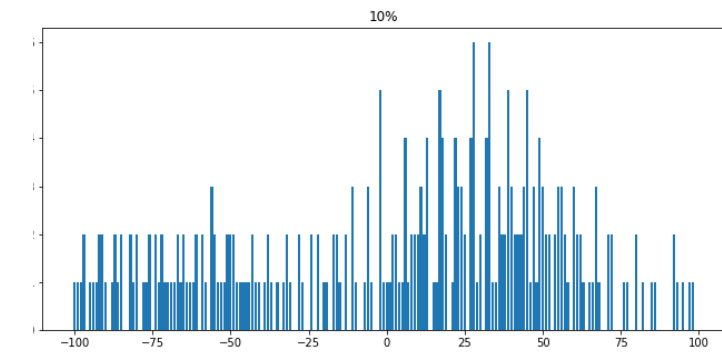
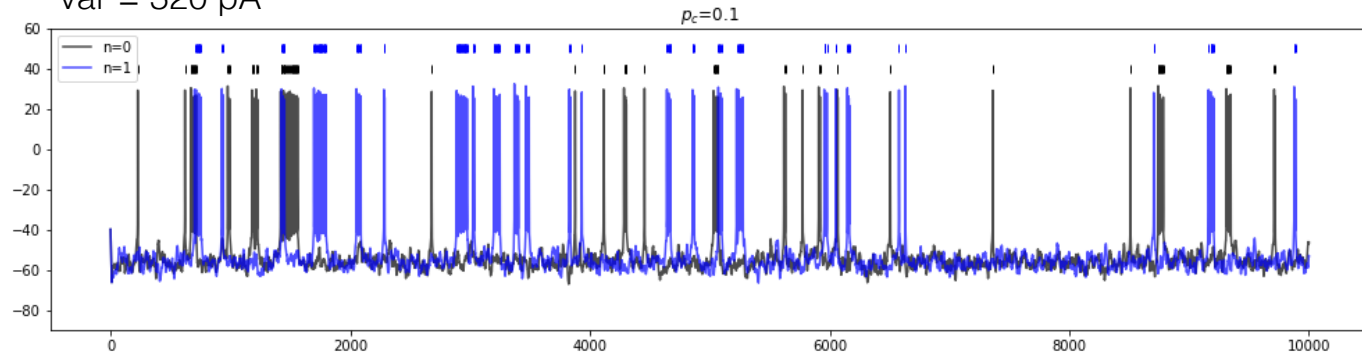


From Izhikevich, 2006

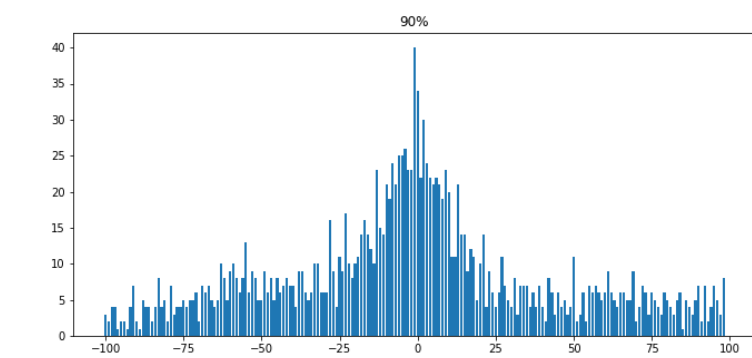
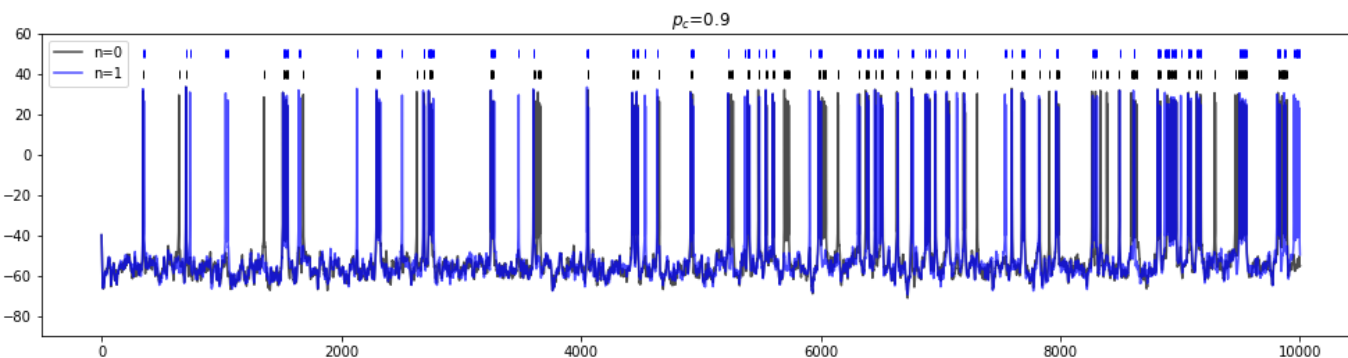
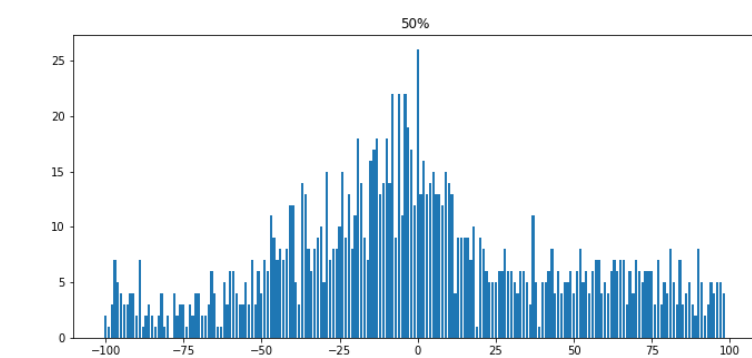
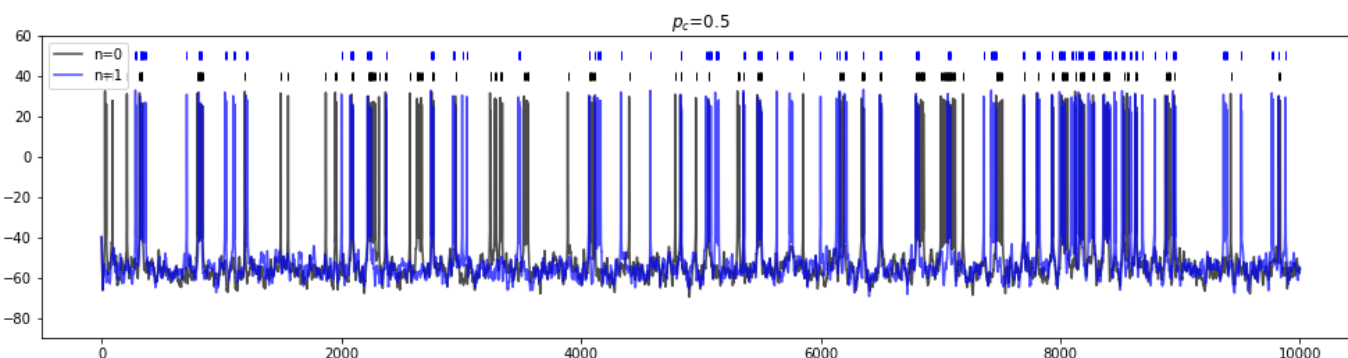
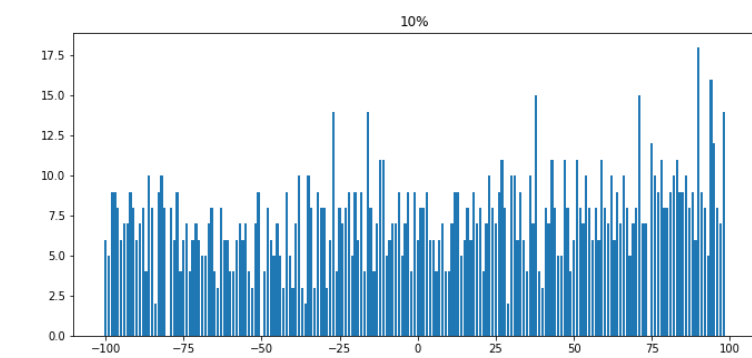
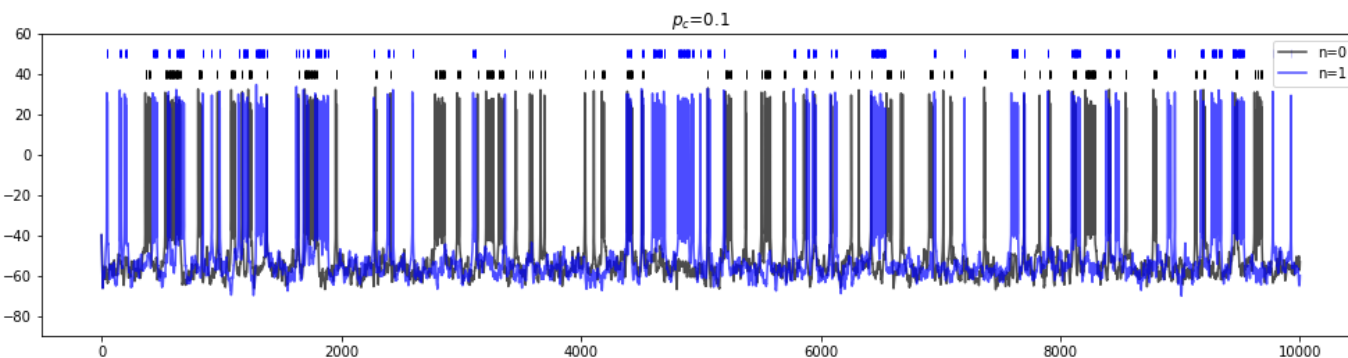
Change in membrane potential: $\partial_t v = f_i(v, w; p) + f_s(v; p) + I_F$

Proportion of open K channels: $\partial_t w = g(v, w; p)$

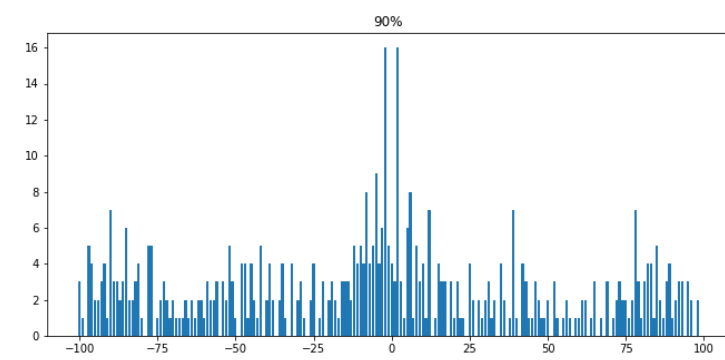
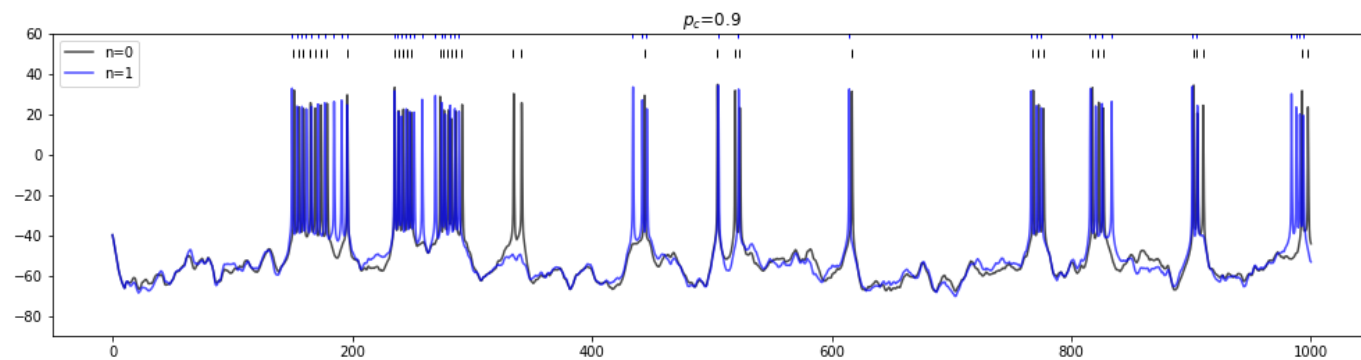
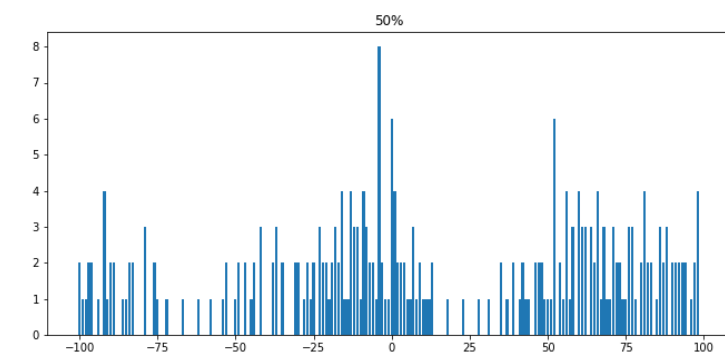
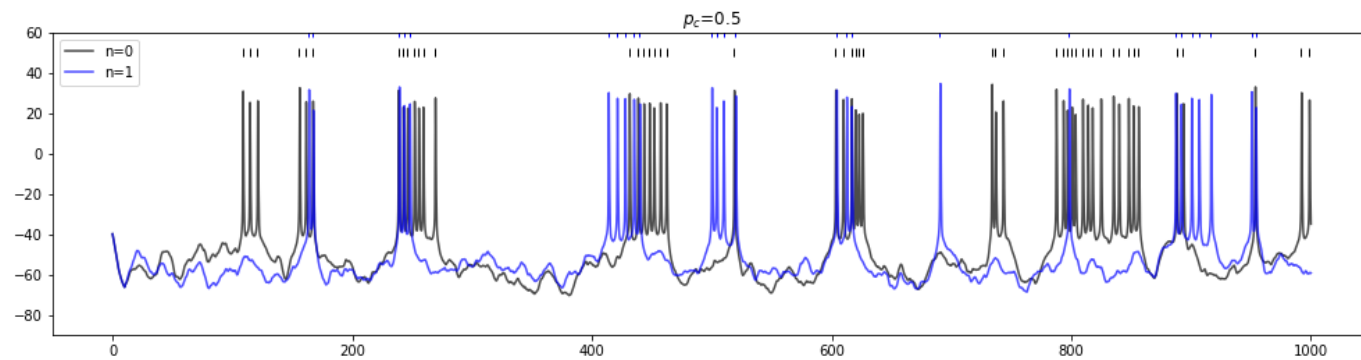
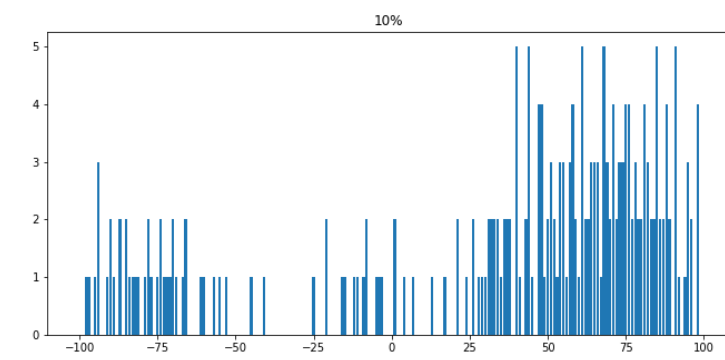
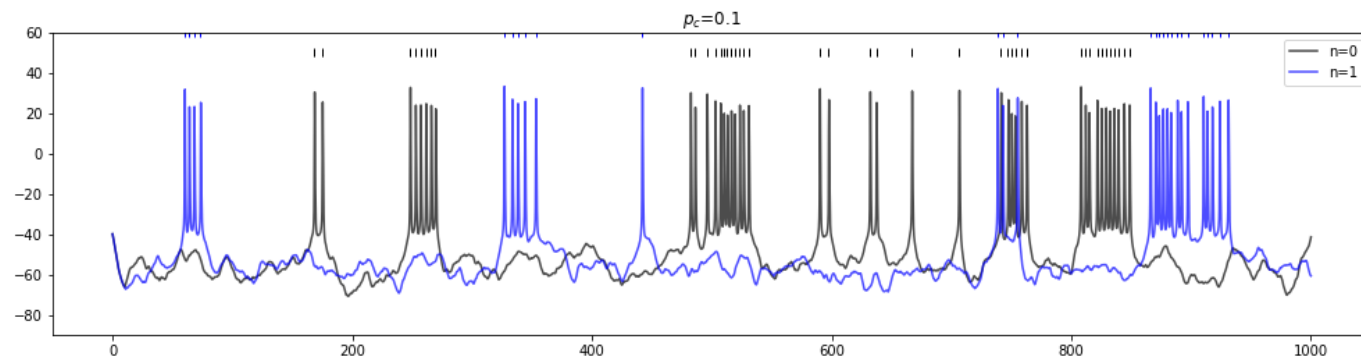
var = 320 pA



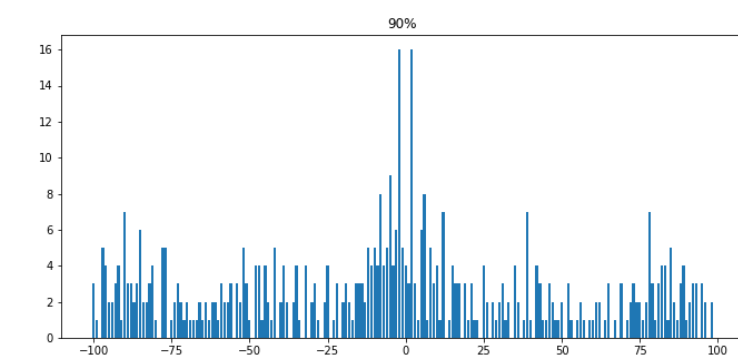
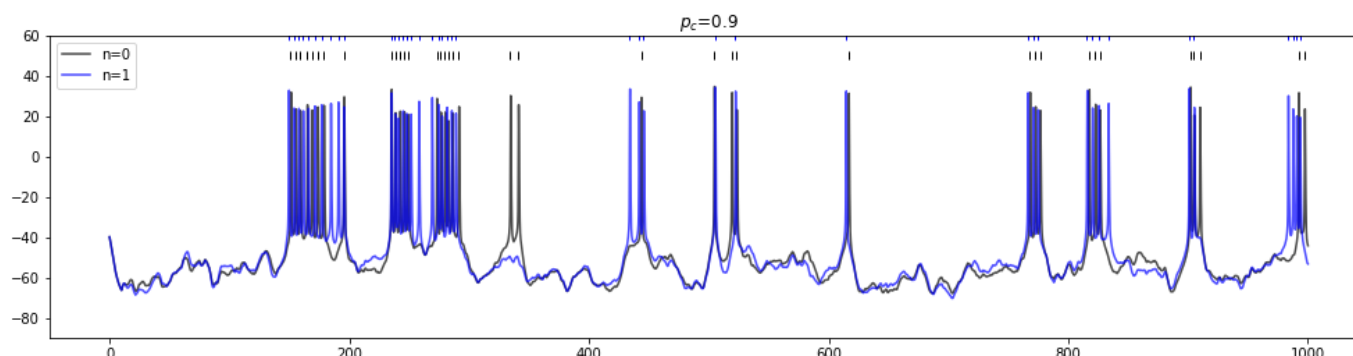
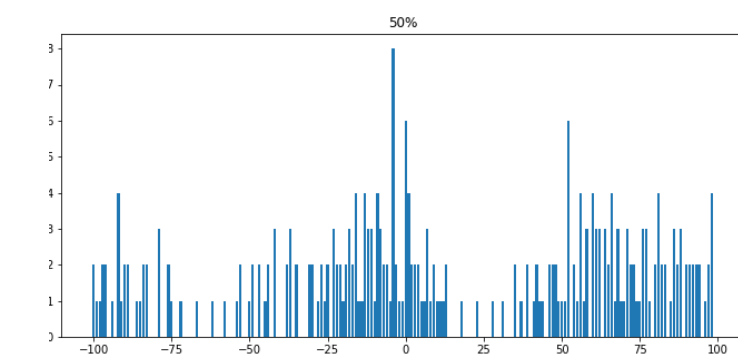
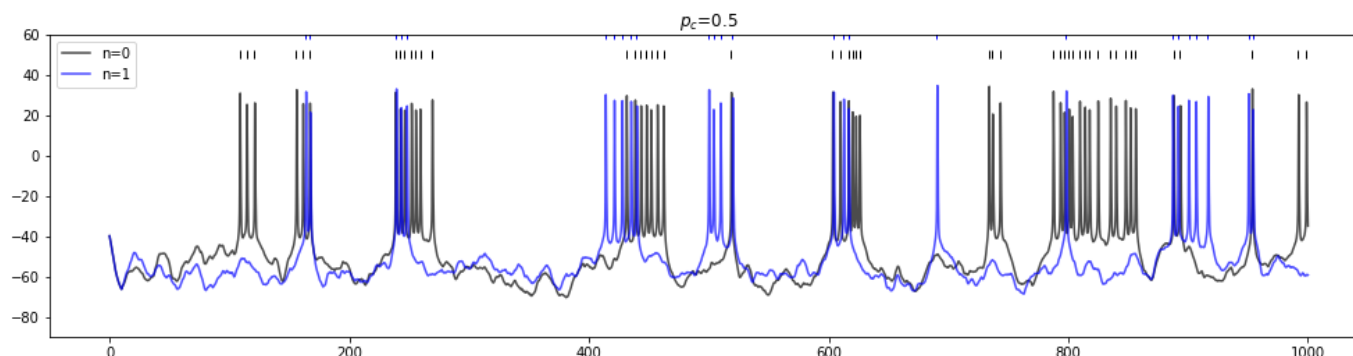
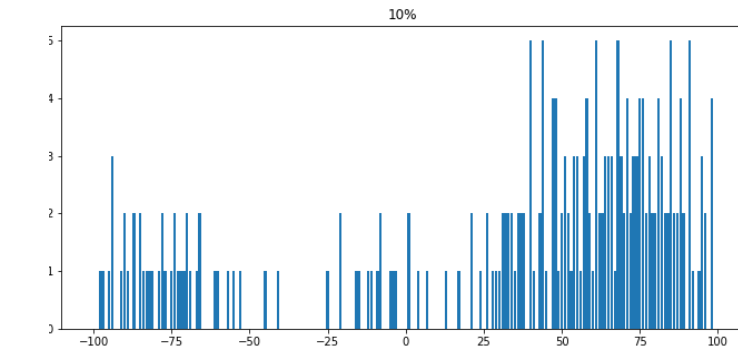
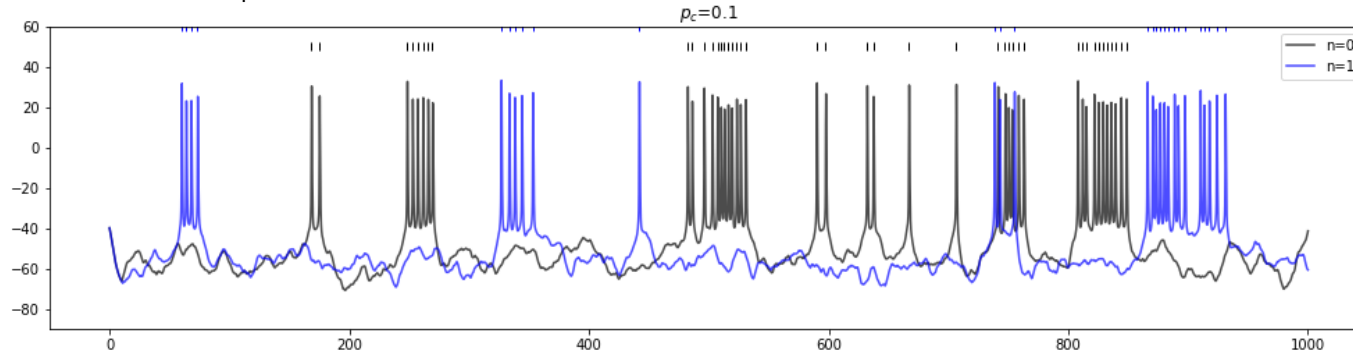
var=640 pA



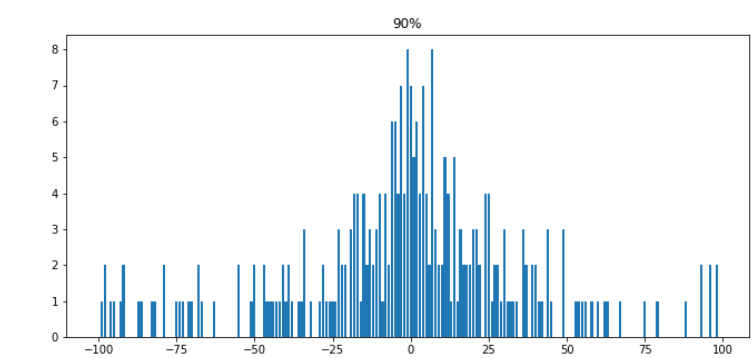
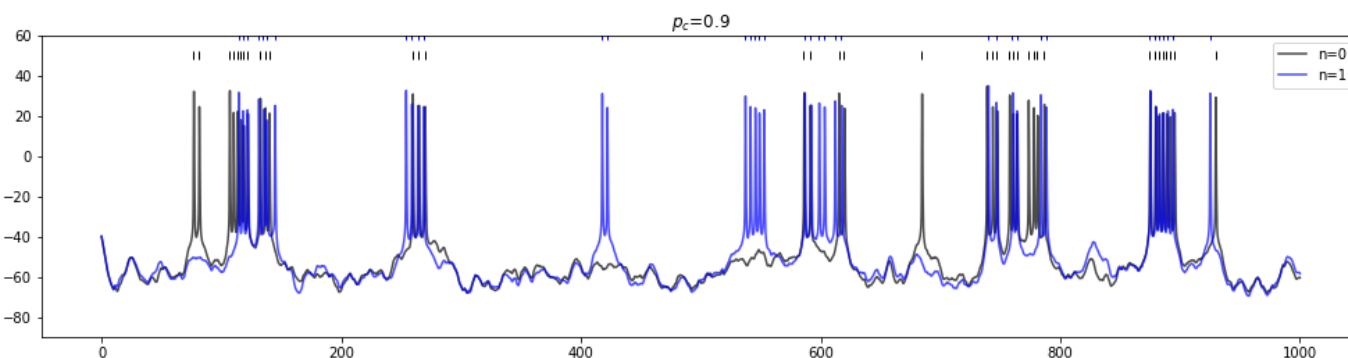
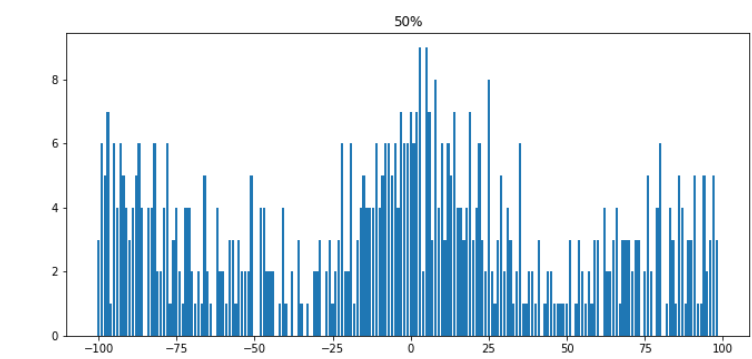
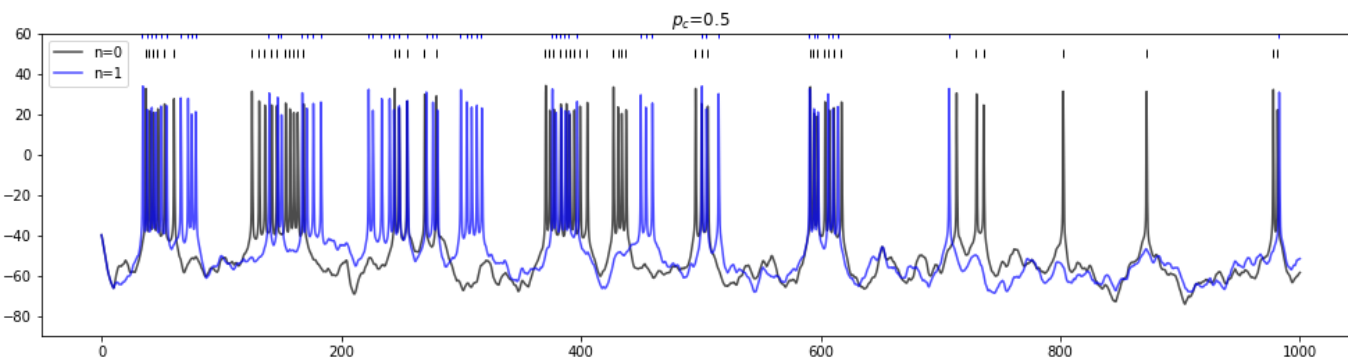
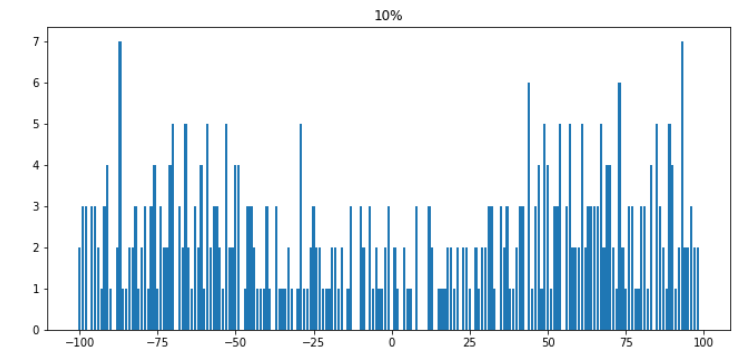
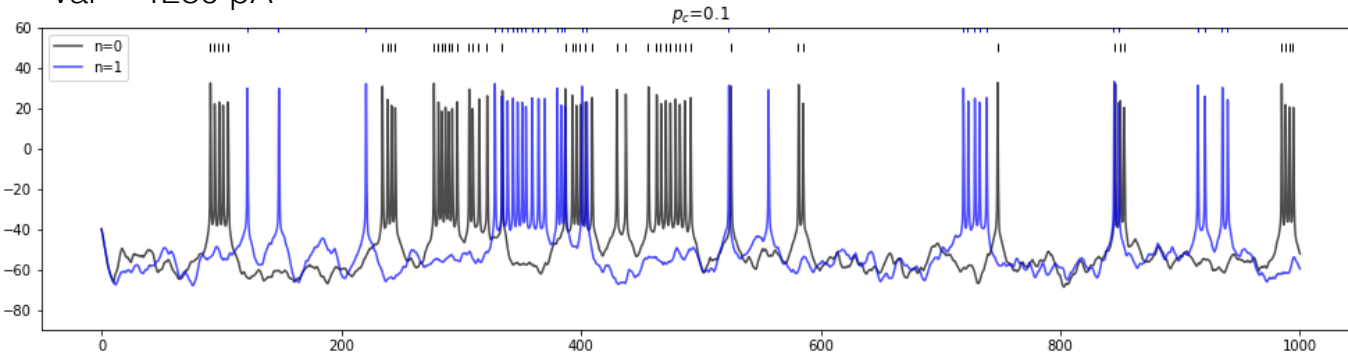
var=960 pA



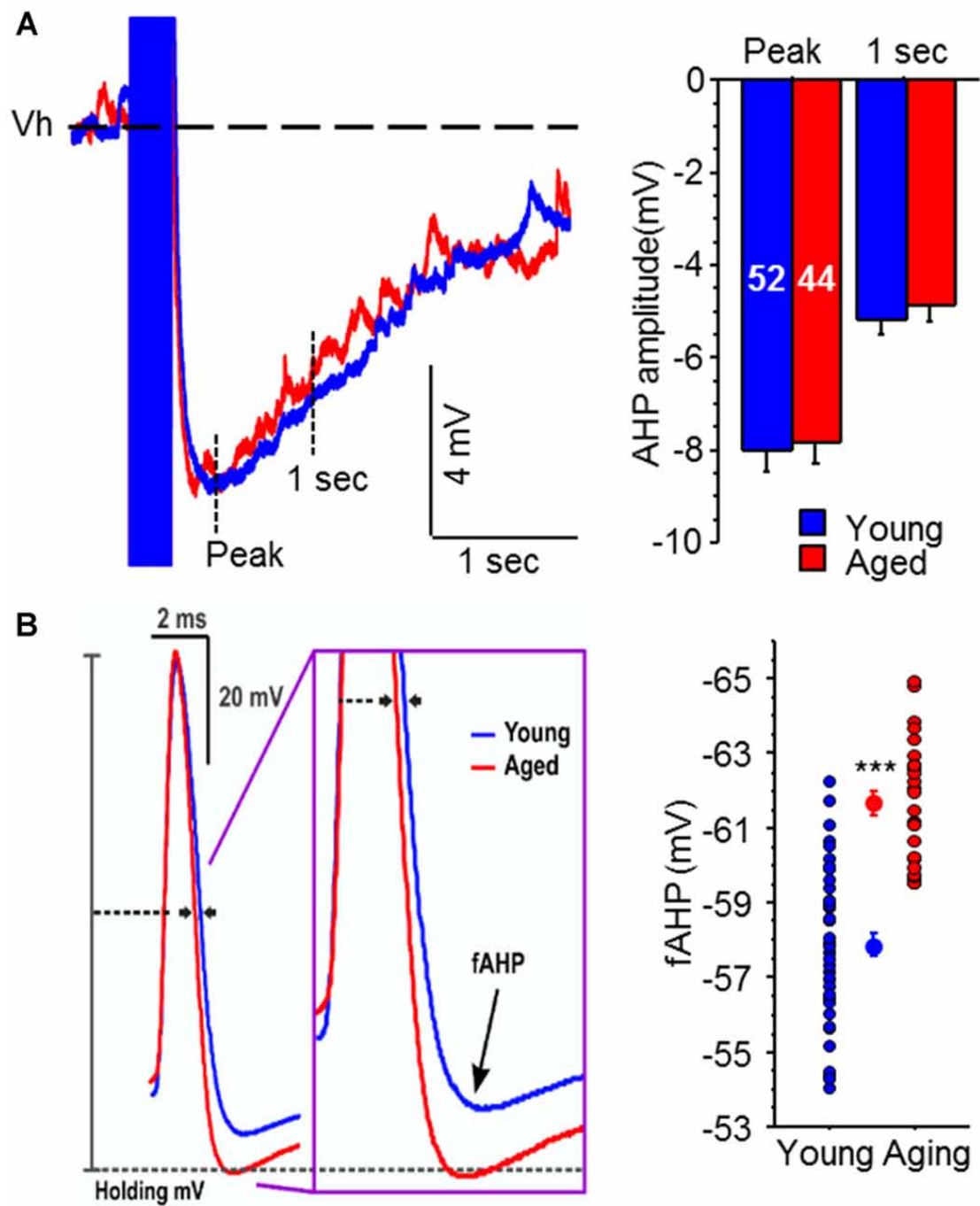
var = 1120 pA



var = 1280 pA



CA1, CA3 neurons: aged vs young



From Oh et al. 2011

These biophysical changes are correlated to learning and behavior.

For instance, older mice and rats show increased latency in acquisition times during specific spatial tasks.

One hypothesis is that the decreased excitability in these neurons affects the way in which representations are built